

AD-A063 392

HUGHES AIRCRAFT CO FULLERTON CALIF GROUND SYSTEMS GROUP
ADAPTIVE TRACKING SYSTEM STUDY. (U)

F/G 17/1

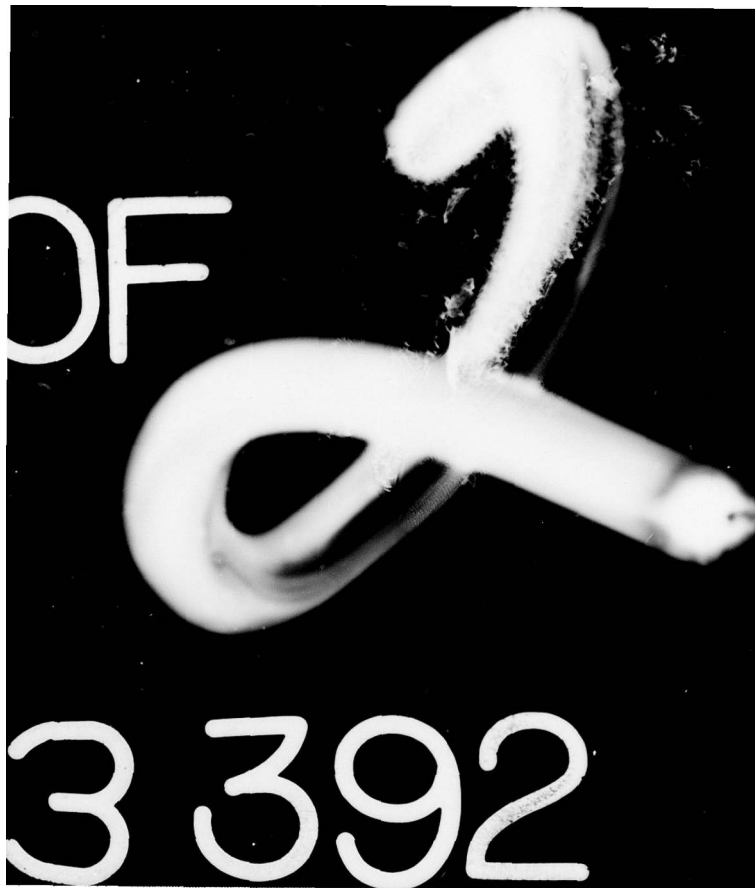
OCT 78 P L FEINTUCH, F A REED, N J BERSHAD
FR78-11-1345

N00024-77-C-6251
NL

UNCLASSIFIED

1 OF 2
AD
A063392





LEVEL

②

A

24

ADA063392

FINAL REPORT ON PHASE 1

OF THE

ADAPTIVE TRACKING SYSTEM STUDY

October 1978

Prepared Under

Contract Number N00024-77-C-6251

DDC FILE COPY

For The

Naval Sea Systems Command Code 06H1

DDC
RECEIVED
JAN 17 1979
A

DISTRIBUTION STATEMENT A

Approved for public release;
Distribution Unlimited

Hughes Aircraft Company
Ground Systems Group
Fullerton, California

79 01 16 152

9 FINAL REPORT ~~CONFIDENTIAL~~ Oct 77-Oct 78 on
OF THE
6 ADAPTIVE TRACKING SYSTEM STUDY.
11 Oct ~~1978~~
12 62 p.

Prepared Under
Contract Number ~~NO0024-77-C-6251~~ *new*

16/FIL121

For The 17/SF11121160
Naval Sea Systems Command Code 06HI

By
10 Paul L. Feintuch,
Francis A. Reed,
N. J. Bershad
B. Beginsky

DISTRIBUTION STATEMENT A
Approved for public release;
Distribution Unlimited

Hughes Aircraft Company
Ground Systems Group
Fullerton, California ✓

172 370 *SM*

FOREWORD

This report documents the first phase of the effort performed for the Naval Sea Systems Command Code 06H1 on contract N00024-77-C-6251, under Project Serial Number SF 11 121 160, Task 20929, and covers the period from October 1977 to October 1978. It includes all of the technical material found in the three ~~Quarterly Reports~~ plus work performed in the fourth quarter, connective material, the conclusions of first phase, and the approach for the second phase of the study. This study has as its goal to examine the application of adaptive filters to perform passive sonar bearing tracking. The first major steps toward this goal have been realized via a combination of statistical modeling and analysis that has been verified via computer simulation.

ACKNOWLEDGMENTS

This work was directed by Mr. John Neely of NAVSEA 06H1. The studies were performed at Hughes by the principal investigator, Dr. Paul L. Feintuch, with the major analytic support of Mr. Francis A. Reed. Consulting services were provided by Dr. N. J. Bershada, and B. Repasky performed most of the computer simulations.

| | |
|---------------------------------|---|
| ADMISSION fee | |
| RT42 | White Section <input checked="" type="checkbox"/> |
| DDC | Gray Section <input type="checkbox"/> |
| UNANNOUNCED | <input type="checkbox"/> |
| JUSTIFICATION | |
| BY | |
| DISTRIBUTION AVAILABILITY CODES | |
| Dist. | AVAIL. CODE OR SERIAL |
| A | |

TABLE OF CONTENTS

| | Page |
|---|--------|
| I. Introduction | 1 |
| II. Statement of Problem | 1 |
| III. Summary of Results | 2 |
| 1. Selection of the Adaptive Filter Configuration for a Bearing Estimator | 3 |
| 2. Extraction of Bearing Estimates from the Adaptive Filter Weights | 4 |
| 3. Frequency Domain Equivalent of the Time Domain Adaptive Filter Bearing Estimator | 4 |
| 4. Delay Estimation with a Discrete Adaptive Tracker | 8 |
| 5. Adaptive Bearing Tracker Performance for Dynamic Signals | 9 |
| 6. Simulations | 9 |
| 7. Conclusions and Relationship to Phase 2 | 14 |
| IV. Figures | |
| V. Appendices | |
| I. Summed Beam vs Split Beam Bearing Estimation | I-1 |
| II. Comparison of Time and Frequency Domain Adaptive Trackers with Broadband Signal Inputs | II-1 |
| III. Mean and Variance of a Single Complex Tap Weight with Signal and Noise Inputs | III-1 |
| IV. Variance of the Split Beam Adaptive Bearing Estimator and Comparison to CRLB | IV-1 |
| V. Delay Estimation with a Discrete Adaptive Tracker | V-1 |
| VI. Tracking Behavior of the Mean Weights for Various Signal Models and a Linearly-Time-Varying Delay | VI-1 |
| VII. Transient Behavior of the LMS Adaptive Filter (Response to Variable Frequency Spectral Lines) | VII-1 |
| VIII. Comparison of Adaptive Tracker Performance with an Existing Automatic Tracker | VIII-1 |

I. INTRODUCTION

This is the final report on the first phase of a study contract to examine the applicability of adaptive filtering to passive sonar bearing tracking. The study was motivated by certain limitations in existing split-beam trackers that might be removed by using an adaptive filter canceller. In particular 1) an adaptive filter does not require a-priori power spectral information on the signal and noise fields, 2) because the filter characteristics are adjusted iteratively (time-varying), the filter has the capability to track dynamic (non-stationary) inputs and 3) since all the correlation information between split array outputs is contained in the adaptive filter canceller weights, the potential exists to perform both broadband and narrowband tracking simultaneously, using all the signal energy rather than separating the energy as in current tracking systems.

This report contains the results reported in the first three quarterly reports with some modifications and new results obtained during the fourth quarter effort. The body of the report is organized so as to present a summary of the results of the analytical effort. The details of the analyses are found in the Appendices.

II. STATEMENT OF PROBLEM

The work effort has been focussed on studying the following set of analysis tasks associated with using the adaptive filter as a bearing tracker:

- 1.0 Analysis of the application of adaptive filters to bearing tracking.
 - 1.1 Determine the best method for obtaining the delay parameter τ from the adaptive filter weights. Compare the bias and variance from this method of estimating τ to that obtained from existing split beam trackers.
 - 1.2 Determine the sensitivity of tracking performance to unknown signal and noise power spectra.
 - 1.3 Evaluate the bias caused by plane wave interference on tracker performance.
 - 1.4 Investigate the design of an adaptive tracker which can use both broadband and narrowband signal components simultaneously to estimate target track. Determine if the ambiguities in the adaptive weights can be resolved for narrowband inputs.
- 2.0 Analysis of adaptive filters with non-stationary inputs.
 - 2.1 Determine the closed form transient response of an adaptive line enhancer having linearly changing input signal frequency from the matrix eigenvalues.

2.2 Model broadband dynamic inputs into the adaptive tracker and analyze the time response and mean squared-error of the cancelled (error) output.

3.0 Simulation, test and evaluation using computer generated data.

- 3.1 Model the adaptive tracker on the HAC simulation facilities and determine performance using synthetic data. Determine tracker bias and variance as a function of signal bearing rate, S/N ratio, and plane wave interference. Broadband and narrowband signals as well as combined broadband and narrowband signals are to be used.

III. SUMMARY OF RESULTS

The results of this study are divided into seven parts. The first part deals with the selection of the adaptive filter configuration to perform bearing estimation. Both sum beam and split-beam tracker configurations were studied.

The second part deals with the extraction of the bearing (or delay) estimate from the adaptive filter, keeping in mind that the AF is basically operating as a waveform estimator. For broadband inputs, the delay estimate is chosen to correspond to the peak value of the weights. The third part deals with a frequency domain equivalent model of the time domain adaptive filter that enables the variance of the adaptive filter delay estimator to be calculated. The variance of the delay estimator is compared to the Cramer-Rao Lower Bound (CRLB) for the variance of any unbiased estimator. The fourth part deals with practical implementation of the delay estimator that, because of the discrete-time locations of the filter taps, differs from the theoretical continuous-time model whose performance was analyzed in Part 3. The discrete time implementation consists of an interpolation routine following the adaptive filter that uses the weight values to interpolate delays between the taps. The degradation of the interpolation model, as compared to the continuous estimator, is investigated.

The fifth part deals with the performance of the adaptive filter bearing estimator as a tracker for signals that are changing bearing. Three signal models are considered -

single frequency signals (narrowband inputs), broadband spectrally white signals, and broadband non-white signals. In each case, it is shown that the adaptive filter is capable of tracking changing bearing. A related dynamical problem is also investigated; the-response of the adaptive filter to a linearly-varying-frequency sine wave.

The sixth part deals with the simulation of the adaptive filter bearing estimator in both the time domain filter configuration and its frequency domain equivalent. For a wide variety of simulation parameters, the two configurations are shown to perform equally well and to yield close agreement with the theoretical predictions. It also compares the adaptive tracker performance to that of a conventional tracking system.

The seventh part deals with the conclusions of the study that are based upon the results of the previous six parts. These conclusions are related to the future tasks to be performed in Phase 2 of the overall study.

Part I - Selection of the Adaptive Filter Configuration for a Bearing Estimator

It would have been highly desirable to apply some type of optimization theory to the selection of the structure containing the adaptive filter and constituting the bearing estimator. For example, what structure, using the adaptive filter, yields the minimum variance unbiased estimate of bearing in the class of allowable structures. Unfortunately, no such optimization theory exists nor does it appear feasible to attempt to derive a theory. Instead, based upon some reasonable assumptions about what structures might be useful for bearing estimation, two bearing estimator structures were selected on an ad hoc basis and studied in detail.

The two bearing estimator structures, sum beam and split-beam, are shown in Figures 1 and 2. It is shown in Appendix I that the sum-beam system tends to obscure the signal correlation properties necessary for the adaptive filter to track. The hydrophone noises produce residual correlations on the beams which the adaptive filter treats as a signal process. To decorrelate the noises, one must form beams from separate elements, so that the two inputs to the adaptive canceller are not linear combinations of the same set of processes. This motivated the consideration of the split-beam processor of Figure 2. It is shown in Appendix I that the split-beam system offers the capability of correctly estimating the delay between the two split-beam inputs. Furthermore, in Appendix IV, it is shown that the performance of the split-beam adaptive bearing tracker is very near to the theoretical lower bound on performance of any tracker. This latter result lends strong support to the ad hoc selection process.

Part II - Estimation of Bearing Estimates from the Adaptive Filter Weights

The structure for estimating bearing (delay) is shown in Figure 3. The left half-beam output is selected to be the desired signal and the right half-beam is selected to be the input to the adaptive filter. Ideally the filter should insert a delay equal to the signal arrival time difference between the two half array phase centers. Hence, one weight (at the correct delay on the delay line) will be unity and all other weights will be zero. However, because the filter is a tapped delay line, only discrete values of the time delay can be estimated exactly by observation of a single non-zero weight. Thus, depending on the spectra of $X_L(t)$ and $X_R(t)$, more than one tap weight will be non-zero. If we also include the effects of noise, it is conceivable that several weights will be non-zero even if the true delay occurs precisely at a tap on the delay line. Hence, some kind of algorithm is needed for determining the correct location of the peak of the weights from noisy sample values of the weights taken at discrete times. The particular algorithm is discussed in Appendix V.

A theoretical analysis of the performance of the bearing estimation scheme in Figure 3 requires statistical knowledge of the filter weights after convergence. Although the mean values of the weights can be determined as a function of the signal and noise powers and the algorithm gain coefficient μ , the variance of the time domain weights in the presence of correlated inputs to the two half-arrays cannot be determined directly at this time. Knowledge of the weight variance is necessary in order to compute the variance of the bearing estimate. Because of this lack of statistical knowledge about the system Figure 3, an equivalent frequency-domain adaptive bearing estimator is studied in the next section. The alternate configuration is analyzed and used to predict the performance of the system in Figure 3. Subsequent analysis and simulations verify the equivalence of the two systems.

Part III - Frequency Domain Equivalent of the Time Domain Adaptive Filter Bearing Estimator

Figure 4 shows an alternate structure for the split-beam adaptive bearing estimator that displays more clearly the ability of the device to track both broadband and narrowband signals. Most conventional trackers are designed to handle either narrowband signals or broadband signals but not both. For example, a bearing tracker that uses a phase-locked loop (PLL) to measure the difference in phase between two half-arrays can effectively track narrowband signals where the phase of a carrier with slowly

varying envelope can be followed. However, broadband signals, which do not have a well-defined carrier are not tracked well by a PLL.

The split-beam adaptive bearing tracker can track either broadband or narrowband signals since the adaptive filter does not need to know the signal statistics a priori. The delay of a broadband signal will be seen as a relatively large peak in the weight values at the correct delay setting. The delay of a narrowband signal will be seen as a phase delayed set of sinusoidal filter weights. In this case, the delay will display itself most easily by FFT'ing the weights and selecting the largest output of the phase estimator in Figure 4.

The significance of the above arguments is that the split-beam adaptive bearing tracker automatically configures itself as a broadband or narrowband tracker as the situation requires. This means that the device is able to track on all the incoming signal energy, whether broadband or narrowband. The processor of Figure 4 is a method for exploiting this behavior. The peak in the adaptive filter weights, or in the Fourier transform of the weights is used to determine the inter-array delay or phase shift.

Figure 4 indicates the structure for extracting bearing estimates from the time-domain adaptive filter. For comparison, Figure 5 shows a frequency domain analog of the time domain adaptive filter. In Figure 4, it is noted that the entire broadband input is the input to M tap adaptive filter. The error signal over the total band controls the weight adjustment algorithm. On the other hand in Figure 5, the input is divided into narrow frequency bins with each narrowband input and error signal controlling the adjustment of a single complex weight for each bin. Since the weight adjustment in each frequency bin occurs independently of errors in other frequency bins, it is not obvious that the two implementations are equivalent. In Appendix II, for the case of a broadband signal in noise, it is shown that the implementations in Figures 4 and 5 converge to essentially the same steady-state weight vector and mean-square error if the FFT time window in Figure 5 is large in comparison to the time delay difference between the signals at the adaptive tracker inputs. Furthermore, by examining the difference equations for the mean value of the weights, it is shown in Appendix II that the time responses are equal. The weight fluctuations are also compared and shown to differ by a ratio that is approximately unity for $\mu \sigma_n^2$ small.

Having verified the equivalence of the time and frequency domain adaptive bearing estimator configurations, we now proceed to determine the performance of the frequency domain bearing estimator.

The performance of the broadband adaptive filter tracker requires the mean and variance of the weights with both signal and noise present. The configuration initially proposed operates entirely in the time domain using a tapped delay line (Figure 4). This is contrasted with the structure in Figure 5 wherein the beam outputs are pre-filtered using, for example a Fast Fourier Transform (FFT) and a single complex adaptive filter weighting is used on each FFT bin on each split beam. The time delay between split array phase centers corresponds to a different phase shift at each frequency. The adaptively filter outputs can subsequently be recombined to produce a broadband output if desired. The key assumption being employed is that the observation time is relatively long compared to the inverse of the bandwidths so that Fourier coefficients provide an adequate second-order statistical realization of the broadband process itself.

If the input processes are wide-sense stationary over the observation time, then disjoint spectral outputs are uncorrelated. Since the input data is assumed to be a narrowband gaussian random process, the disjoint bins therefore provide statistically independent outputs. Thus each complex tap is operating on independent data just as the time domain taps along the delay line are assumed to operate on samples that are independent in time. This interpretation casts the analysis in a form that is tractable. In Appendix III, the mean and variance of the complex weight is calculated with both signal and noise present. This result is then used to obtain steady-state tracker performance.

The principle results of Appendix III are

$$\lim_{n \rightarrow \infty} E [W(n+1)] = \frac{\alpha \sigma_I^2}{\sigma_I^2 + \sigma_n^2}$$

$$\text{Var} [W(\infty)] = \mu \sigma_n^2 \left[\frac{(|\alpha|^2 + 1) \sigma_I^2 + \sigma_n^2}{(\sigma_I^2 + \sigma_n^2) [2 - 2\mu (\sigma_I^2 + \sigma_n^2)]} \right]$$

where

- α = normalized signal correlation between two half arrays
- σ_I^2 = signal power
- σ_n^2 = noise power
- μ = algorithm feedback coefficient
- E = denotes statistical expectation

Furthermore, the steady-state mean-square error is given by

$$E \left[|\epsilon(\infty)|^2 \right] = \sigma_I^2 \left\{ \left(\frac{|\alpha| \sigma_n^2}{\sigma_I^2 + \sigma_n^2} \right)^2 + \frac{\mu \sigma_n^2 (|\alpha|^2 + 1)}{2 - 2 \mu \sigma_I^2} \right\} \\ + \sigma_n^2 \left\{ 1 + \frac{\mu \sigma_n^2 (|\alpha|^2 + 1)}{2 - 2 \mu \sigma_I^2} + \left(\frac{|\alpha| \sigma_I^2}{\sigma_I^2 + \sigma_n^2} \right)^2 \right\}$$

The above results can be used to determine the performance of a continuous version of the adaptive bearing estimator shown in Figure 3. Figure 6 differs from Figure 3 in that the tapped delay line in the adaptive filter is assumed to be infinitely dense (i. e., the tap separations are infinitesimal). This allows us to view the weight values as a function of a continuous parameter, say τ , rather than as a function of a discrete parameter, m , as in Figure 3. The advantage of this viewpoint will be evident shortly.

We furthermore assume the time domain-frequency domain equivalence of Figures 4 and 5 is valid as verified in Appendix II and apply the results of Appendix III to Figure 6.

The model and statistical weight analysis of Appendices II and III are used to make a first-order approximation analysis of the time-domain adaptive filter when configured as a bearing estimator. This analysis uses the model in Figure 5 for broadband inputs. The objective is to operate the broad adaptive filter (in any implementation, time or frequency domain) and compare its performance with the Cramer-Rao Lower Bound (CRLB). The parametric behavior at low signal-to-noise ratios is a fundamental concern of the analysis. It is shown in Appendix IV that the variance of the split-beam

adaptive bearing estimator is very near to CRLB lower bound on the variance of any split beam estimator.

The variance of the estimator is within 0.5 db of the CRLB. Hence, the split-beam adaptive bearing estimator performs close to the theoretical lower bound on the variance of any unbiased estimator. Hence, the adaptive bearing estimator is nearly optimum and, in effect, makes a maximum likelihood estimate of the bearing without a priori knowledge of the signal and noise spectra. The price of unknown input spectra is the 0.5 db difference in performance in comparison to the CRLB.

Part IV - Delay Estimation with a Discrete Adaptive Tracker

In Part 3, an expression for the variance of the bearing estimate of a continuous adaptive filter configured as an adaptive tracker was developed. The estimate is based upon determination of the peak of the continuous impulse response of the adaptive filter. In practice, however, the adaptive filter is discrete in time and of finite length, and the peak of the impulse response must be determined by interpolating between the discrete sample points. The interpolation process increases the variance of the bearing estimate with respect to that of the continuous case.

Appendix V describes a numerical method of determining the peak of an interpolated impulse response, and develops an expression for the variance of the estimate using this method.

Part V - Adaptive Bearing Tracker Performance for Dynamic Signals

The previous analysis has considered the behavior of adaptive bearing estimator for signals at a fixed bearing angle; that is, how does the performance of adaptive bearing estimator compare to the CRLB for static signals. Although the static analysis gives a good indication of how the estimator performs, the real case of interest is in the tracking mode where the bearing angle of the target is changing. In Appendix VI the time-varying mean weights are derived for a signal that is moving such that the delay between split-array phase centers is linearly changing with time. Three signal models are considered - a narrowband signal, a broadband spectrally white signal and a broadband non-white signal. For the single frequency case, the mean filter weights correct for a frequency shift and phase precession due to the angular movement of the target in bearing. For a spectrally white process, the mean filter weights are a travelling wave with a decaying exponential envelope. Tracking the bearing involves estimating the delay location of the leading edge of the weights. For the broadband non-white signal, the mean weights behave in a similar manner to the previous case except, because of correlation between the taps, the peak of the travelling wave is much larger and the decaying exponential envelope is dependent on the signal dynamics and correlation. Thus, tracking non-white signals is easier than tracking white signals.

A subject related to the tracking behavior of the adaptive filter is treated in Appendix VII. The transient behavior of the LMS adaptive filter is studied when the filter is configured as a canceller operating in the presence of a fixed or variable complex frequency sine-wave signal buried in white noise. For a fixed frequency signal, the mean weights are shown to respond to signal more rapidly than to noise alone. For a chirped signal, a fixed parameter matrix first order difference equation is derived for the mean weights and a closed form steady-state solution obtained. The transient response is obtained as a function of the eigenvectors and eigenvalues of the input covariance matrix. Sufficient conditions for the stability of the transient response are derived and an upper bound on the eigenvalues obtained. Finally, the mean-square error is evaluated when responding to a chirped signal. The gain coefficient of the LMS algorithm is determined that minimizes the mean-square error for chirped signals as a function of chirp rate and signal and noise powers.

Part VI - Simulations

The last part of this report deals with simulations of adaptive bearing trackers in both the time and frequency domain implementations followed by time domain interpolation.

The simulations serve three purposes:

- 1) Verification of the equivalence of the time and frequency domain implementations of the tracker,
- 2) Support for the theoretical model of the frequency domain implementation,
- 3) Provide initial sets of data for design of the adaptive bearing tracker.

Figures 17 - 46 show the delay estimates as a function of the various system parameters indicated on the figures.

In order to verify the results of the previous sections and the appendices, the adaptive tracker has been simulated on the computer. The simulation is configured to implement both the time and frequency domain trackers, and provides for broadband or narrowband signal inputs with a variable delay between the simulated array inputs. The capability is included to band limit the input via a finite impulse response (FIR) filter in each input path. The delay may also be varied linearly with time. A $\sin(x)/x$ interpolator, as described in Appendix V, is included to estimate delays when the true delay lies between discrete filter taps. A phase estimator, corresponding to the narrowband case, is also included. Figures 13 and 14 illustrate the simulation for time and frequency domain trackers, respectively.

A primary result of the second quarterly report was that the time delay can be extracted from the weight vector even at low signal-to-noise ratios where the reduction in mean square error is small. For a broadband signal with a delay equal to an integral number of sampling intervals, this would be evidenced by the filter weight corresponding to the correct delay appearing larger than the other filter taps. The ability to distinguish that the correct tap is largest at input signal to noise ratios as low as -20 dB has been verified by simulation. Figures 15, 16, and 17 show the time domain weight vector as a function of time for one sample interval (0.4167 msec) delay between tracker inputs for a broadband signal with 0, -10, and -20 dB signal-to-noise ratios, respectively. The 2nd weight, corresponding to one unit of delay, clearly has the largest mean value in all cases. Figures 18, 19, and 20 show similar results with the signal delayed 3-sample intervals between inputs.

The results of the simulations using the frequency domain implementation verify the analytical prediction of the steady state weight vector derived earlier in the report.

Table 1 below gives the value of the largest steady state time domain, mean weight for broadband examples simulated with the frequency domain tracker. The remaining weights should have mean zero in steady state. These results can be predicted using equation (8) of Appendix II. The theoretical predictions can be compared to the simulation results given in Tables 3 through 8. These show the time domain weight vector as a function of time for each of the six cases of Table 1. The value of the weights shows good agreement with the above analytical results once the weights approach steady state, as they have in the lower part of each table. It should be noted that each 2400 iterations constitutes one second in these simulations. The tables also indicate that it is possible to determine the correct delay from the weight vector for these signal-to-noise ratios, since the correct weight is largest in all cases.

TABLE 1. PREDICTED VALUE OF LARGEST STEADY STATE MEAN WEIGHT IN THE TIME DOMAIN

| SNR | μ | Delay | Simulation Results in Table No. | Largest Steady State Mean Weight |
|--------|-----------|-------|---------------------------------|----------------------------------|
| 0 dB | 2^{-10} | 1 | 3 | $W_2 = 0.4375$ |
| 0 dB | 2^{-10} | 3 | 4 | $W_4 = 0.3125$ |
| -10 dB | 2^{-10} | 1 | 5 | $W_2 = 0.0795$ |
| -10 dB | 2^{-10} | 3 | 6 | $W_4 = 0.0568$ |
| -20 dB | 2^{-14} | 1 | 7 | $W_2 = 0.00867$ |
| -20 dB | 2^{-14} | 3 | 8 | $W_4 = 0.00619$ |

Using the delay interpolator described in Appendix V, a number of simulations with broadband signal have been run. The inputs to the adaptive tracker are low pass filtered with a cutoff of 800 Hz and sampled at 2400 Hz. A 16-tap time domain filter is used to provide the weights to the interpolator, which has its bandwidth parameter, B , matched to the filter input bandwidth, 800 Hz. Figures 21 through 23 show the delay estimate, $\hat{\tau}$ versus time for $\mu = 2^{-10}$ and an actual delay halfway between the 8th and 9th taps (3.541667 msec), with signal-to-noise ratios (SNRs) of 10, 0, and -10 dB. The one standard deviation (1σ) limits for the estimate as predicted using the results of Appendix V is also shown. Figures 24 through 26 show the same cases with a feedback coefficient of $\mu = 2^{-14}$, which reduces the variance of the estimate. Finally,

Figure 27 shows a -20 dB SNR case with $\mu = 2^{-16}$. These cases are repeated for the actual delay coincident with the 8th tap, or 3.3333 msec, in Figures 28 through 34.

The following observations may be made concerning these simulation results:

- (1) For static delays, the adaptive tracker with interpolation between weights can provide high accuracy delay, and hence, bearing estimation for broadband targets. Table 2 below, converts the delay estimate accuracies obtained in the simulations shown in Figures 21 through 27 to broadside bearing accuracies for split arrays with a 7.5 and 75 foot spacing between phase centers.

TABLE 2. BEARING ACCURACIES FOR TYPICAL ADAPTIVE TRACKER SIMULATIONS WITH BROADBAND INPUTS

| SNR | μ | Figure No. | r. m. s. Bearing Error | |
|-----|-----------|------------|------------------------|----------------|
| | | | 7.5 Ft Baseline | 75 Ft Baseline |
| 10 | 2^{-10} | 21 | .187° | 1.87° |
| 10 | 2^{-14} | 24 | .057° | .57° |
| 0 | 2^{-10} | 22 | .67° | 6.7° |
| 0 | 2^{-14} | 25 | .185° | 1.85° |
| -10 | 2^{-14} | 26 | .877° | 8.77° |
| -20 | 2^{-16} | 27 | 5.88° | 58.8° |

As pointed out in Appendix V, μ must be set sufficiently small to assure that the mean of the peak weight vector exceeds the standard deviation if accurate estimation is to result.

- (2) The results of the simulations are in excellent agreement with the predictions given in Appendix V, as long as μ is set sufficiently small. This is most evident in Figure 11. Further, the criterion for setting μ given in that appendix, is verified by the simulation results. For example, from Appendix V, $\mu = 2^{-10}$ is marginal for an SNR of -10 dB, and Figure 23 shows that occasionally the weight maximum appears in the wrong bin.
- (3) Selection of μ sufficiently small to make the mean of the weights exceed the standard deviation requires small μ , and hence, long time constants for

operation with low SNR targets. This raises some question as to whether an adaptive filter with these long time constants can track a moving target. It can be seen from the simulations, however, that estimation within the predicted accuracy is achieved in less than a single time constant. For example, the time constant for the simulations with $\mu = 2^{-14}$ is 6.28 seconds, but the estimate is within predicted steady state limits within nominally 1 second. This suggests an ability to track dynamics while utilizing large time constants to give high accuracy estimates of static targets.

- (4) When μ is marginal for a particular SNR, so that occasionally the peak weight appears in the wrong tap, the estimate falls within predicted steady state error limits most of the time. In this case large deviations from the average could be rejected as "wild points," and the remaining values would be good estimates.

In order to relate these results to existing trackers, a first order performance comparison between the adaptive tracker and a clipped two point correlator tracking scheme is provided in Appendix VIII. The latter is similar to many existing tracking systems. The comparison is not valid for high signal to noise ratio, and should be used only to compare the two trackers in terms of order of magnitude of performance. This is because the assumptions necessary to make two trackers of markedly different structures equivalent in some sense can only be considered approximate. Table 9 shows the bearing accuracy predicted for both the adaptive tracker and the clipped two point correlator for several typical cases, along with the results of the simulations. The results are for the same broadband signal considered in Table 2, with the target stationary at broadside of a split array with 7.5 ft between phase centers. The performance is comparable with the adaptive filter having slightly smaller variances for all cases.

Appendix VI of this report considered the ability of the adaptive tracker to track linearly varying delays. Such a delay is representative of a target with constant bearing rate passing through broadside relative to the split array centers. Simulations were run with the same adaptive tracker/interpolator configuration used in the static runs, but with the delay varying linearly with time. Again, the input is broadband, and both tracker inputs are bandlimited to 800 Hz. The adaptive filter has 16 taps, and the interpolator bandwidth is matched to that of the input.

TABLE 9. COMPARISON OF BEARING ACCURACY OF AN ADAPTIVE TRACKER WITH CLIPPED TWO POINT CORRELATOR TRACKER WITH EQUAL TIME CONSTANTS

| SNR | μ | r. m. s. Bearing Error | | |
|-----|-----------|-----------------------------|------------------------------|---|
| | | Predicted, adaptive tracker | Simulation, adaptive tracker | Predicted, clipped two point correlator |
| 0 | 2^{-10} | .819° | .67° | 2.57° |
| 0 | 2^{-14} | .202° | .185° | .642° |
| -10 | 2^{-14} | 1.3° | .877° | 3.54° |
| -20 | 2^{-16} | 5.8° | 5.88° | 16.25° |

In Appendix VI, it was shown that the mean weight vector, as a function of time is a peak at the actual instantaneous delay between array halves, moving through the filter at the delay rate of change, and with an exponentially decaying trailing edge. This analysis is verified by Figure 35, which shows the weight vector at 5000, 6000, and 7000 iterations for a 10 dB signal and a delay changing at 1.0 msec per second. Figure 36 shows another view of the behavior of the weight vector with time. Here, the delay is changing at 0.2618 msec per second, $\mu = 2^{-10}$, and the signal-to-noise ratio is 10 dB. The peak of the weight vector can be clearly seen moving through the filter with time.

A more quantitative assessment of the tracking behavior of the adaptive tracker can be had from Figures 37 through 39, showing the delay estimate as a function of time for a linearly increasing delay of 261.8 μ sec/sec. This is representative of a 1°/sec target at the split array outputs of an array with 75 feet between phase centers. Figures 37 and 38 show the estimate for the 261.8 μ sec/sec case with $\mu = 2^{-10}$ and SNRs of 10 dB and 0 dB respectively. The same rate of change is shown for $\mu = 2^{-14}$ and SNR of -10 dB in Figures 39.

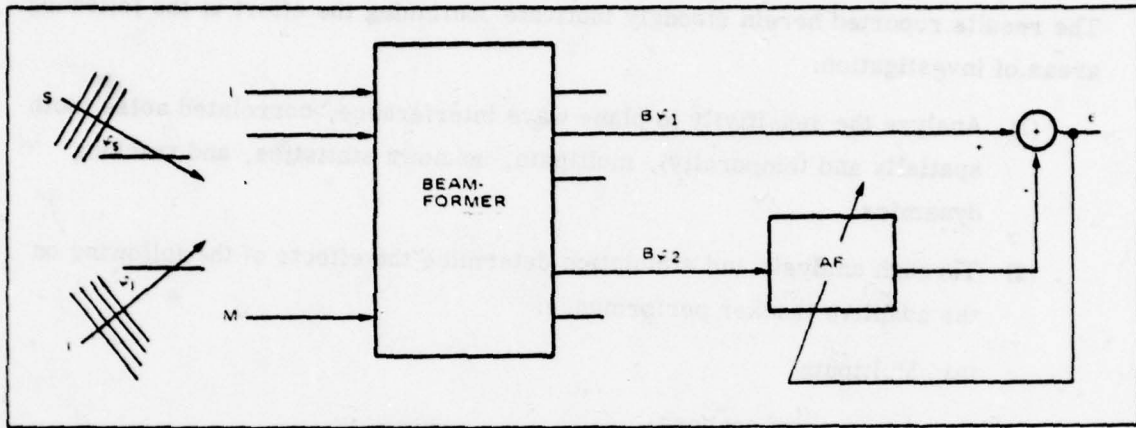
Part VII - Conclusions and Relationship to Phase 2

It can be concluded that the application of an adaptive filter to split beam bearing tracking has the potential to offer performance improvements as discussed in the introduction. In the static case, bearing estimates are comparable to the Cramer-Rao Lower Bound. In the dynamic case, time averages of simulated weights behave

as the theoretical predictions for the mean of the weights. In addition, both narrowband and broadband signals can be tracked with the same processor, suggesting that all target energy can be used for tracking.

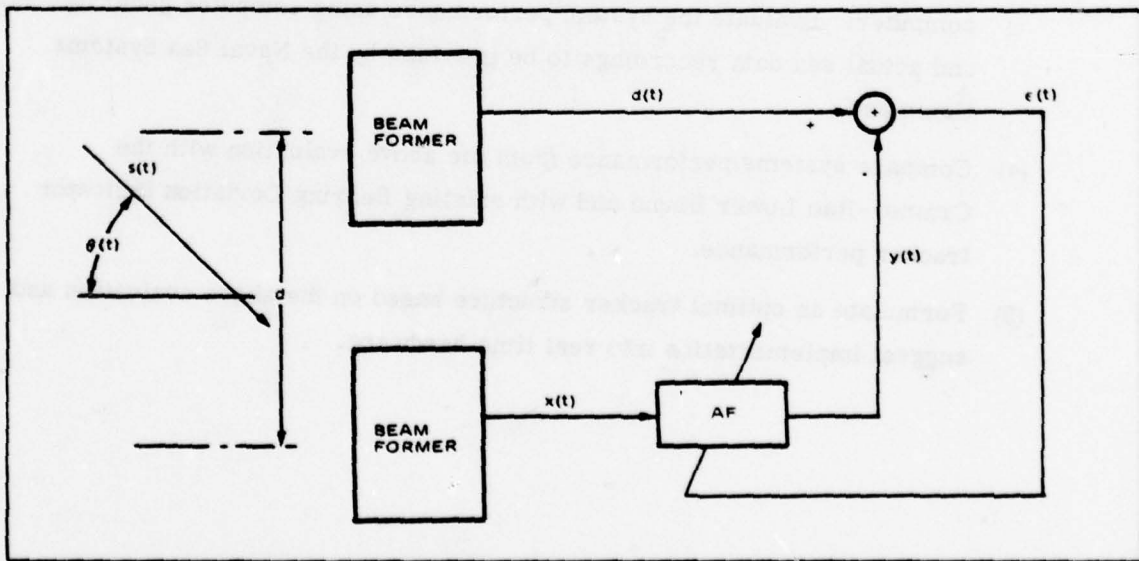
The results reported herein strongly motivate continuing the effort in the following areas of investigation:

- (1) Analyze the sensitivity to plane wave interference, correlated noise (both spatially and temporally), multipath, unknown statistics, and tracking dynamics.
- (2) Through analysis and simulation determine the effects of the following on the adaptive tracker performance:
 - (a) Multipath
 - (b) An array of sensors
 - (c) Multiple targets to be tracked at different bearing rates
 - (d) Multiple interferences to be removed
 - (e) The number of filter taps required
 - (f) The design of filter feedback and gain control parameters
- (3) From the above analysis derive a system configuration and simulate on a computer. Evaluate the system performance using computer generated data and actual sea data recordings to be provided by the Naval Sea Systems Command.
- (4) Compare systems performance from the above evaluation with the Cramer-Rao Lower Bound and with existing Bearing Deviation Indicator tracker performance.
- (5) Formulate an optimal tracker structure based on the above evaluation and suggest implementation into real time hardware.



81156-1

Figure 1. Configuration for Summed Beam Adaptive Tracker



81156-2

Figure 2. Configuration for Split-Beam Adaptive Tracker

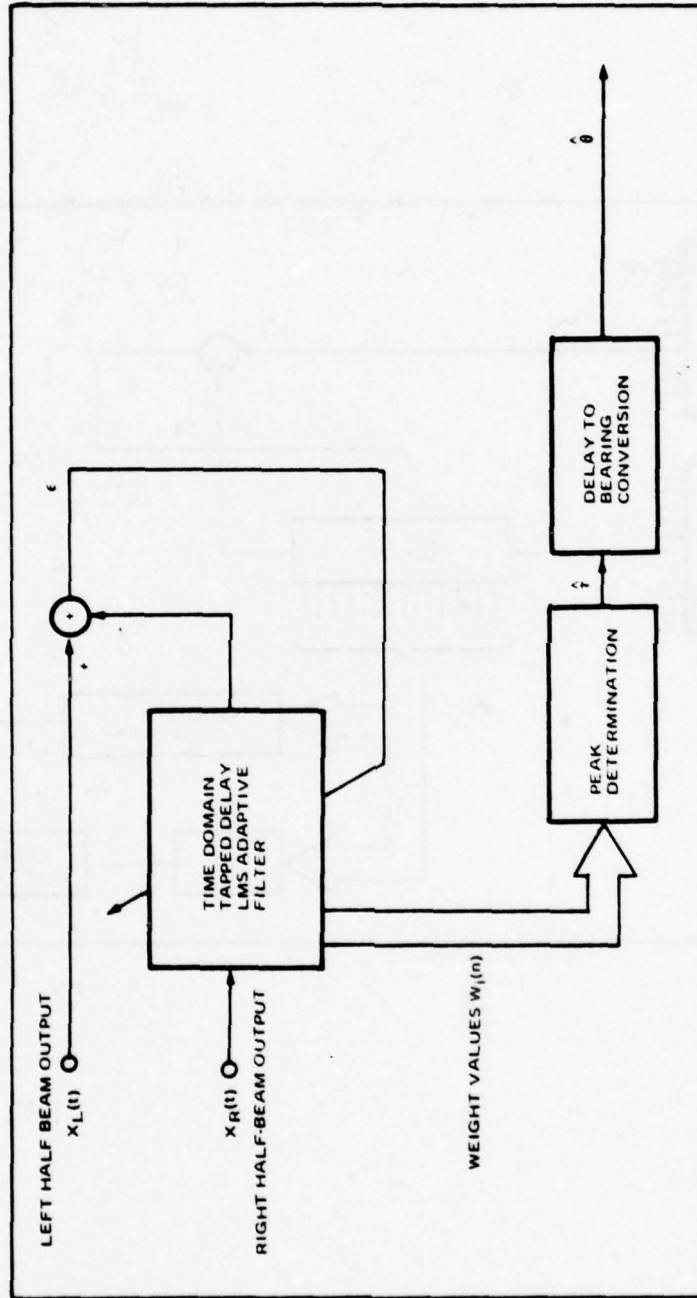


Figure 3. Split Beam Adaptive Bearing Estimator Structure

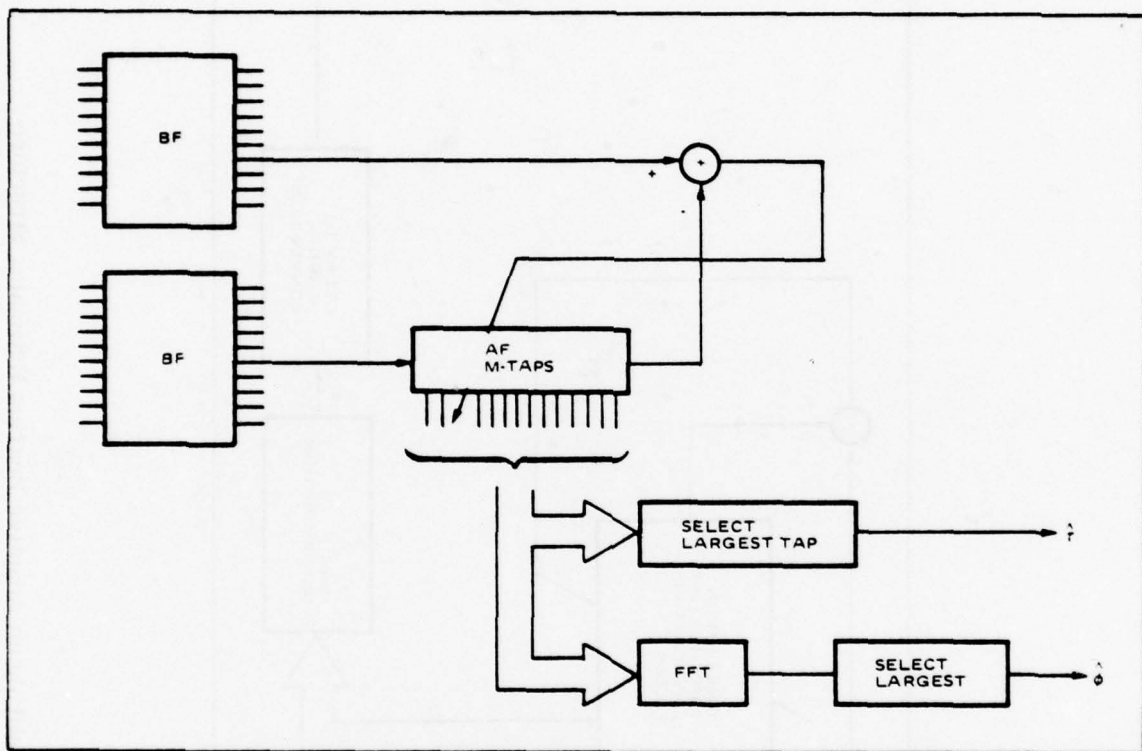
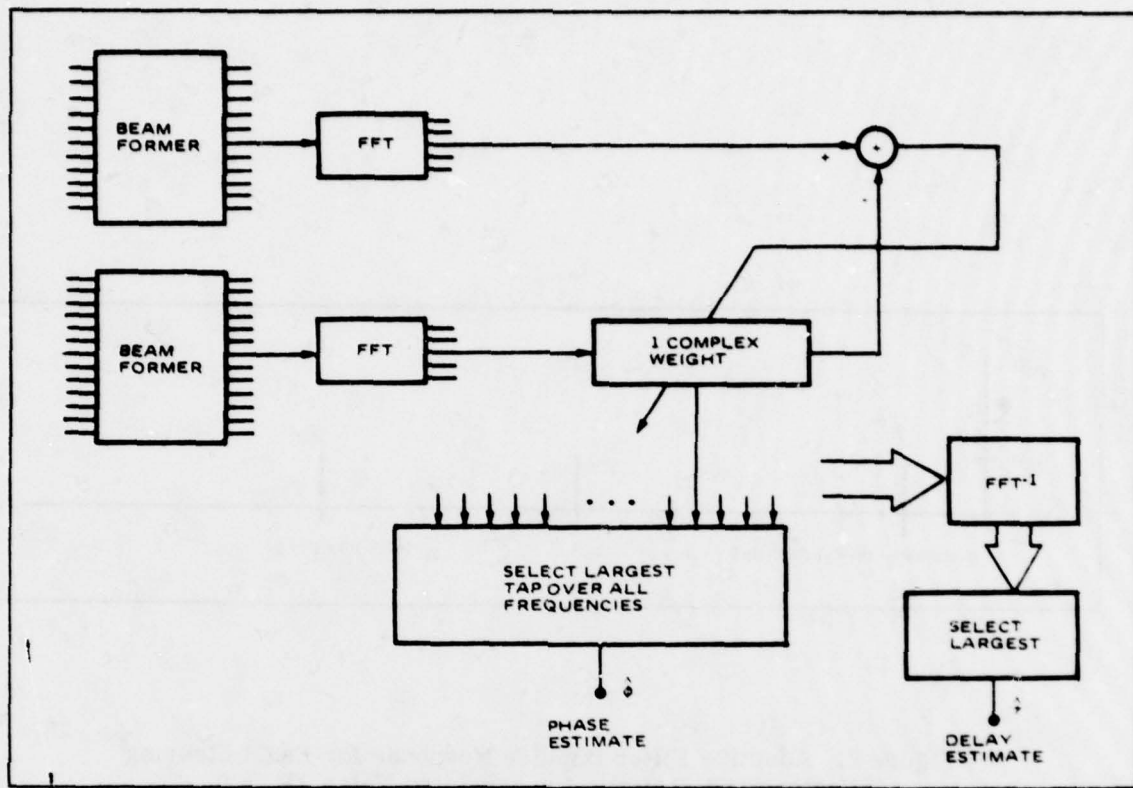
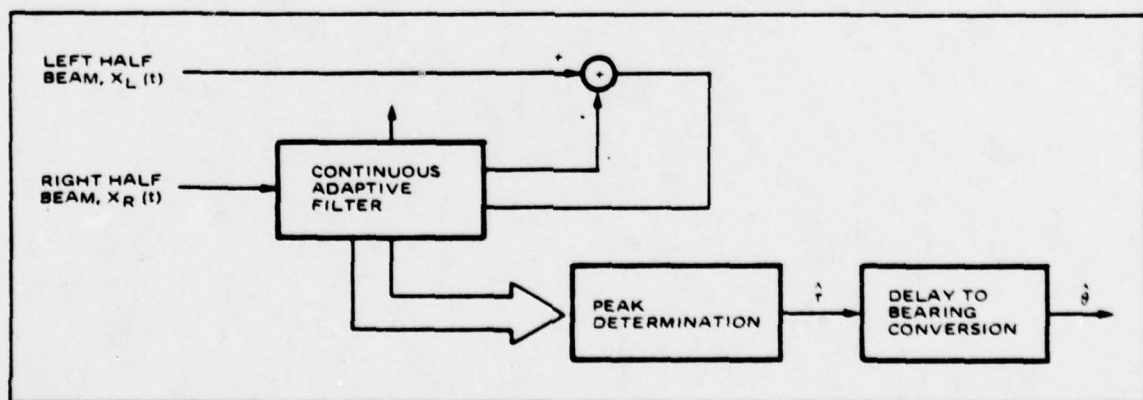


Figure 4. Split-Beam Adaptive Bearing Estimator Structure
 (Alternate Configuration)
 for Both Broadband and Narrowband Signals



8156-5

Figure 5. Frequency Domain Equivalent Model of System in Figure 4



8156-6

Figure 6. Split Beam Continuous Time Adaptive Bearing Estimator

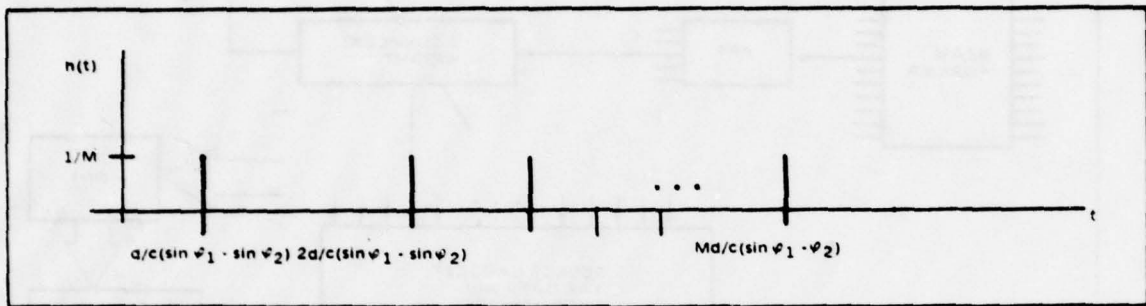


Figure 7. Adaptive Filter Impulse Response for Exact Steering Vectors and Spatially Uncorrelated Noise, $P_s = 0$

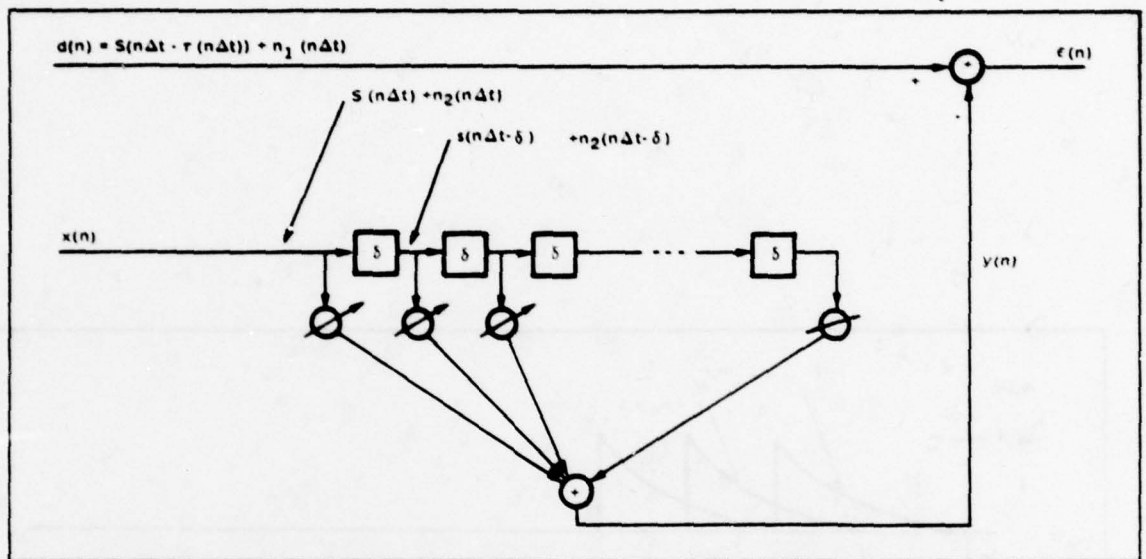


Figure 8. Data in the Delay Line

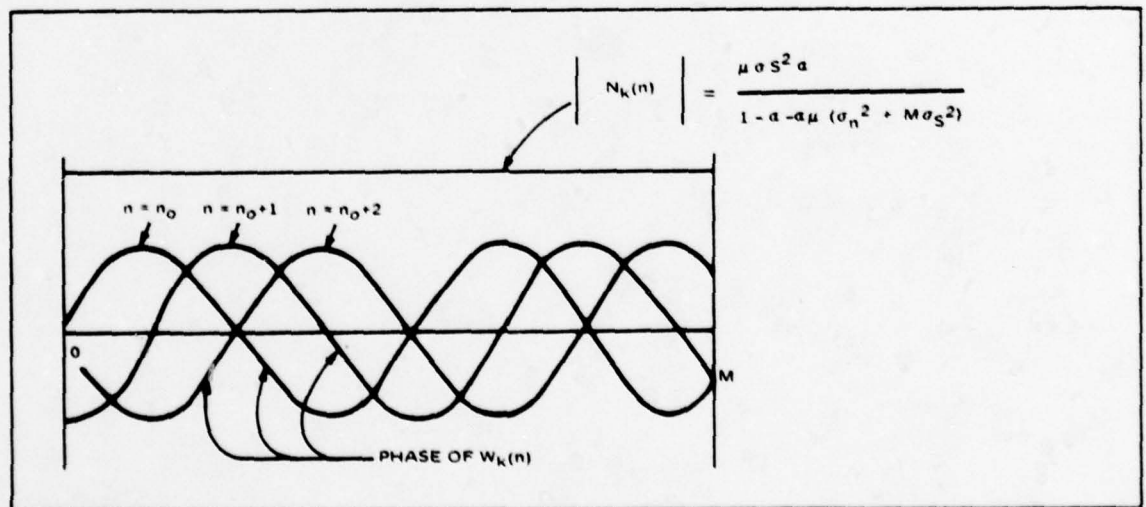
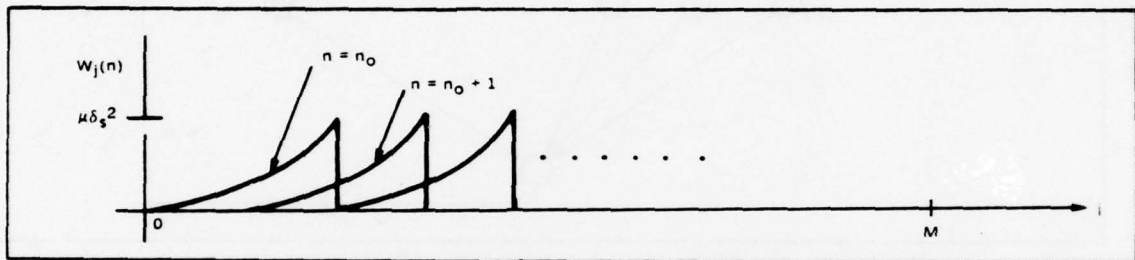


Figure 9. Steady-State Adaptive Filter Weights as Time Changes, Tracking the Changing Time Delay



81156-10

Figure 10. Envelope of the Tracker Weights as They Move in Time

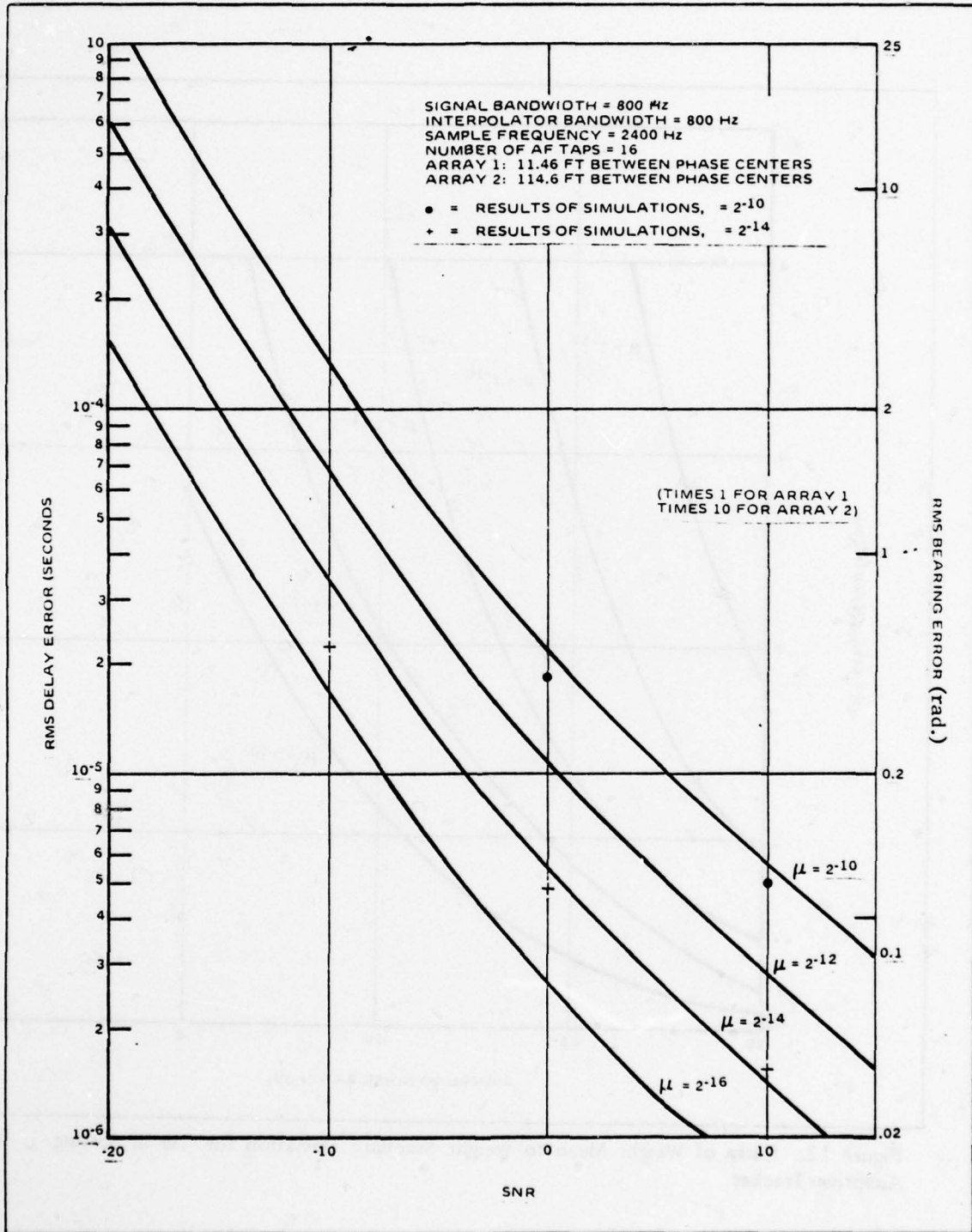
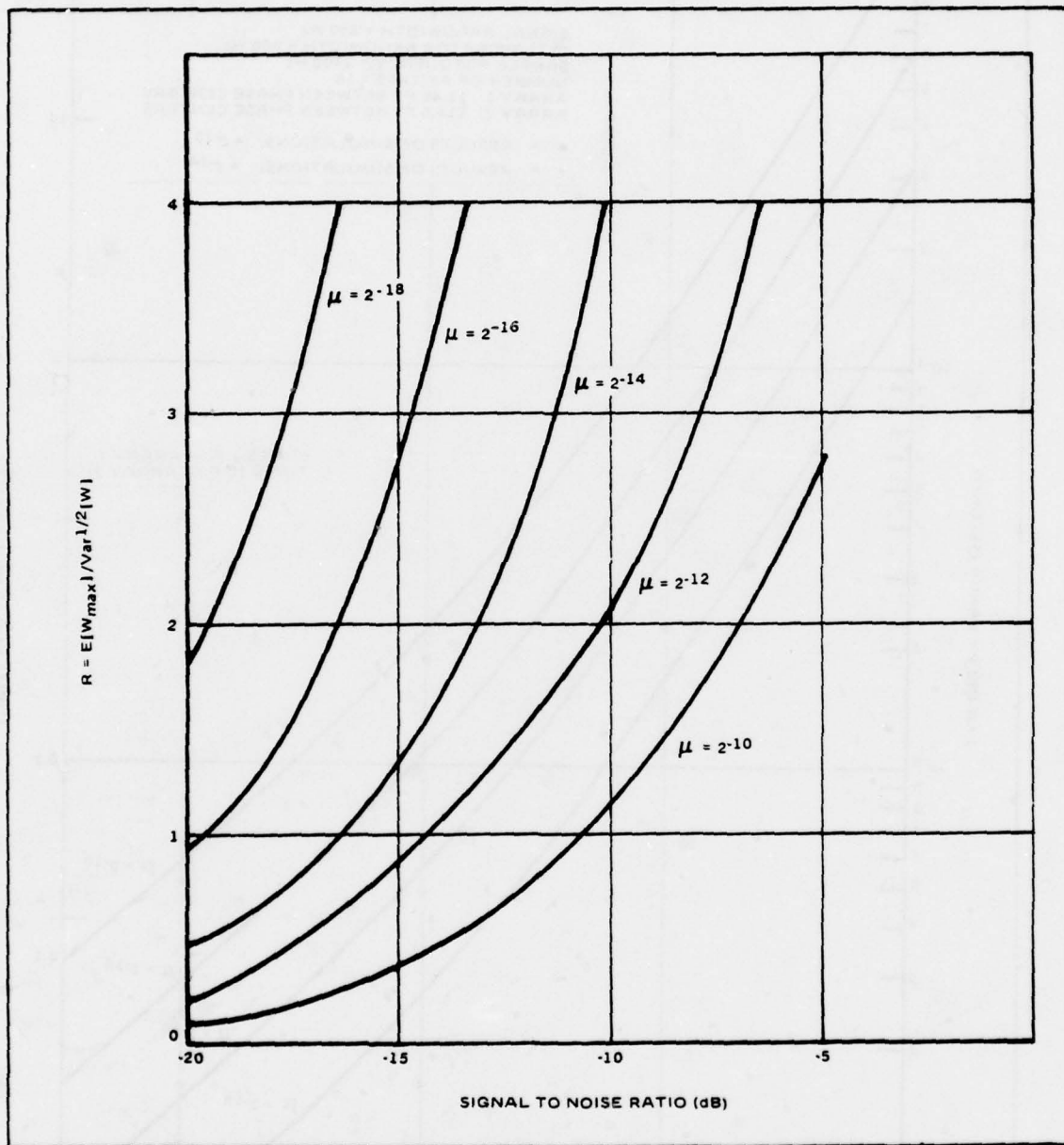
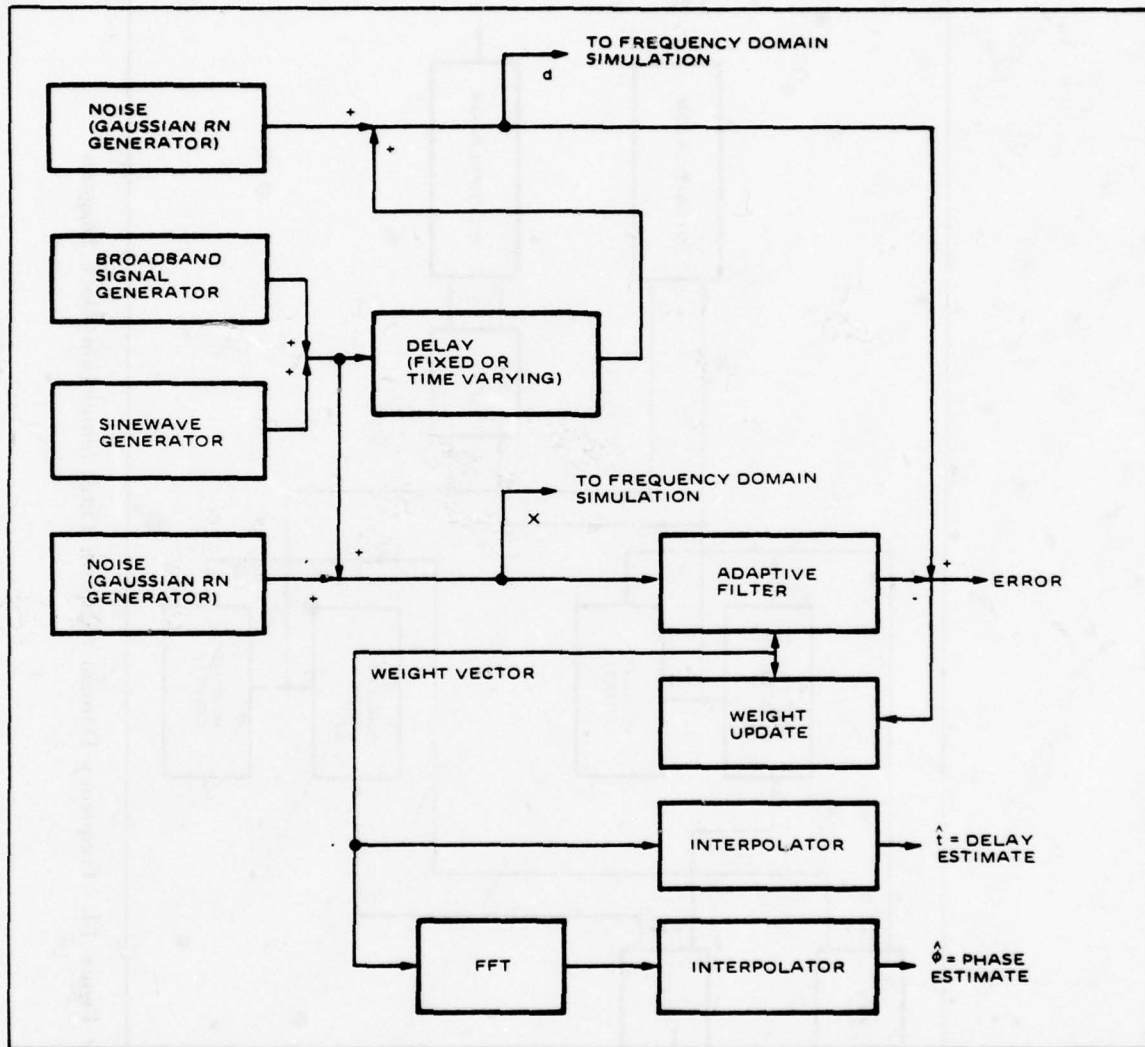


Figure 11. Bearing and Time Estimation Error for Adaptive Tracker with Sine Interpolator



81156-12

Figure 12. Ratio of Weight Mean to Weight Standard Deviation for Use in Setting μ for Adaptive Tracker



81156-13

Figure -13. Time Domain Adaptive Tracker Simulation Block Diagram

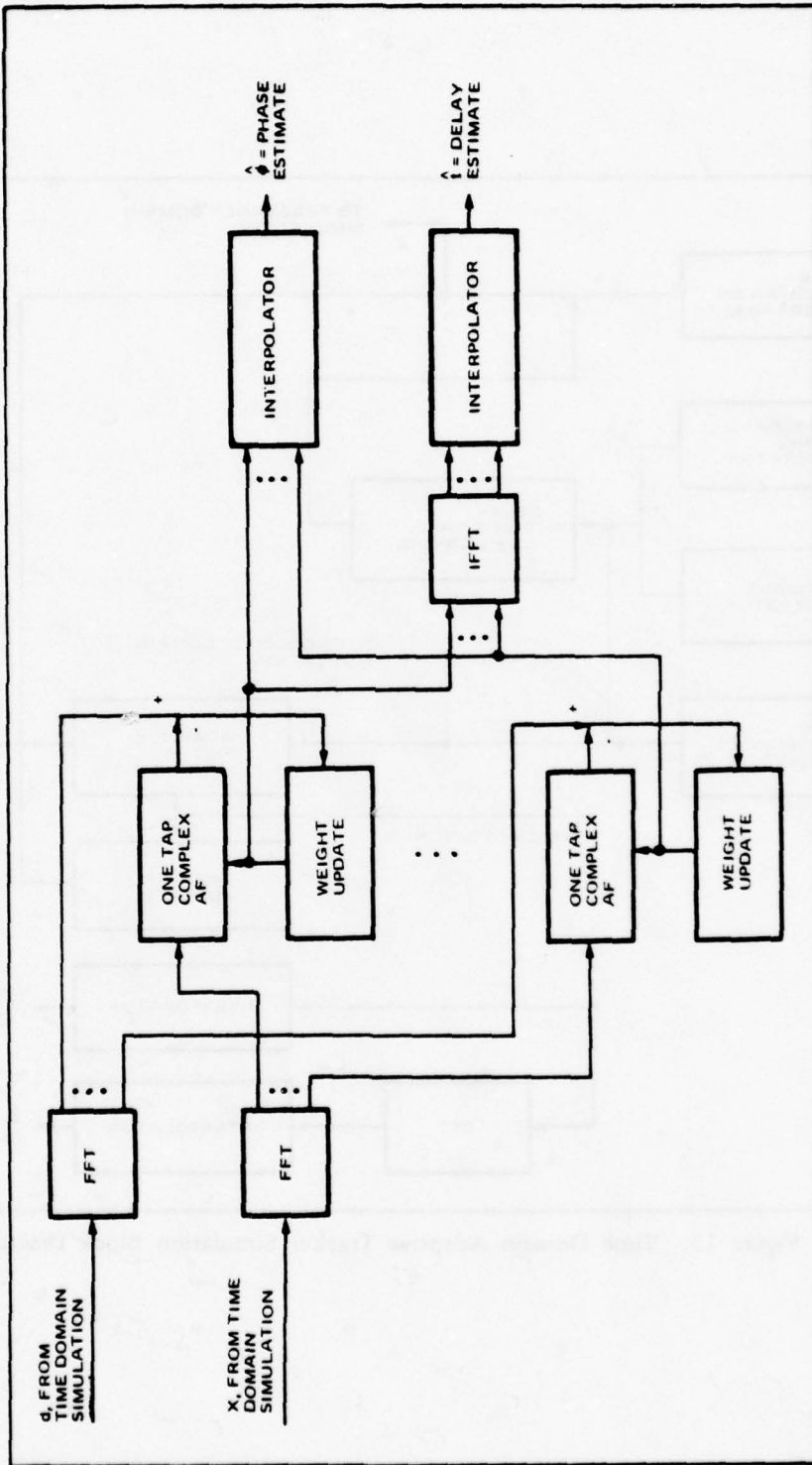


Figure 14. Frequency Domain Adaptive Filter Simulation Block Diagram

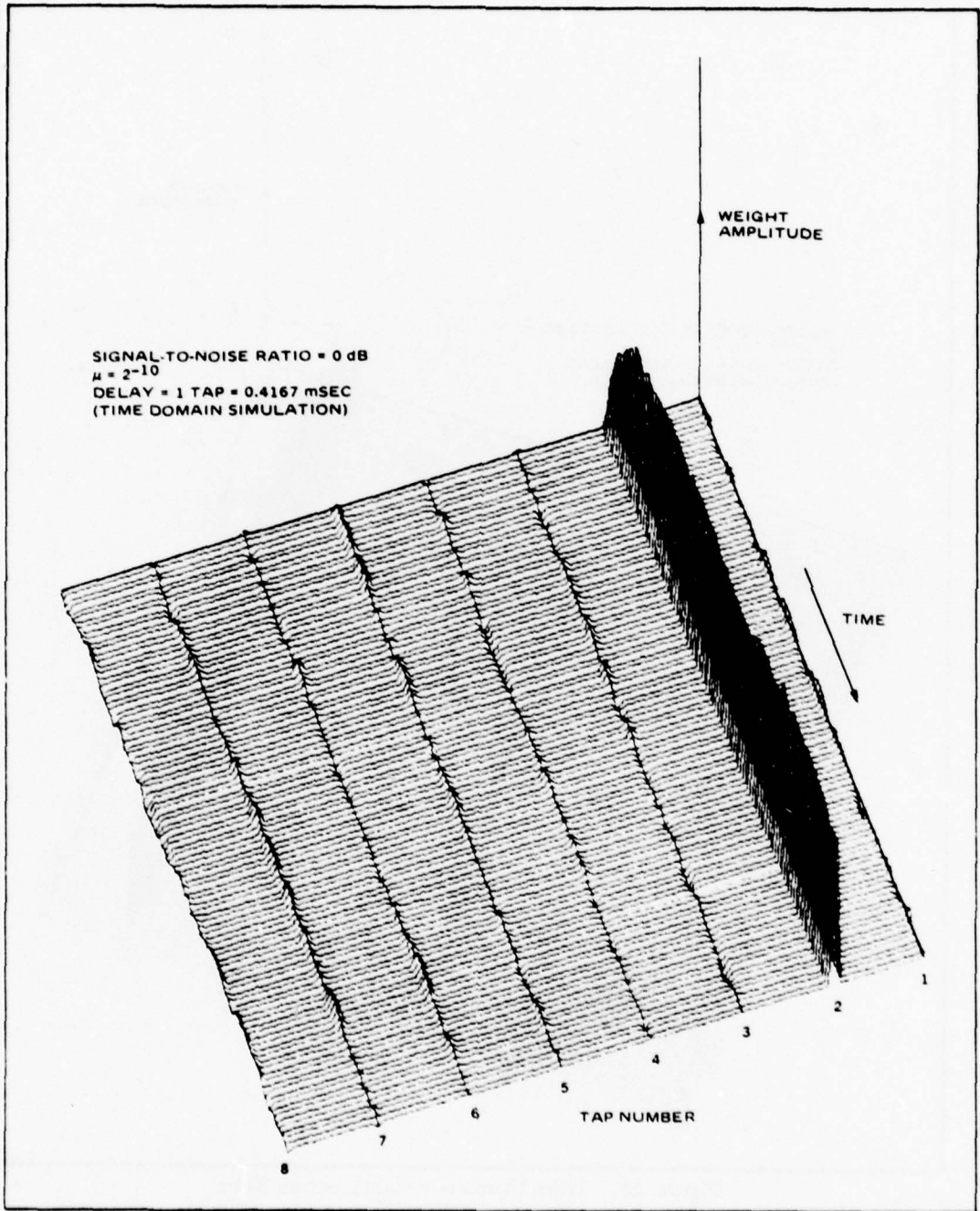


Figure 15. Time Domain Weights versus Time

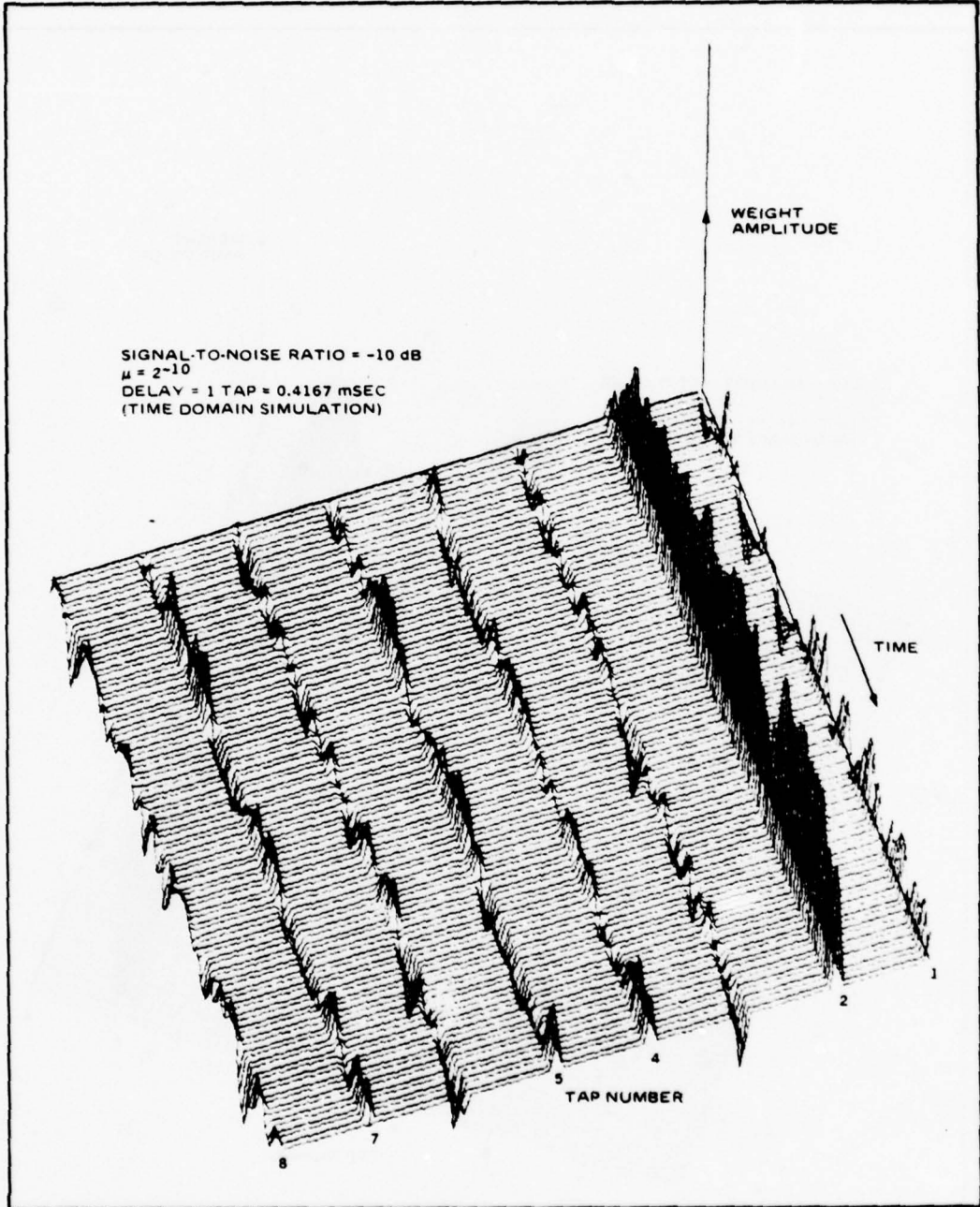


Figure 16. Time Domain Weights versus Time

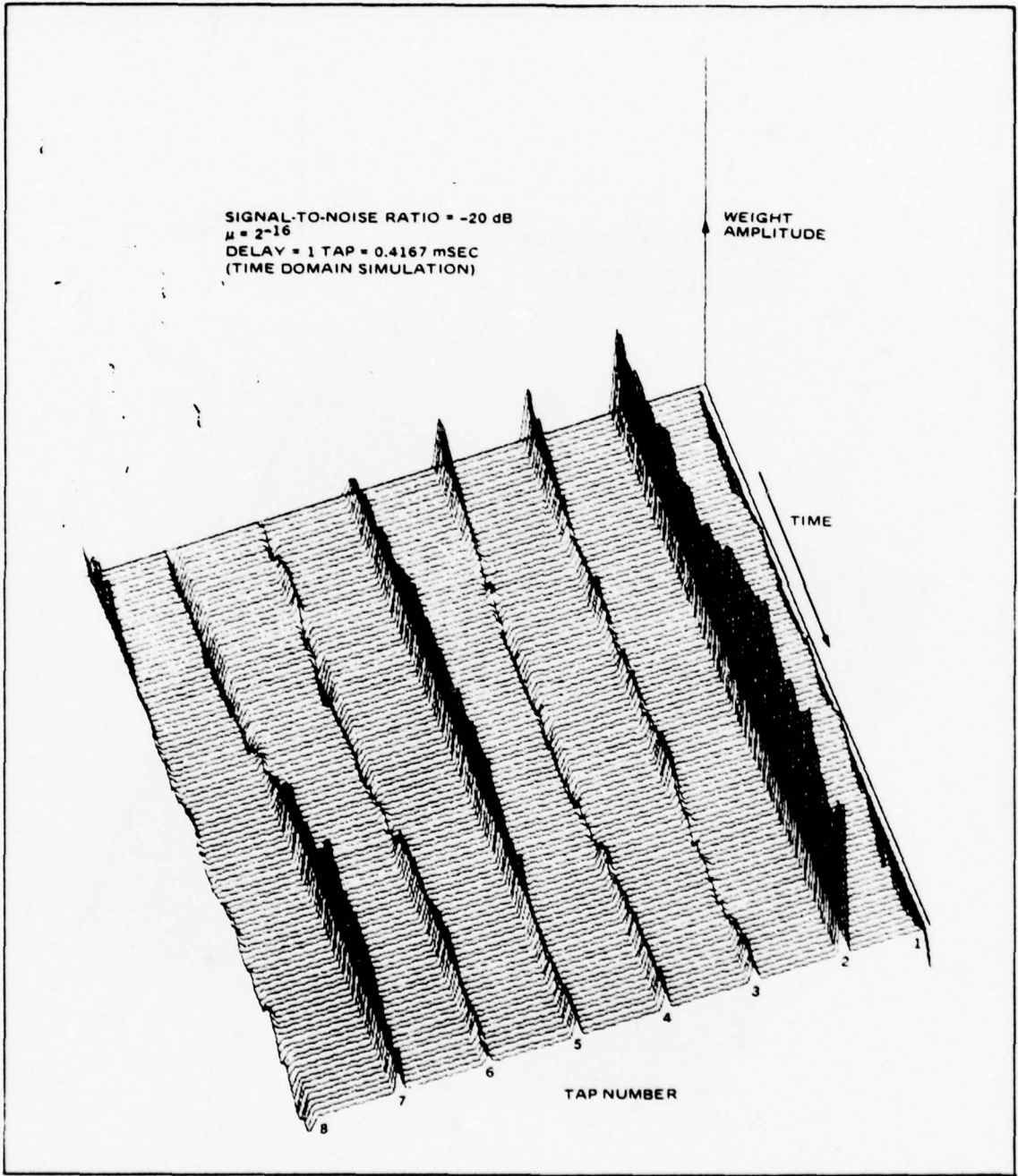


Figure 17. Time Domain Weights versus Time

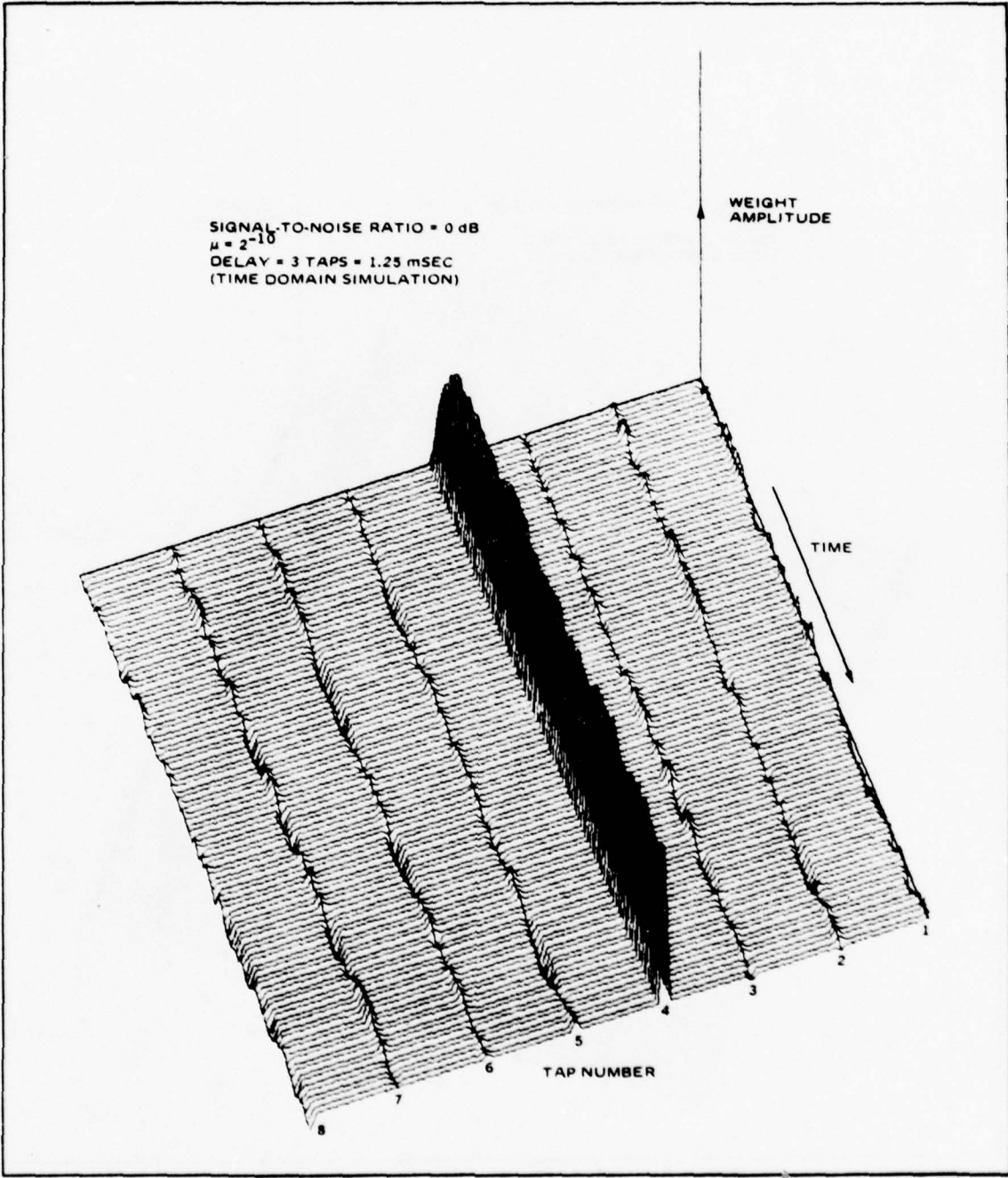


Figure 18. Time Domain Weights versus Time

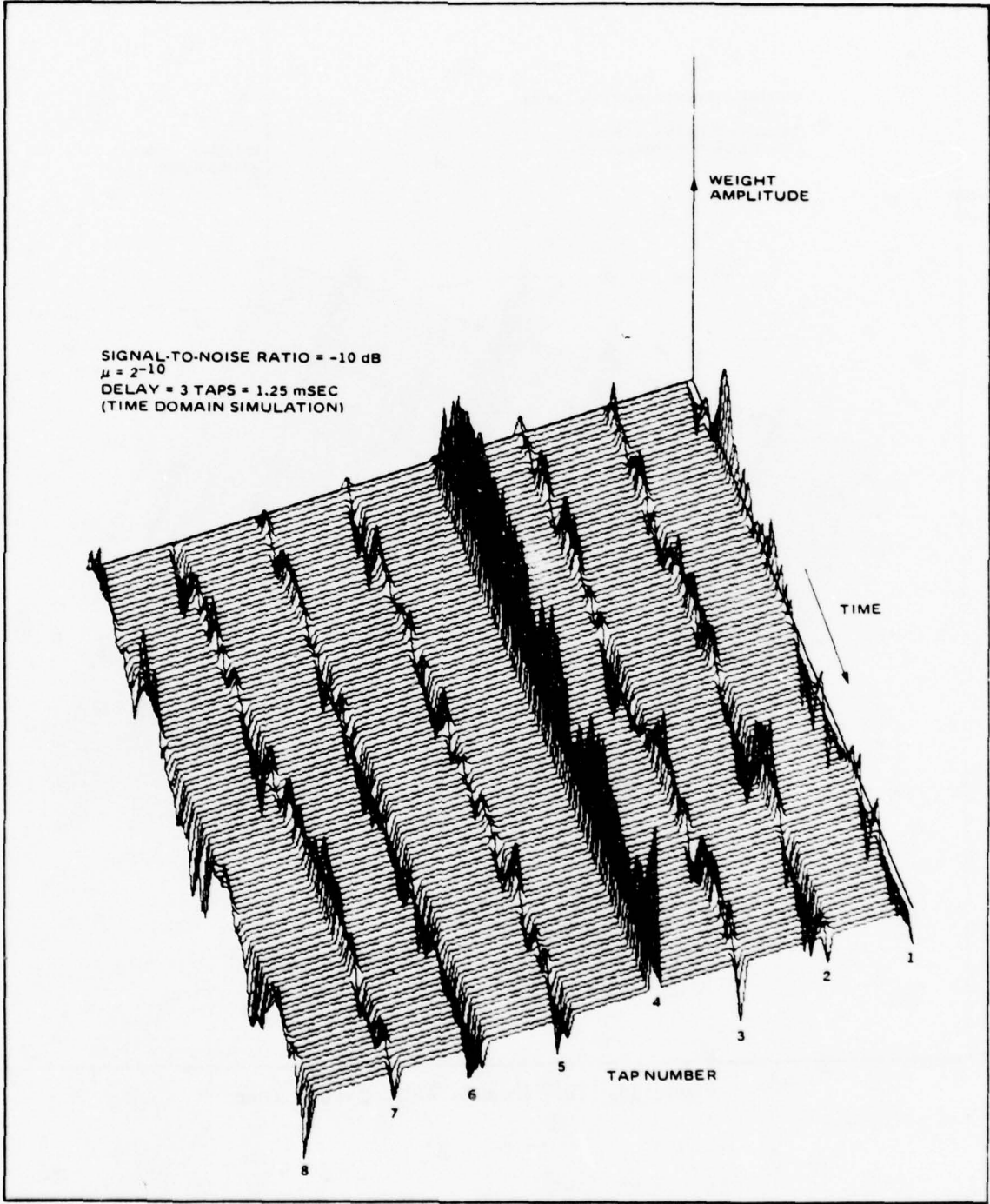


Figure 19. Time Domain Weights versus Time

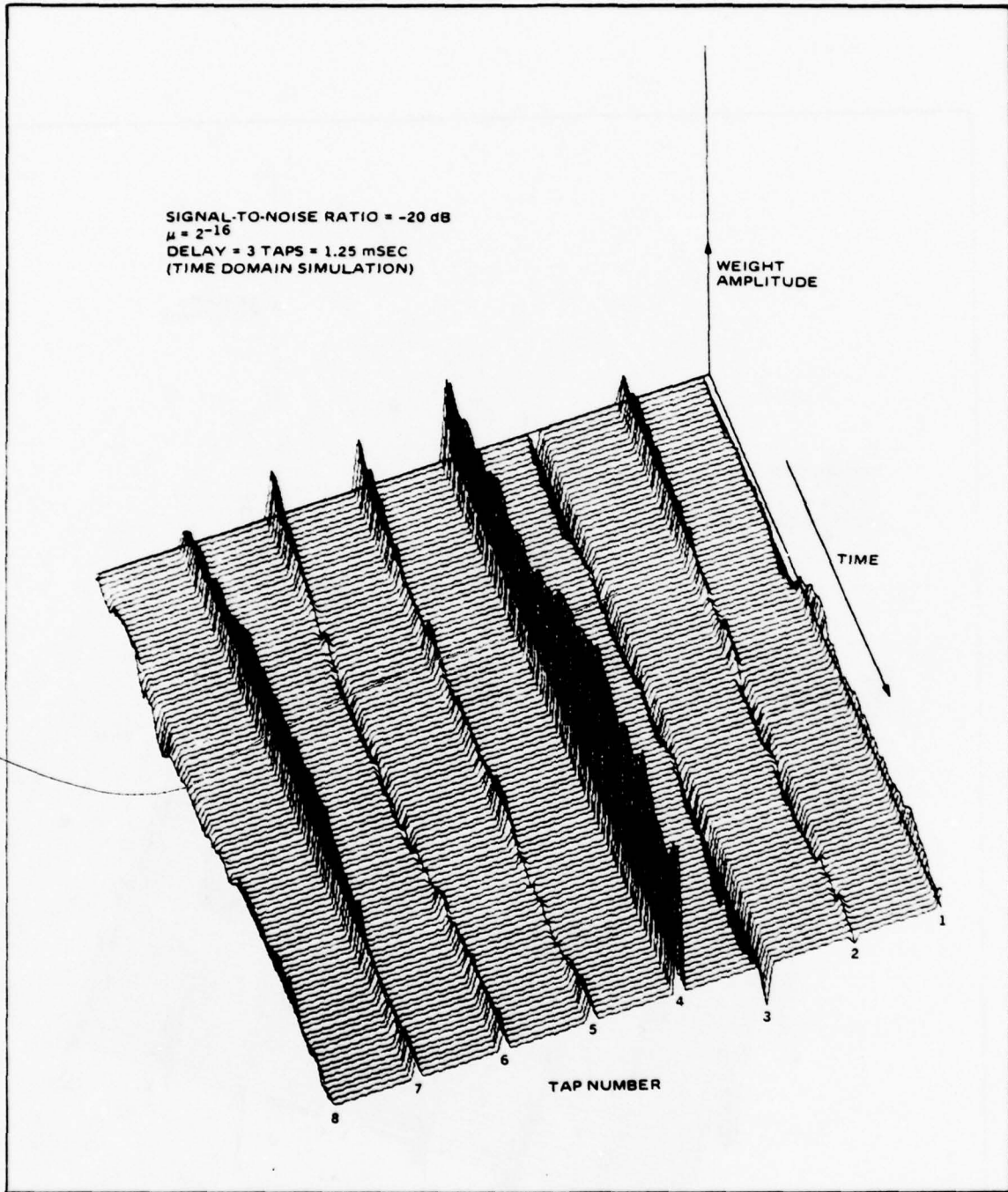


Figure 20. Time Domain Weights versus Time

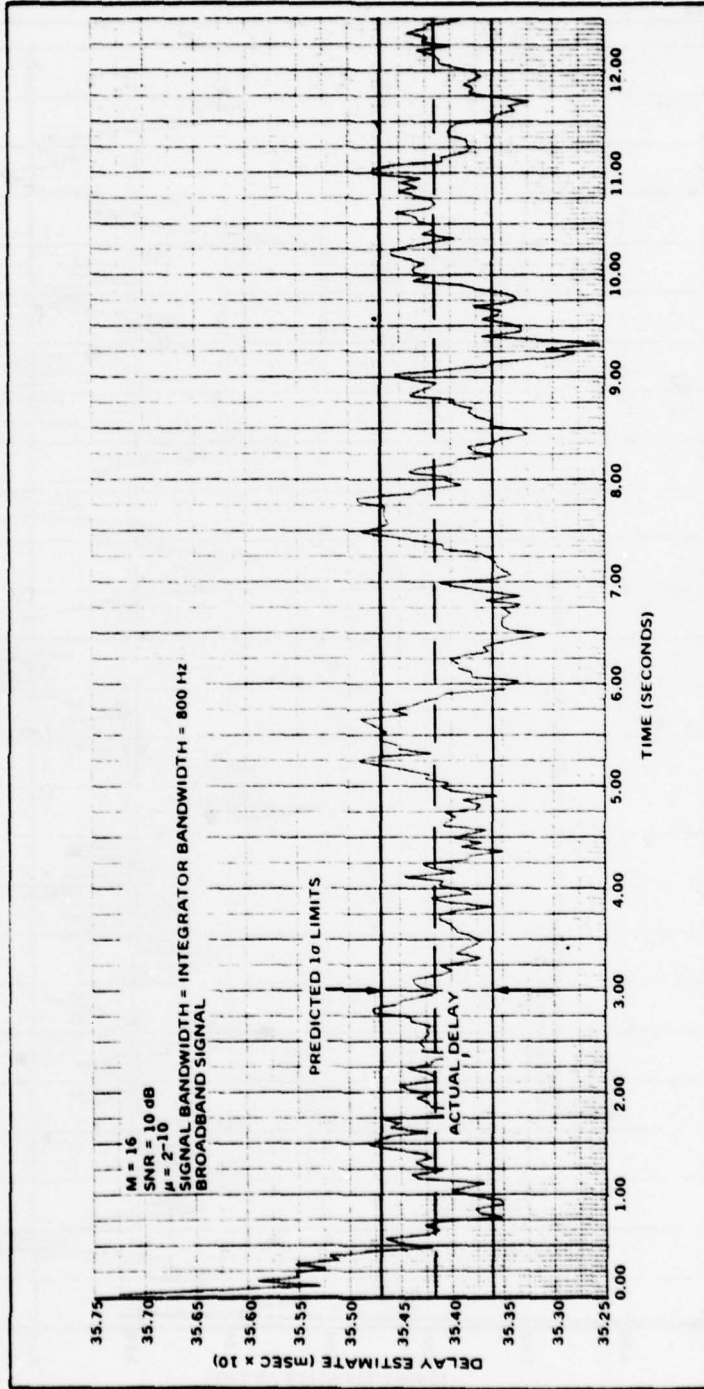


Figure 21. Delay Estimate versus Time (Actual Delay = 3.541667 mSEC)

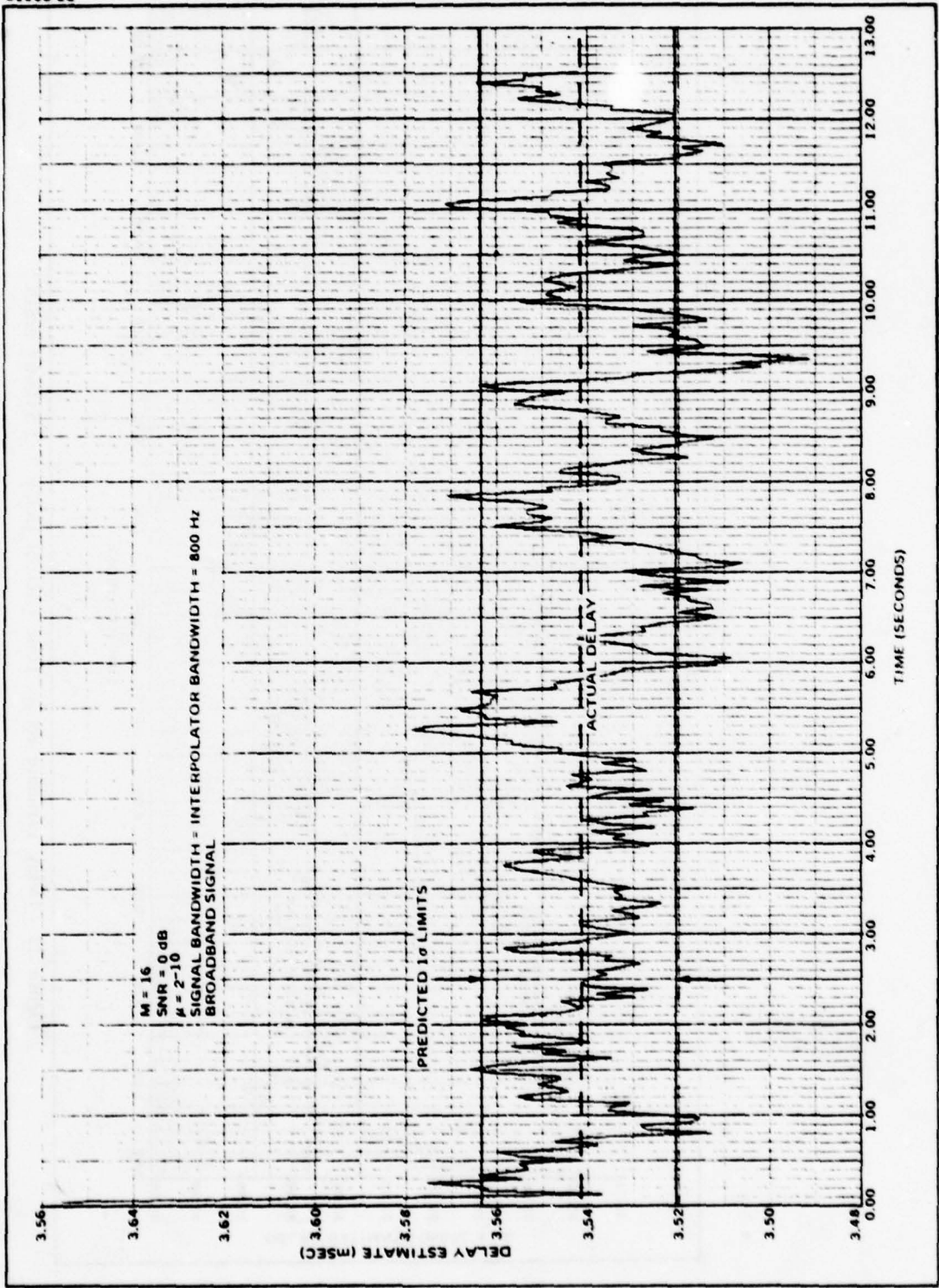


Figure 22. Delay Estimate versus Time (Actual Delay = 3.541667 msec)

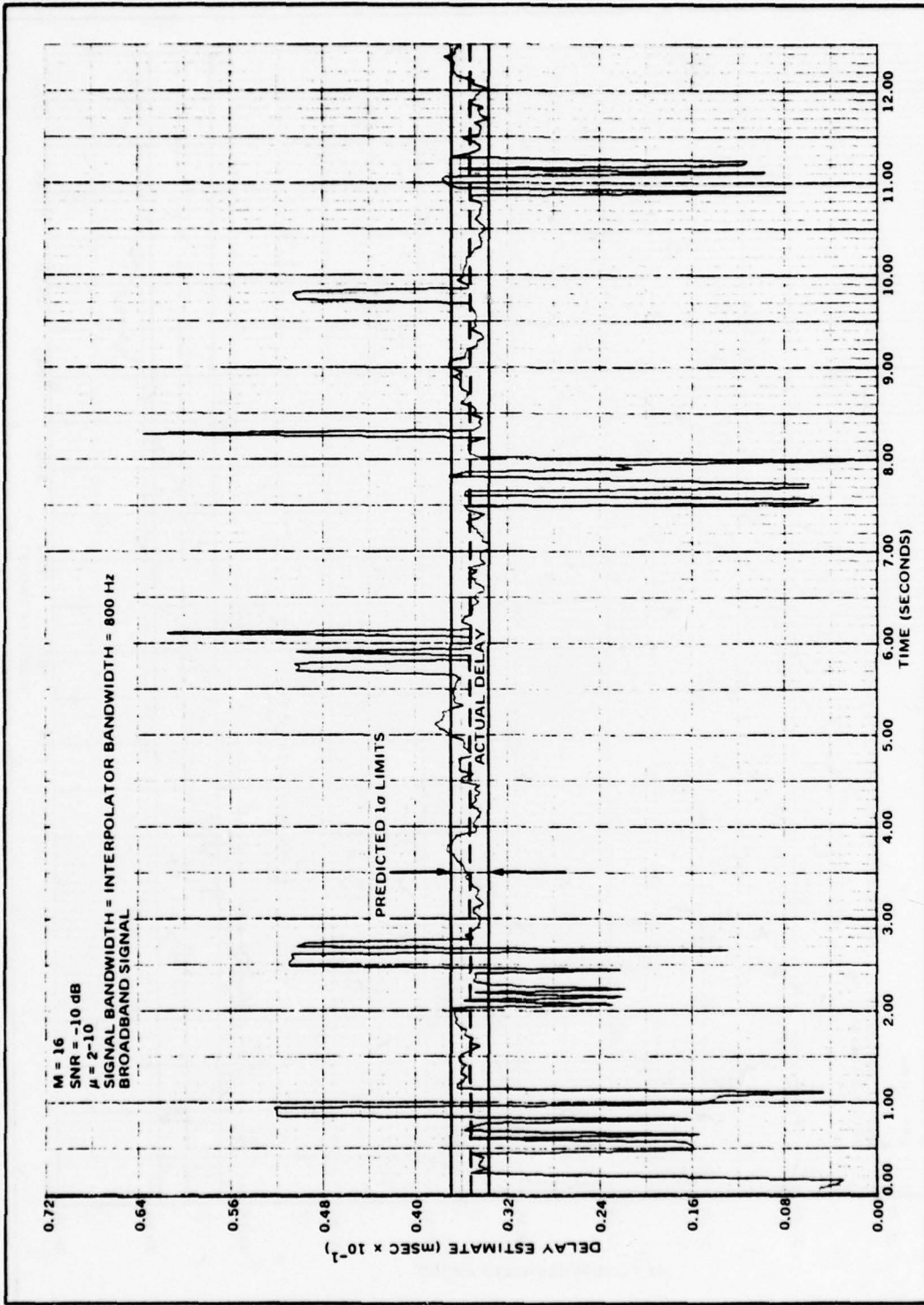


Figure 23. Delay Estimate versus Time (Actual Delay = 3.541667 msec)

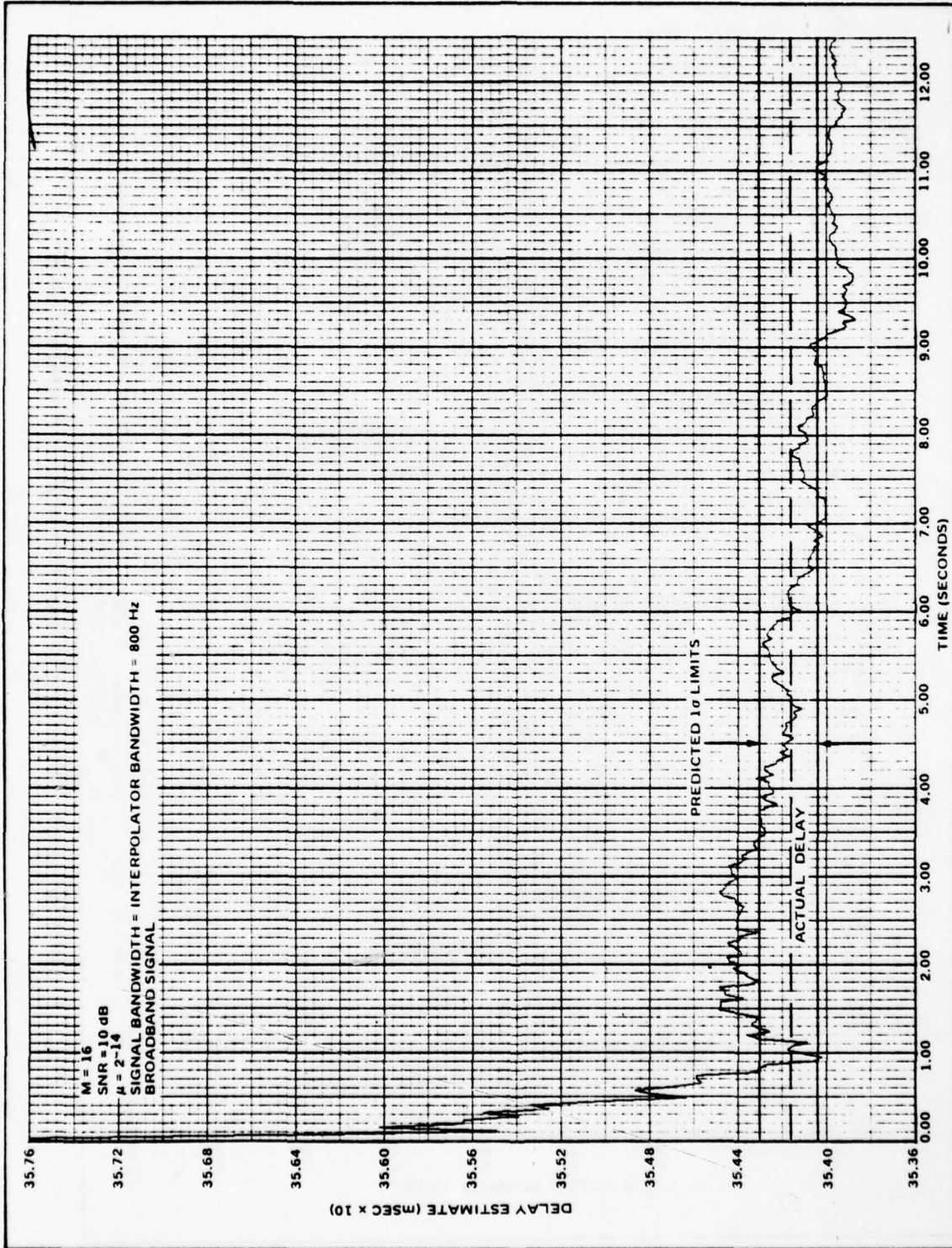


Figure 24. Delay Estimate versus Time (Actual Delay = 3.541667 mSEC)

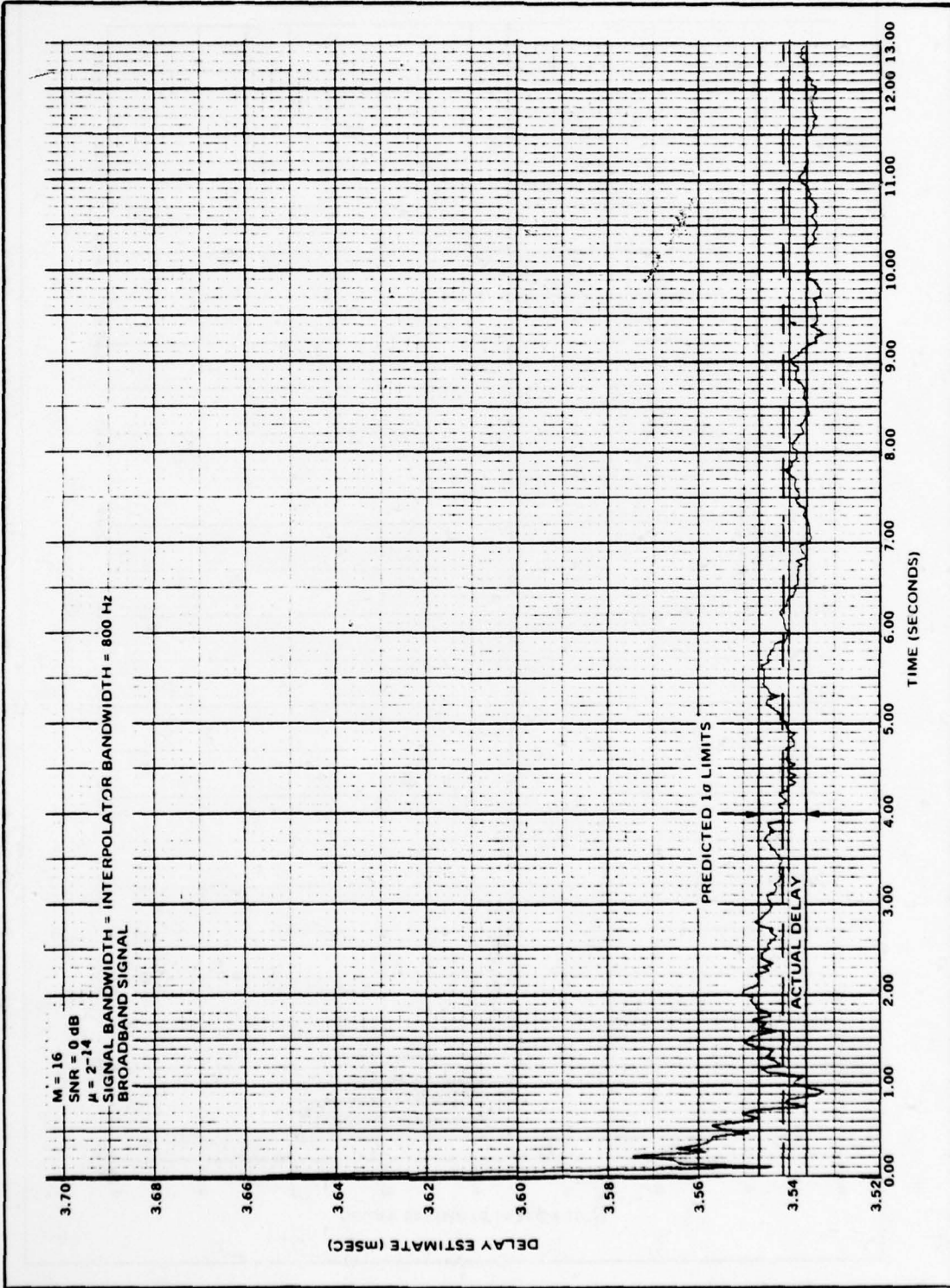


Figure 25. Delay Estimate versus Time (Actual Delay = 3.541667 mSEC)

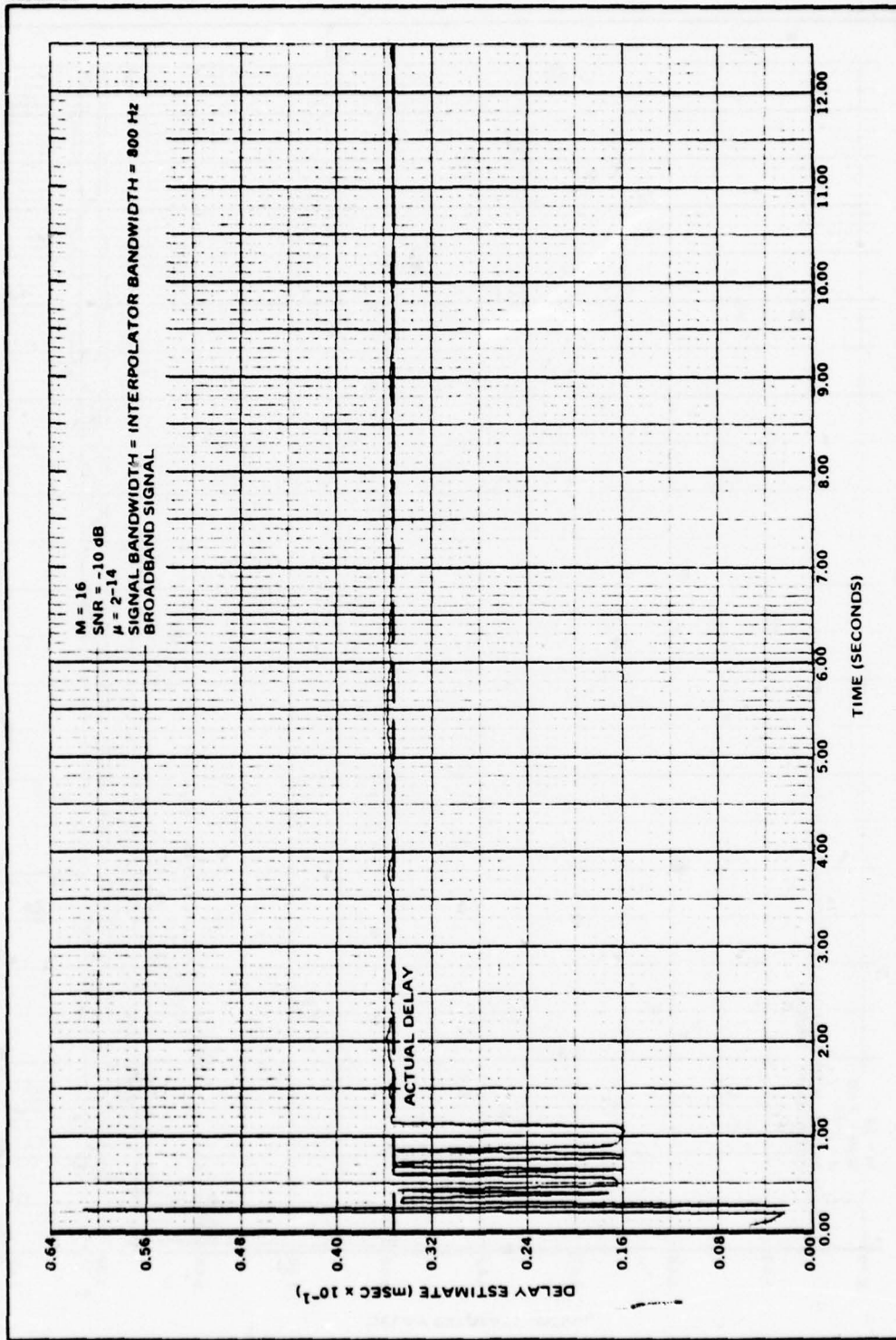


Figure 26. Delay Estimate versus Time (Actual Delay = 3.541667 mSEC)

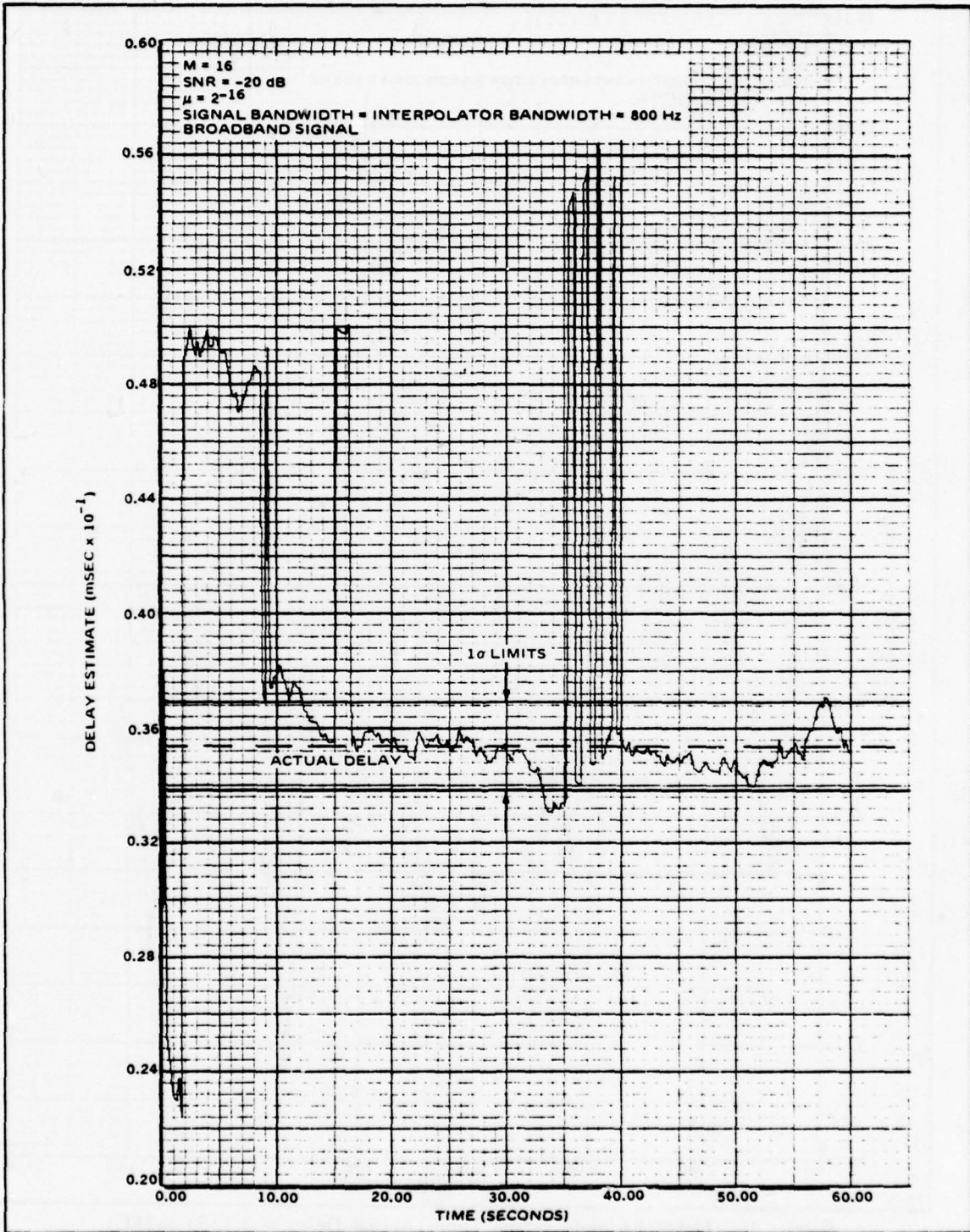


Figure 27. Delay Estimate versus Time (Actual Delay = 3.541667 mSEC)

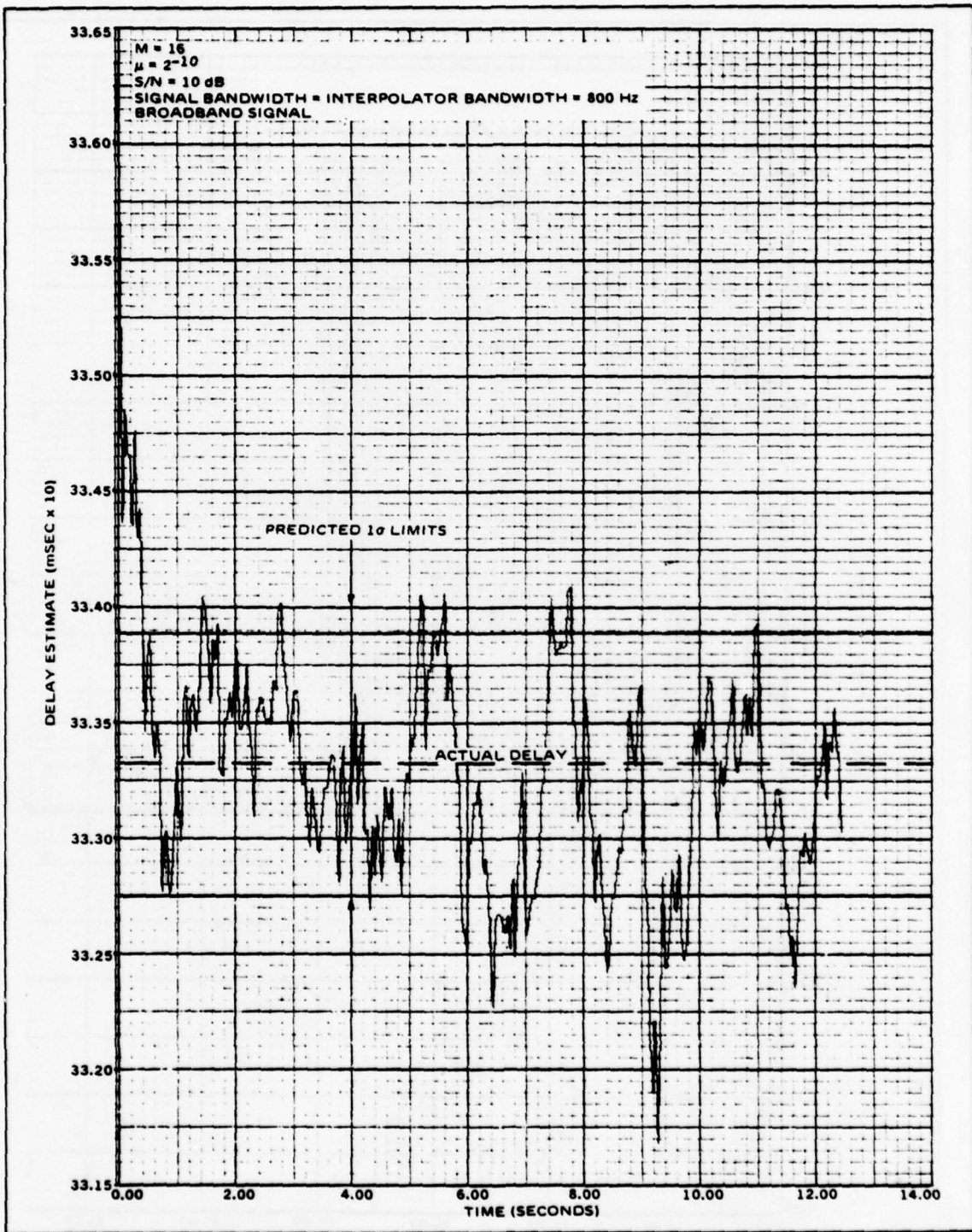


Figure 28. Delay Estimate versus Time (Actual Delay = 3.3333 mSEC)

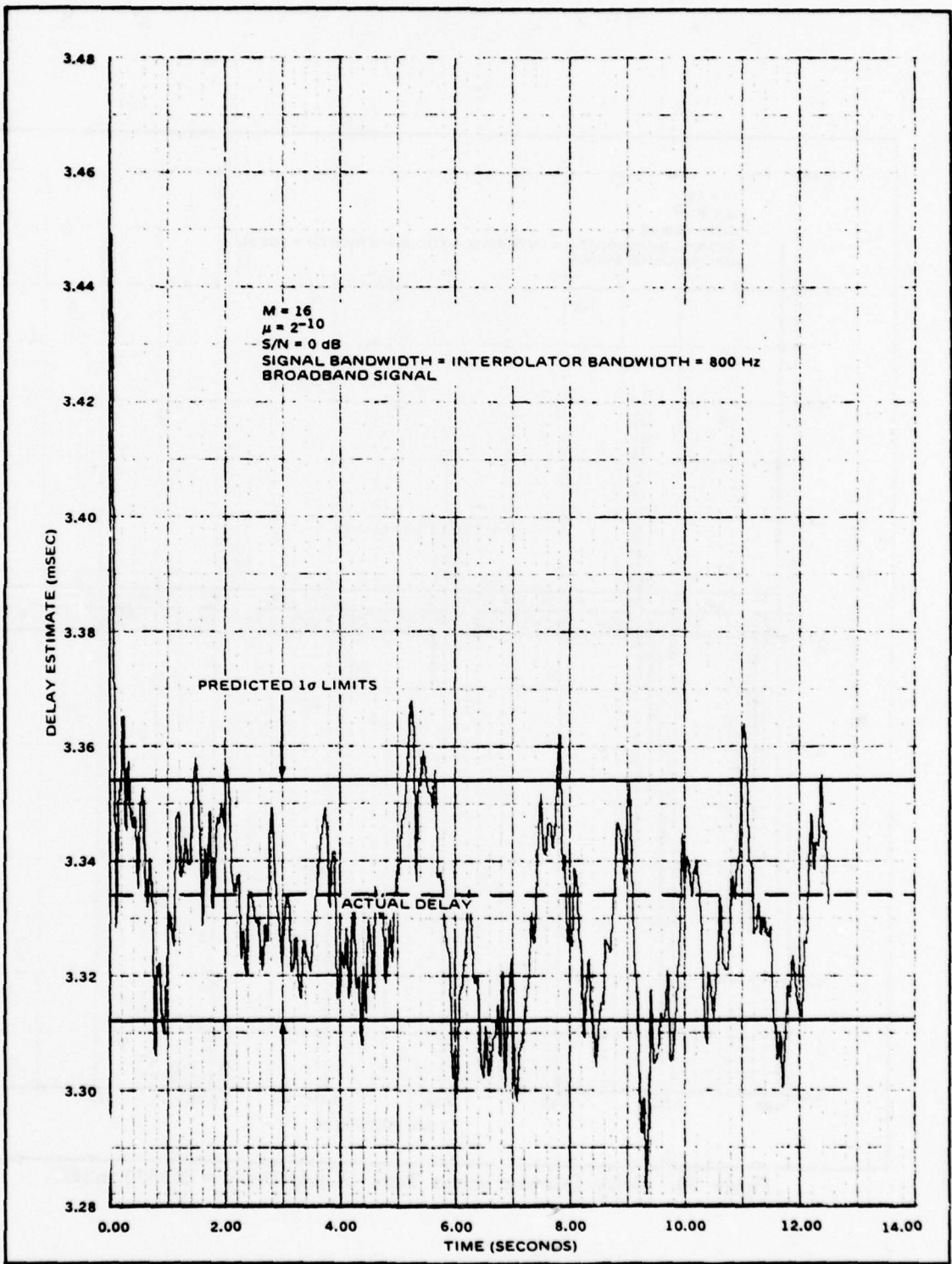


Figure 29. Delay Estimate versus Time (Actual Delay = 3.333 mSEC)

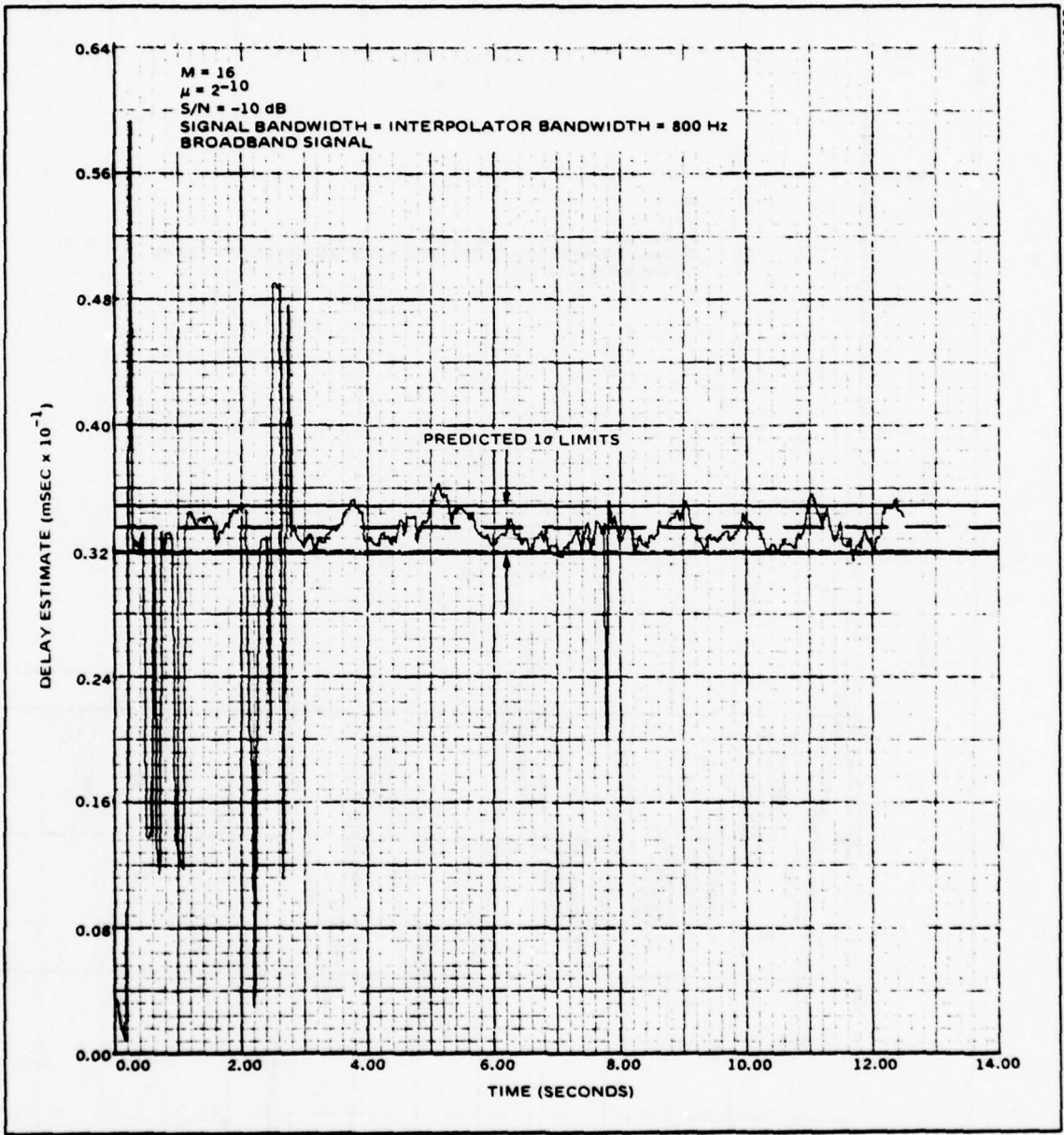


Figure 30. Delay Estimate versus Time (Actual Delay = 3.3333 mSEC)

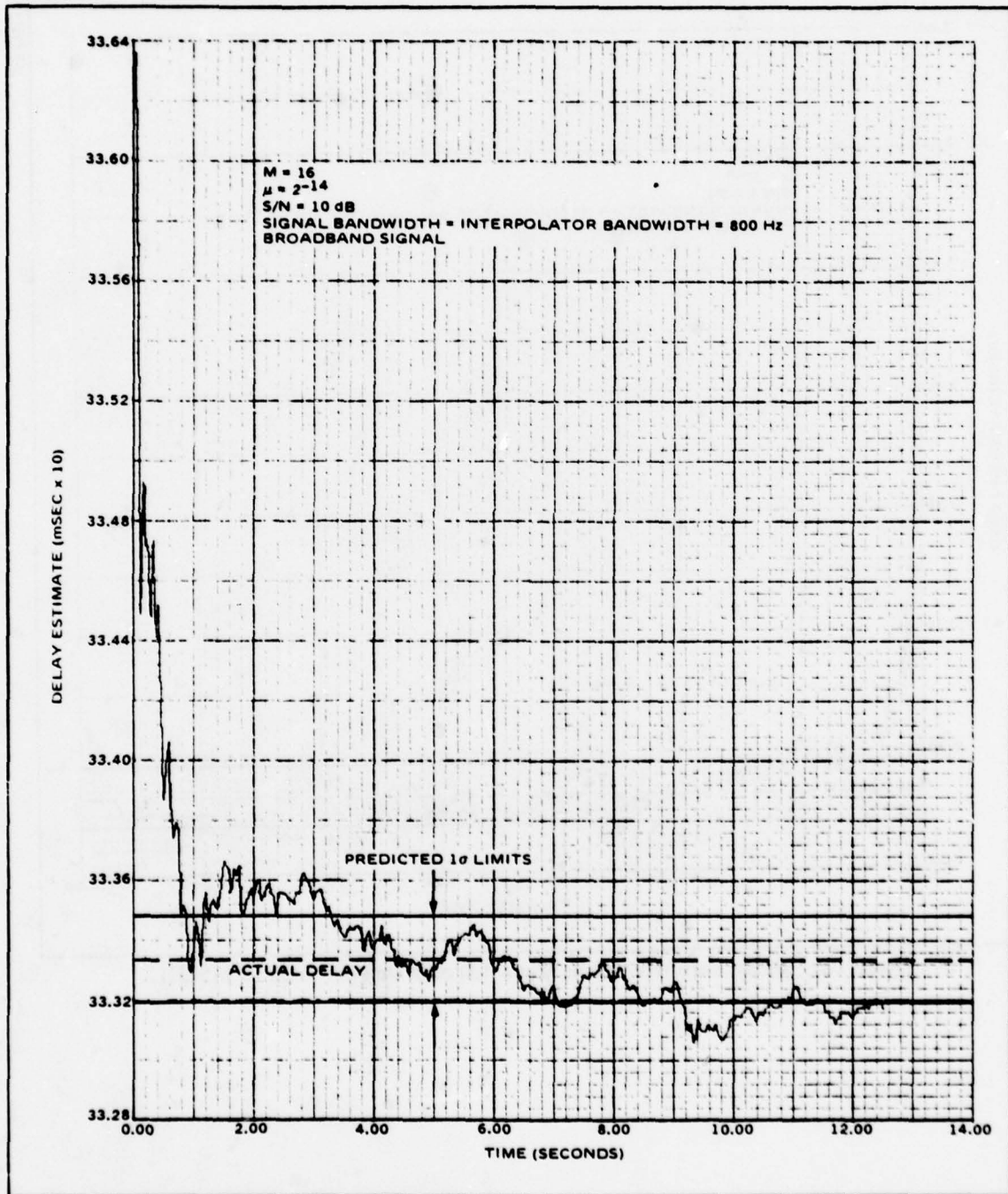


Figure 31. Delay Estimate versus Time (Actual Delay = 3.3333 mSEC)

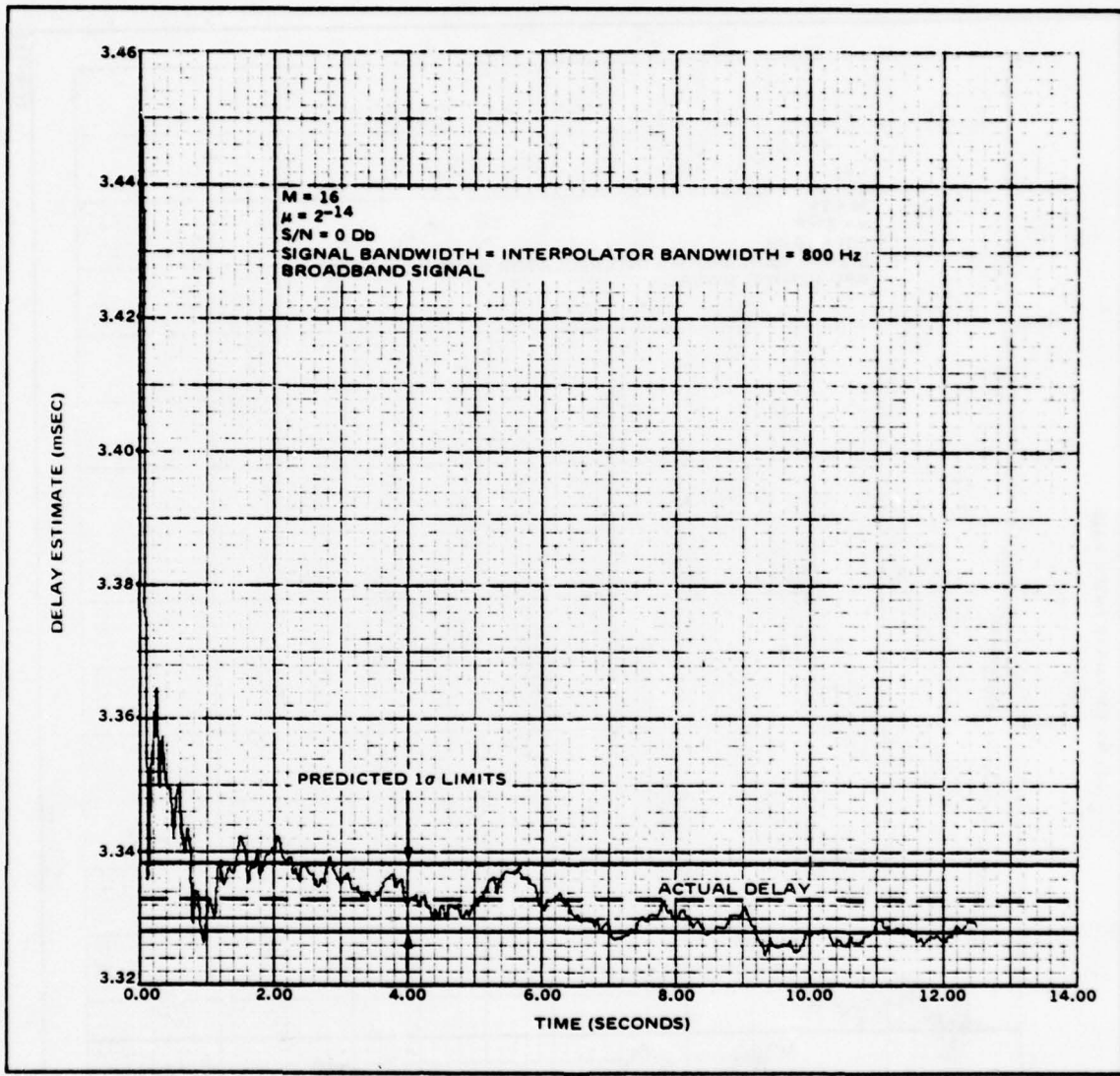


Figure 32. Delay Estimate versus Time (Actual Delay = 3.3333 mSEC)

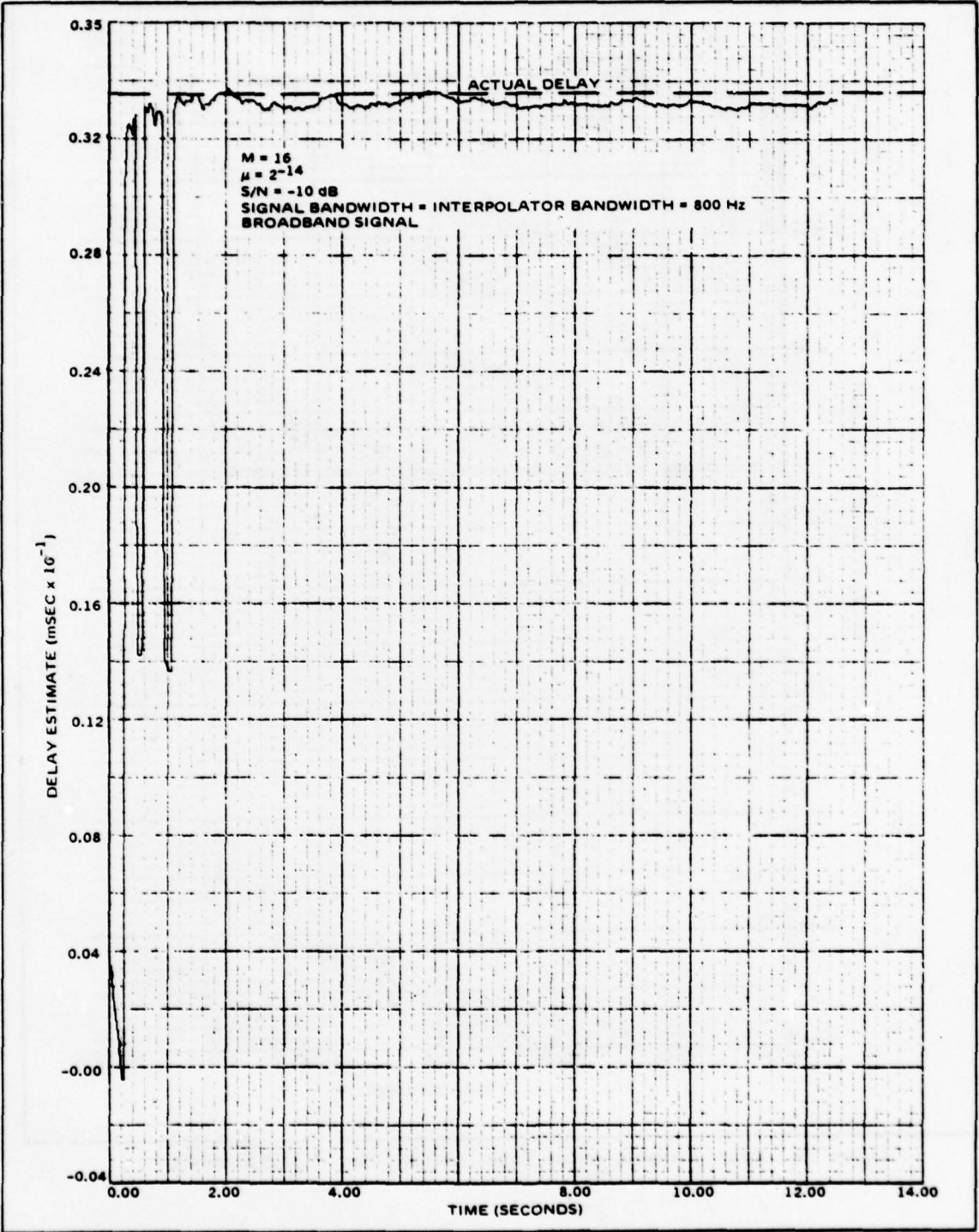


Figure 33. Delay Estimate versus Time (Actual Delay = 3.3333 mSEC)

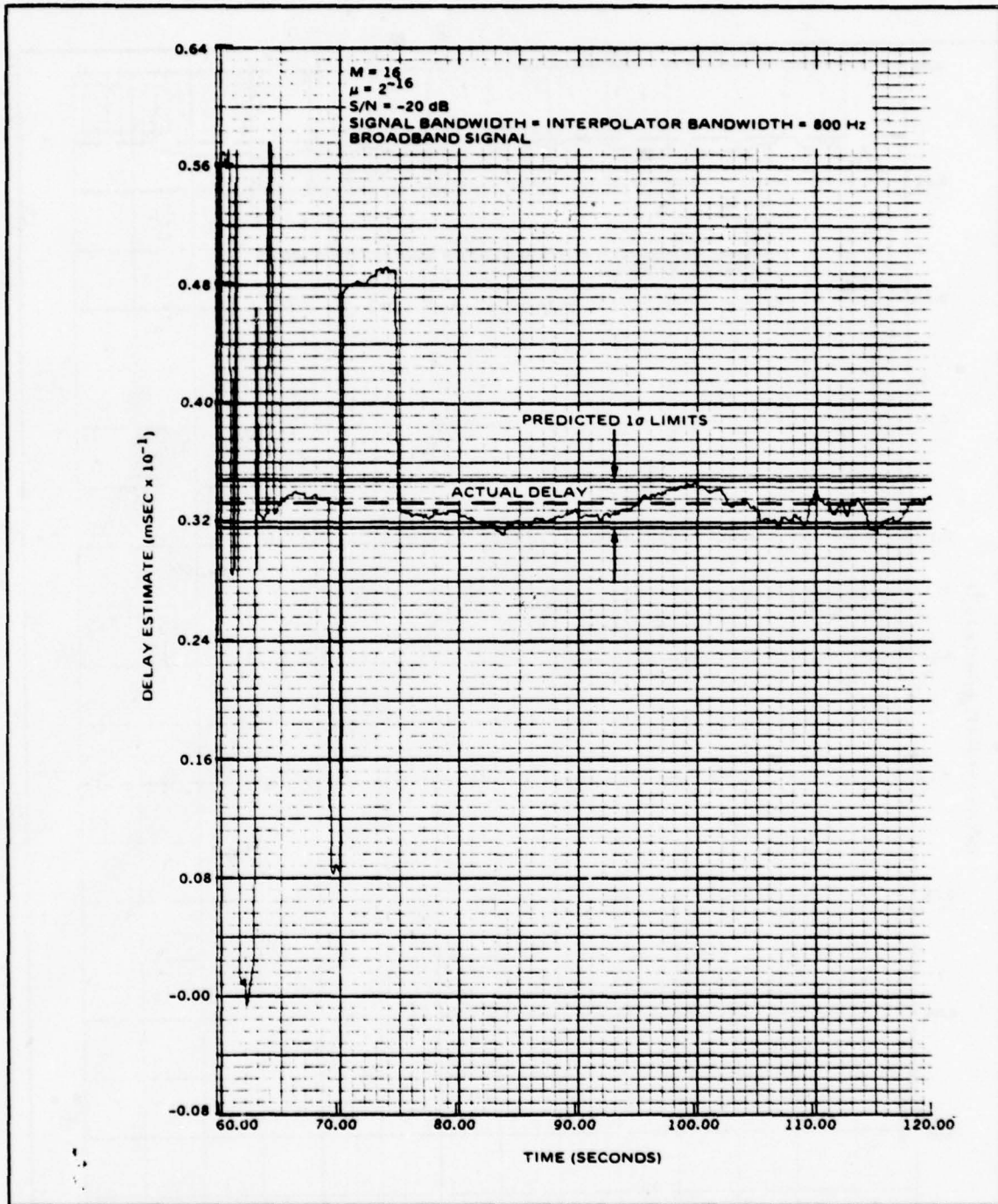
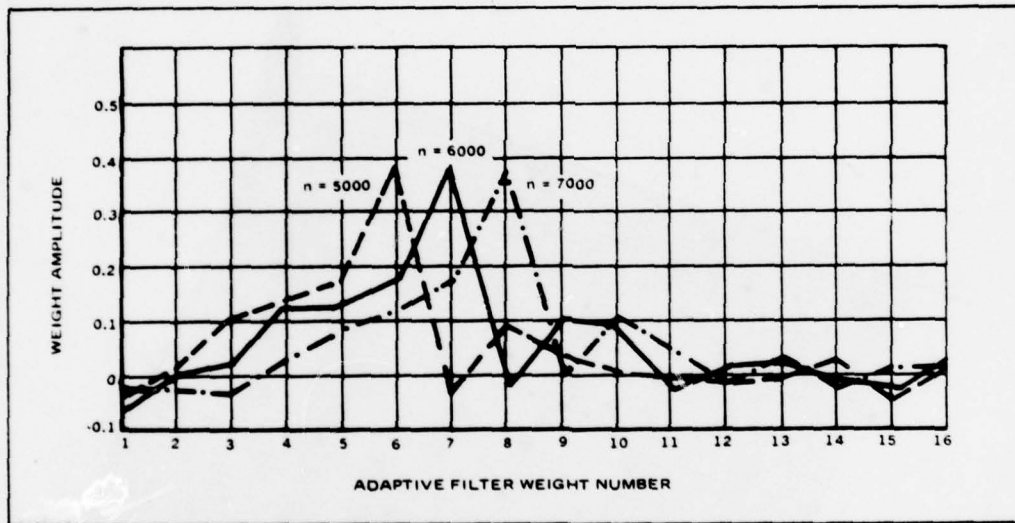
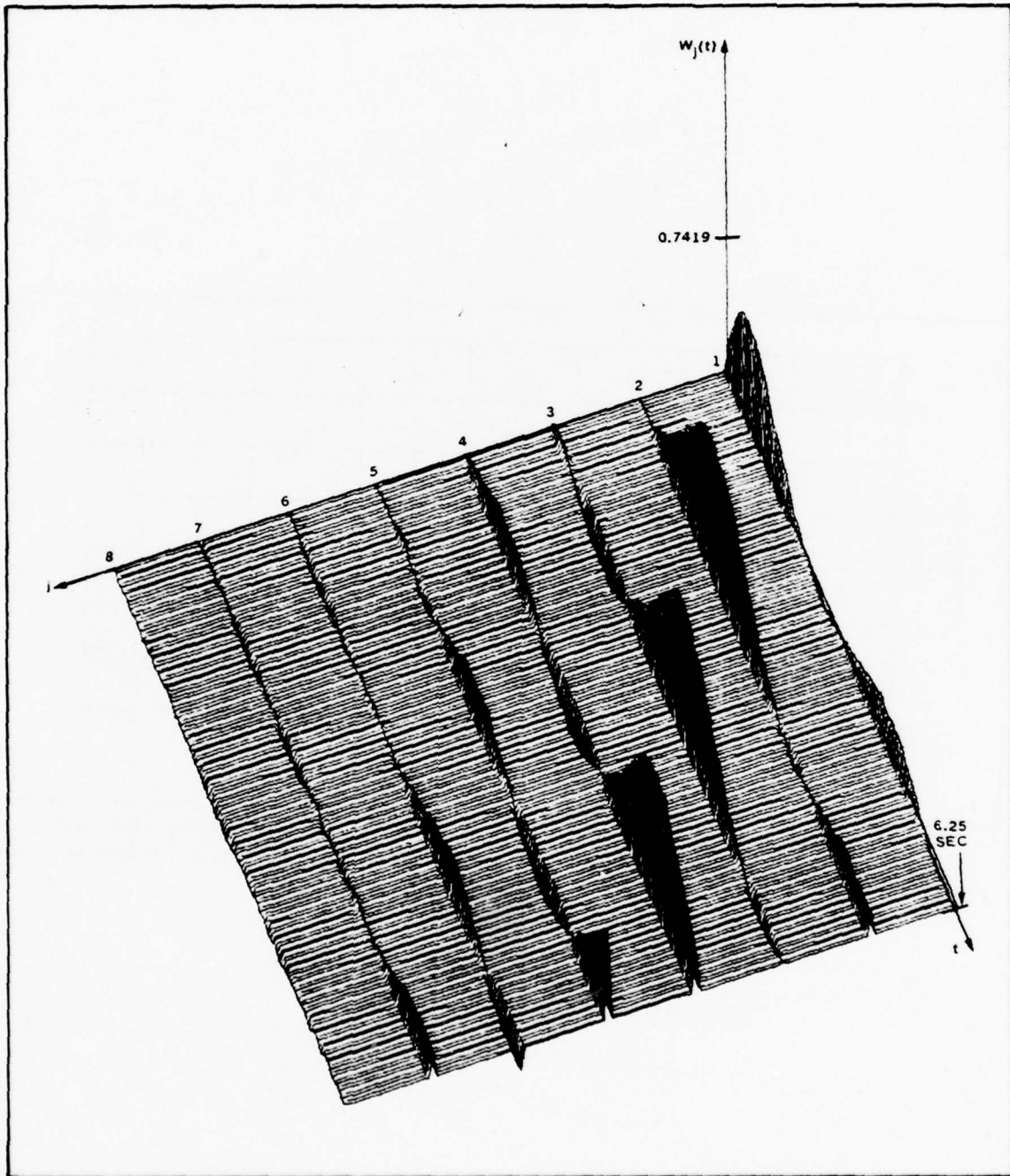


Figure 34. Delay Estimate versus Time (Actual Delay = 3.3333 mSEC)



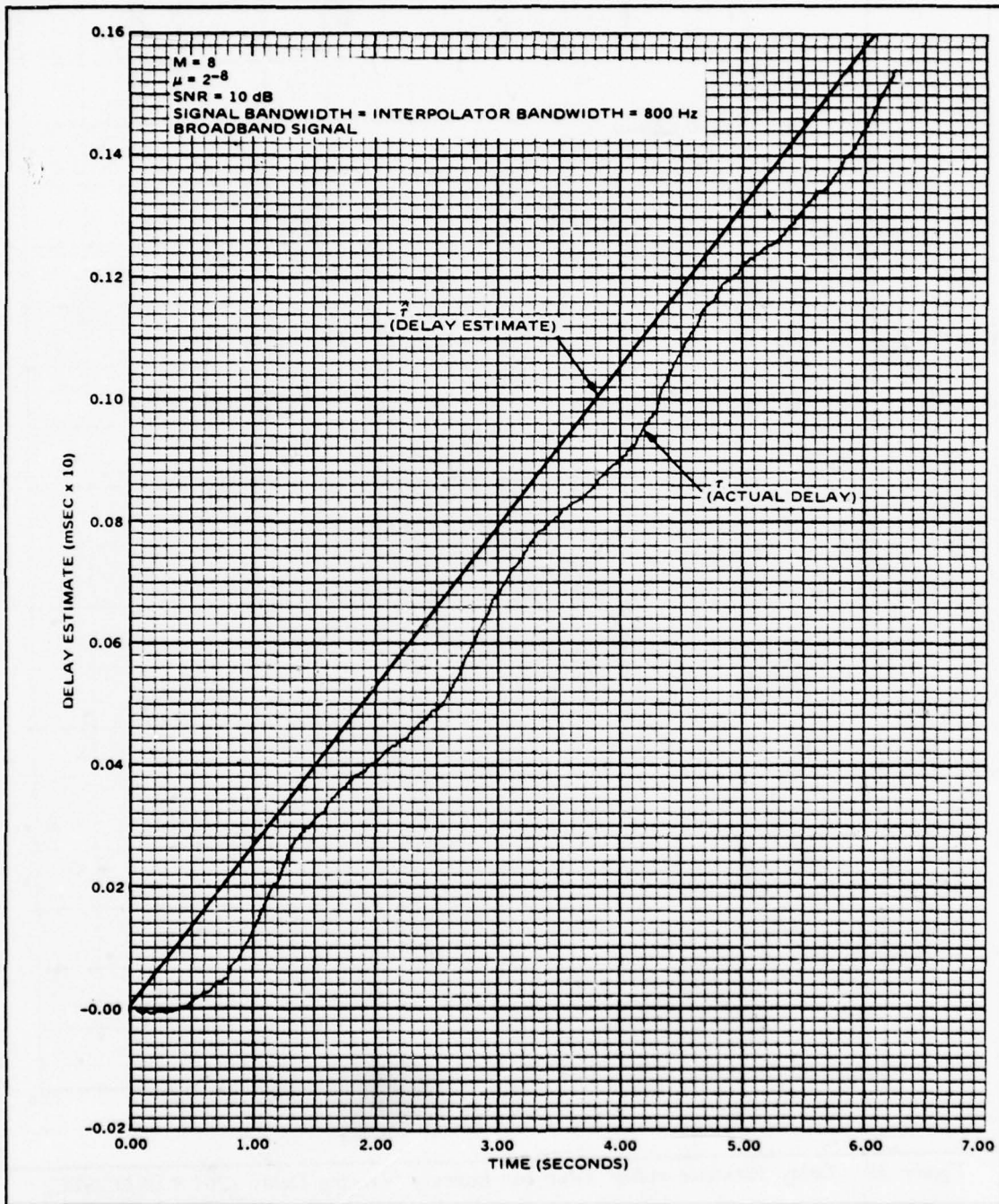
81156-35

Figure 35. Weight Vector as a Function of Time (n) for Linearly Varying Delay and Broadband Input. M = No. of Taps = 16, SNR = 10 dB, $\mu = 2^{-10}$, C = 1.0 msec/sec



81156-36

Figure 36. Weight Vector versus Time for Linearly Varying Delay (Broadband Signal, 8 Tap Time Domain Adaptive Filter)



01156-37

Figure 37. Delay Estimate versus Time for Linearly Varying Delay (261.0 $\mu\text{SEC/SEC}$)

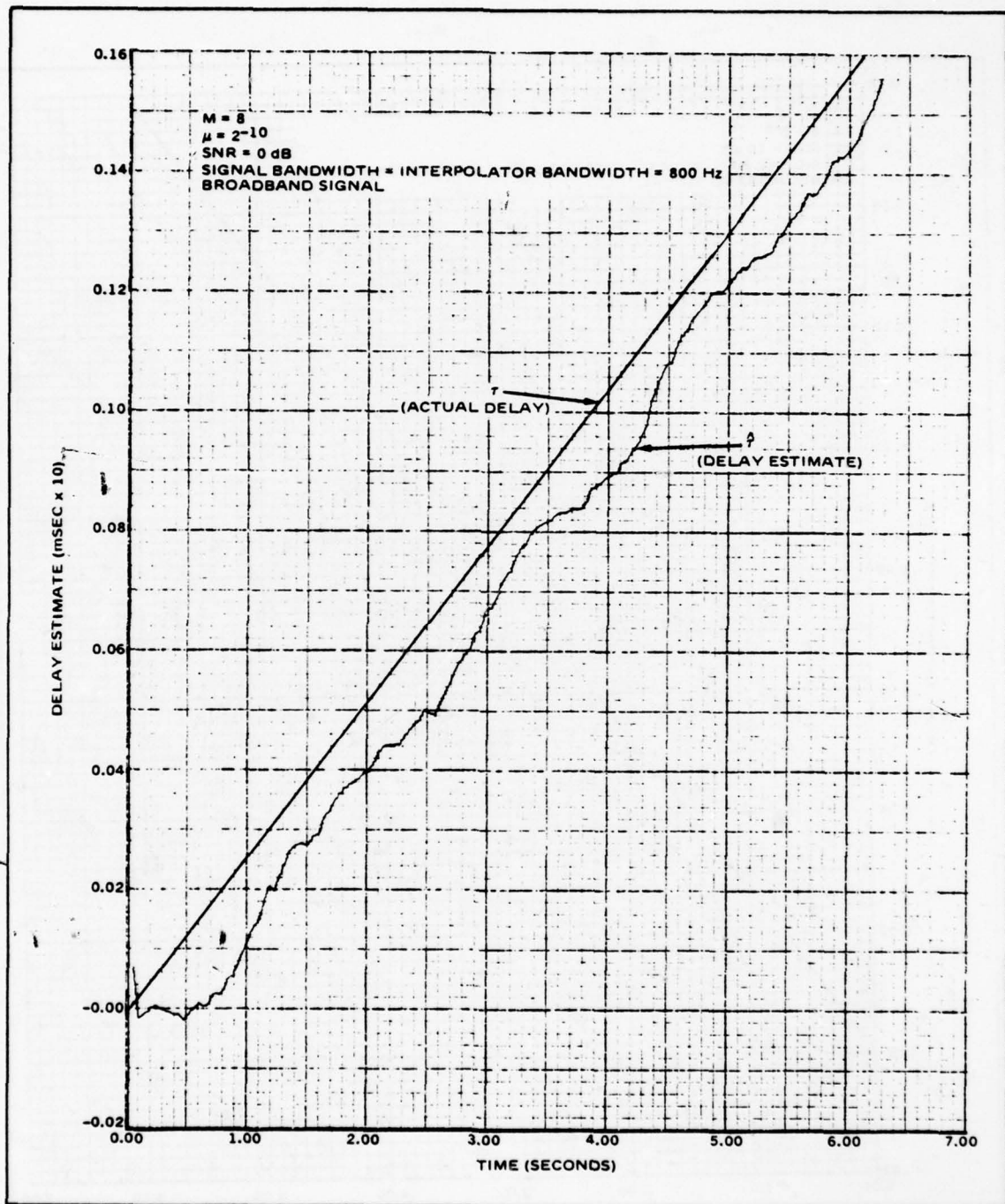


Figure 38. Delay Estimate versus Time for Linearly Varying Delay ($261.8 \mu\text{SEC/SEC}$)

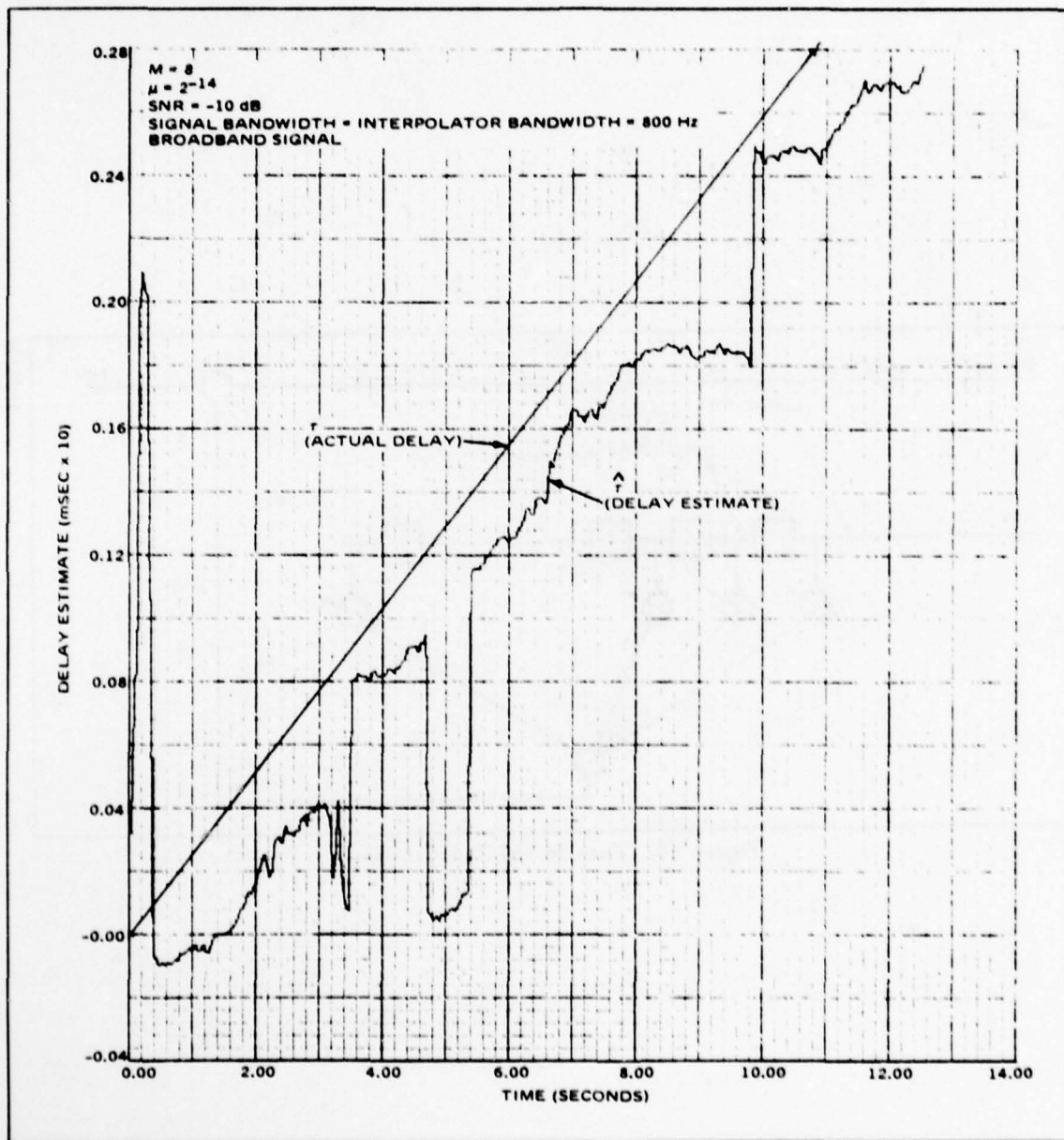
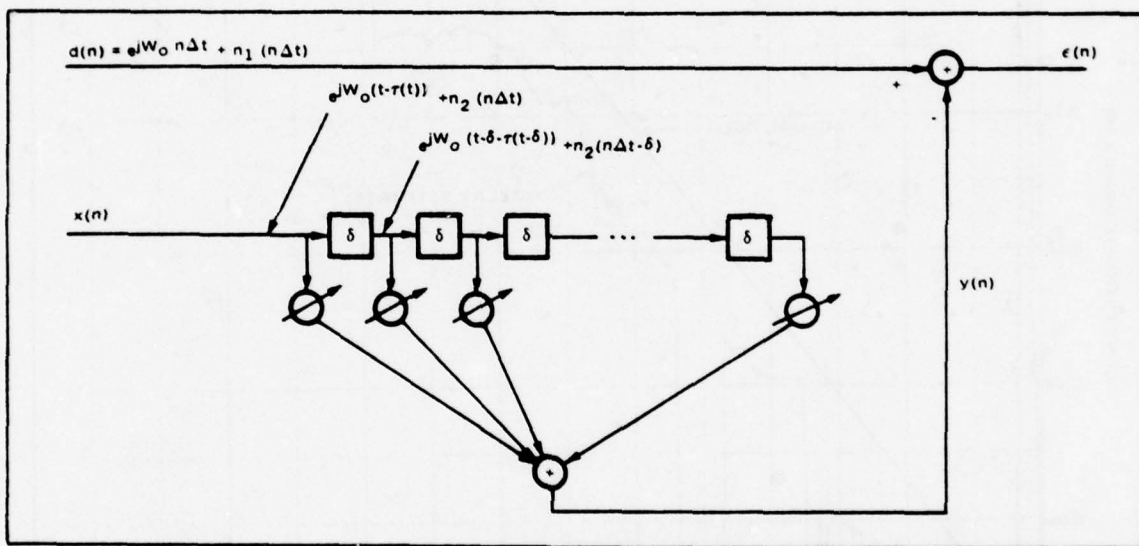


Figure 39. Delay Estimate versus Time for Linearly Varying Delay ($261.8 \mu\text{SEC/SEC}$)



81156-46

Figure 40. Data in the Delay Line

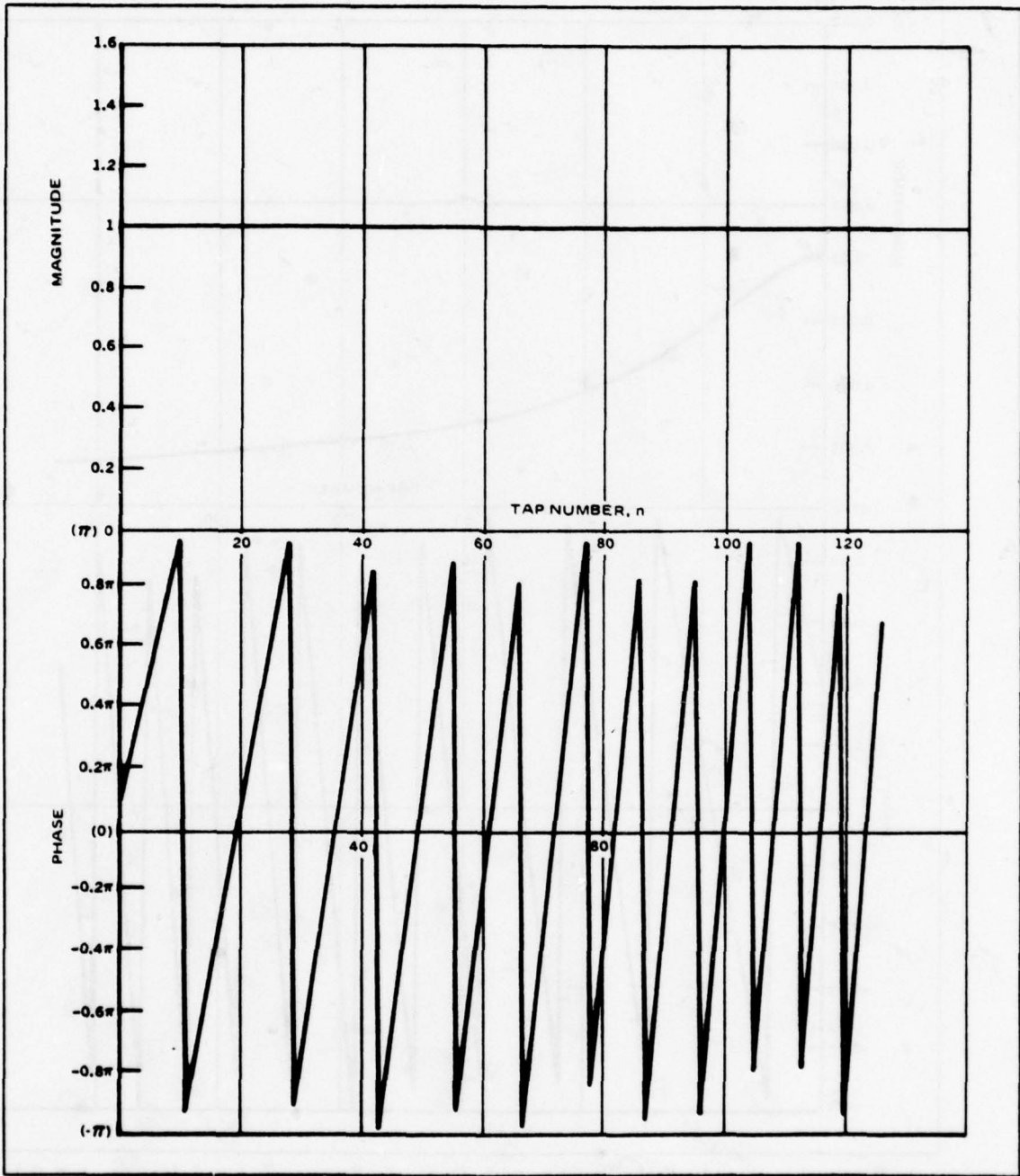


Figure 41. Undistorted Signal in Tapped Delay Line, $D(n) f = 5 \text{ Hz/sec}$
 No. of Taps = 128

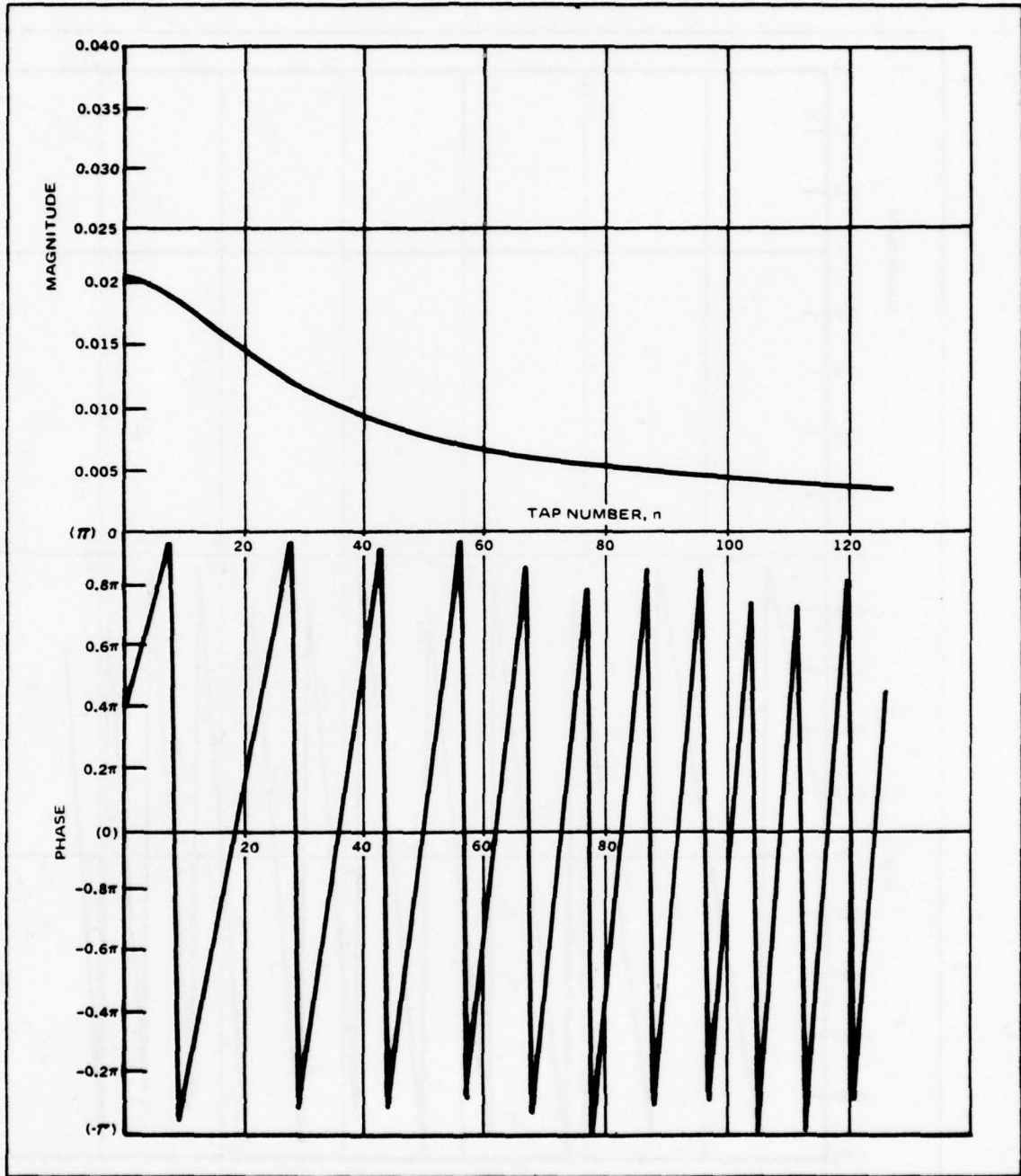


Figure 42. Steady State Weights with Dynamic Frequency $f = 5$ Hz/sec $\mu = 0.1$
No. of Taps = 128 SNR = 1

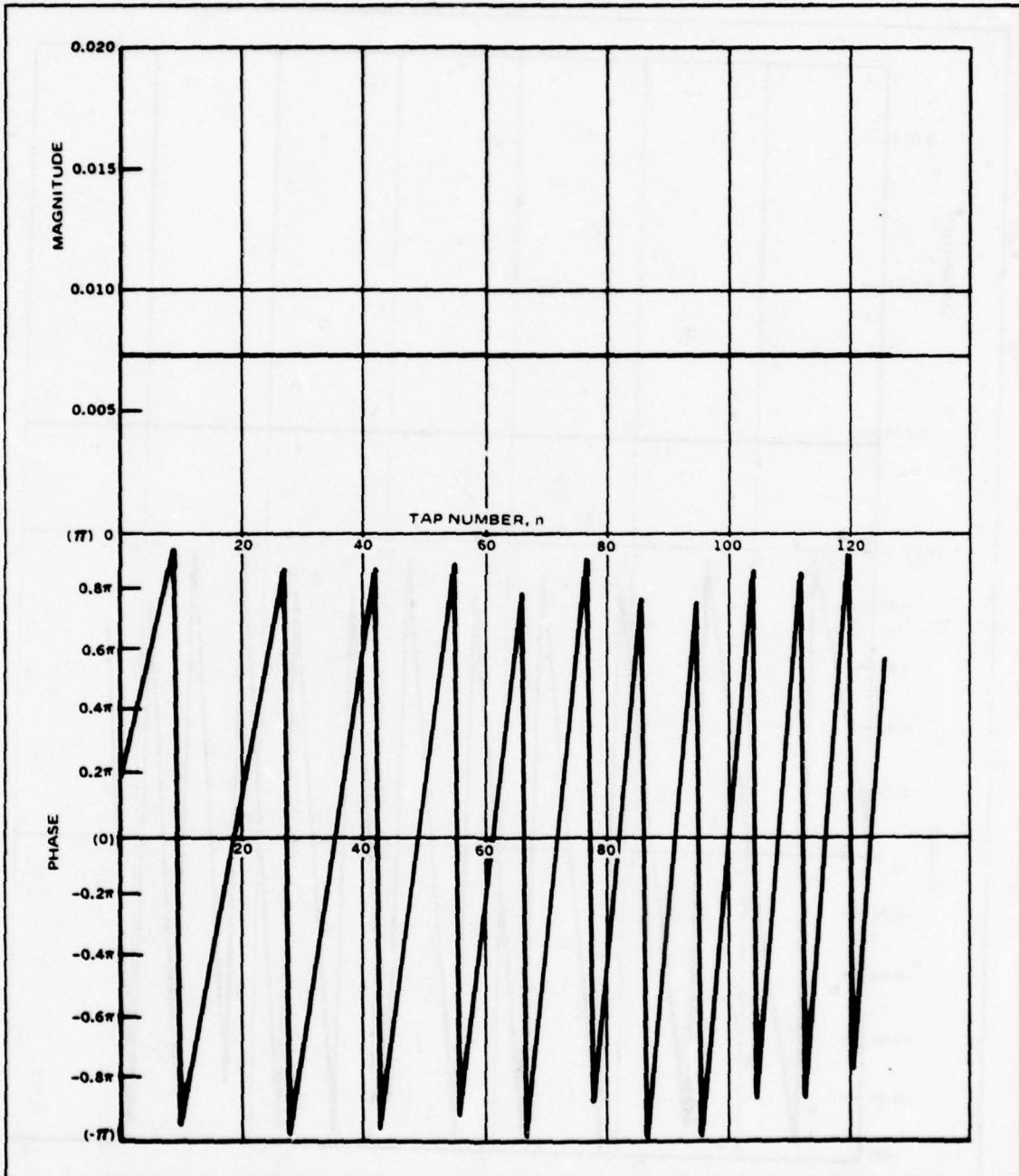
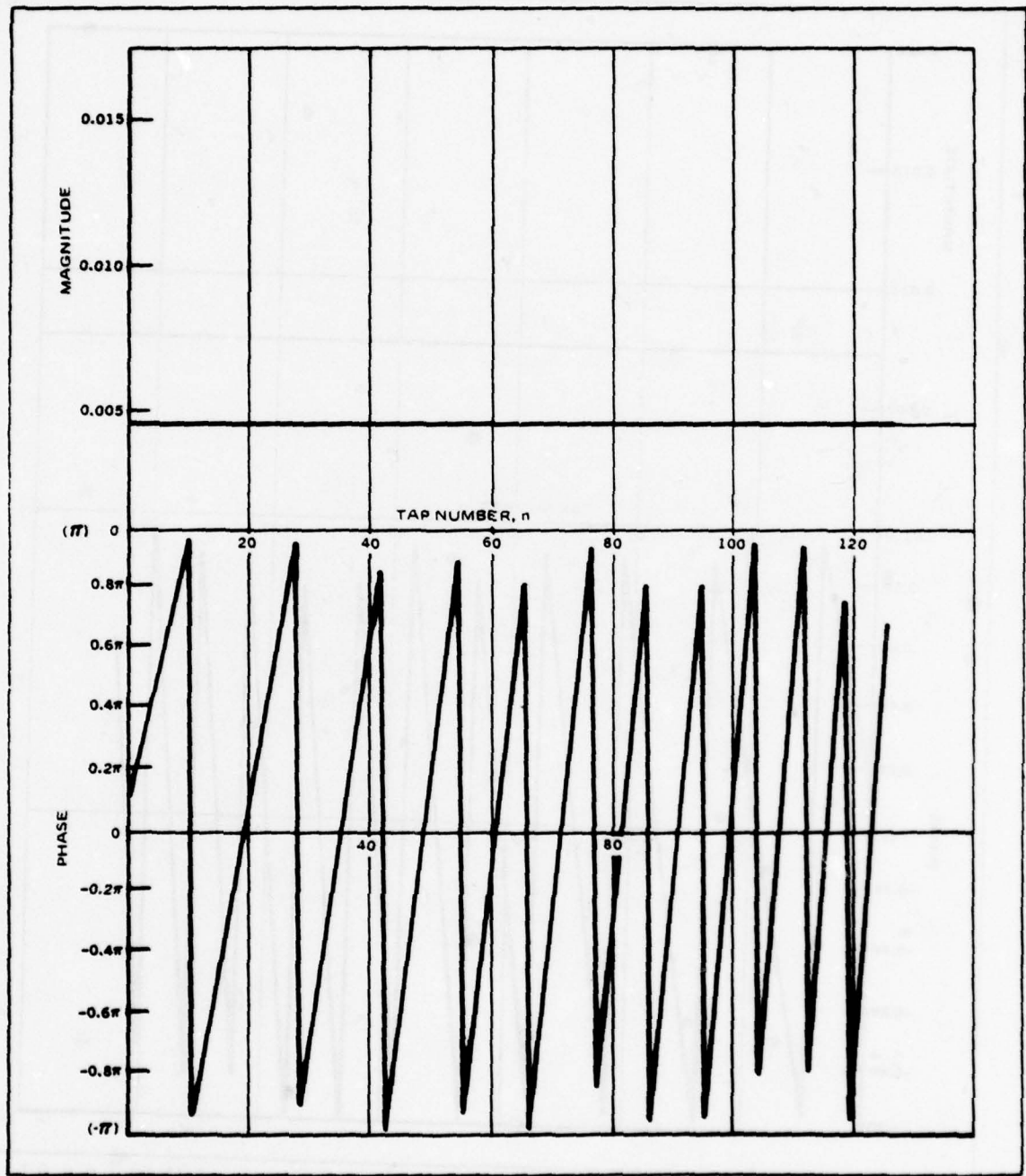
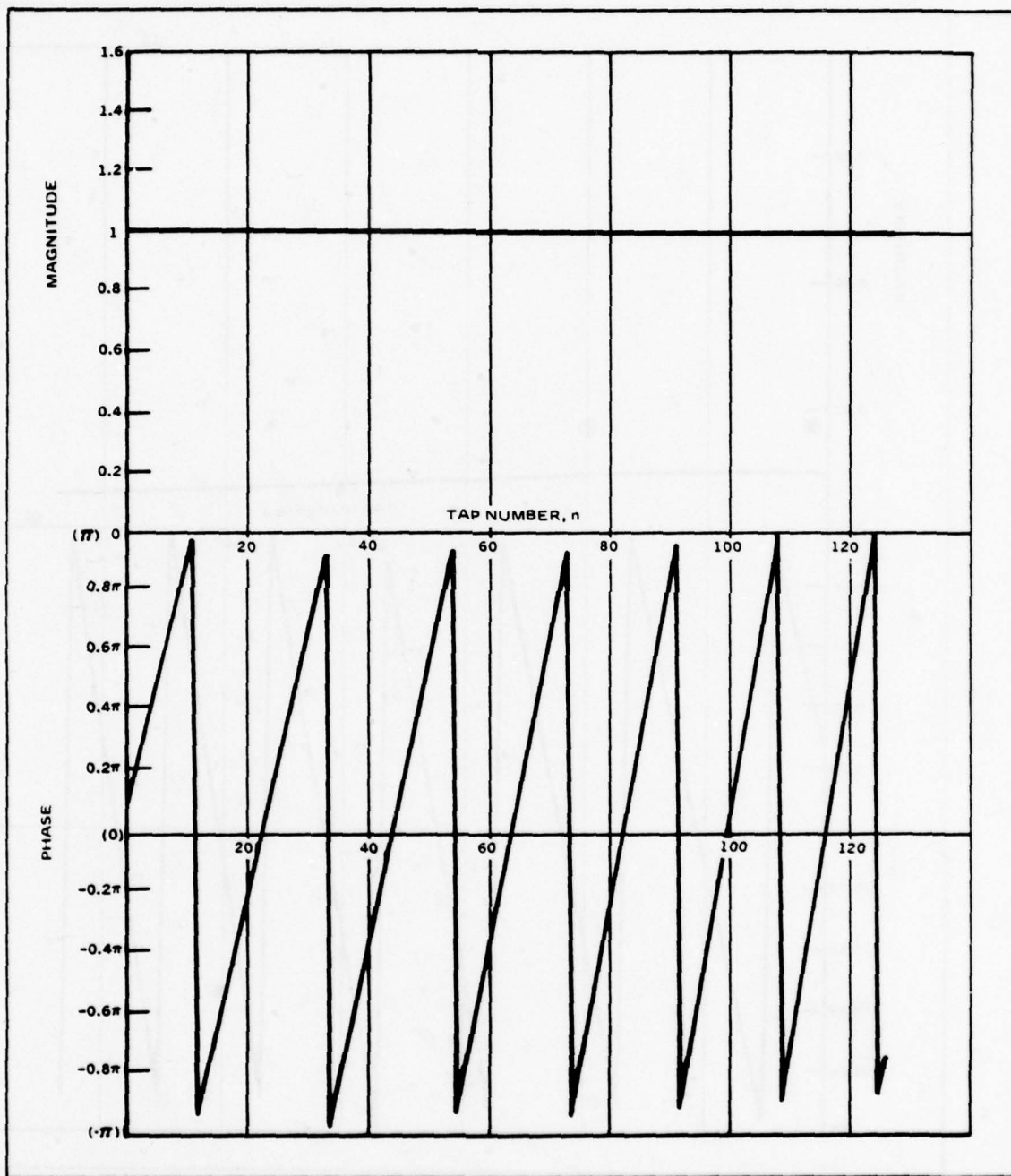


Figure 43. Steady State Weights with Dynamic Frequency $f = 5$ Hz/sec $\mu = 0.1$
No. of Taps = 128 SNR = 0.1



81156-50

Figure 44. Steady State Weights with Dynamic Frequency $f = 5$ Hz/sec $\mu = 0.1$
 No. of Taps = 128 SNR = 0.01



81156-51

Figure 45. Undistorted Signal in Tapped Delay Line $f = 1.25$ Hz/sec No. of Taps = 128

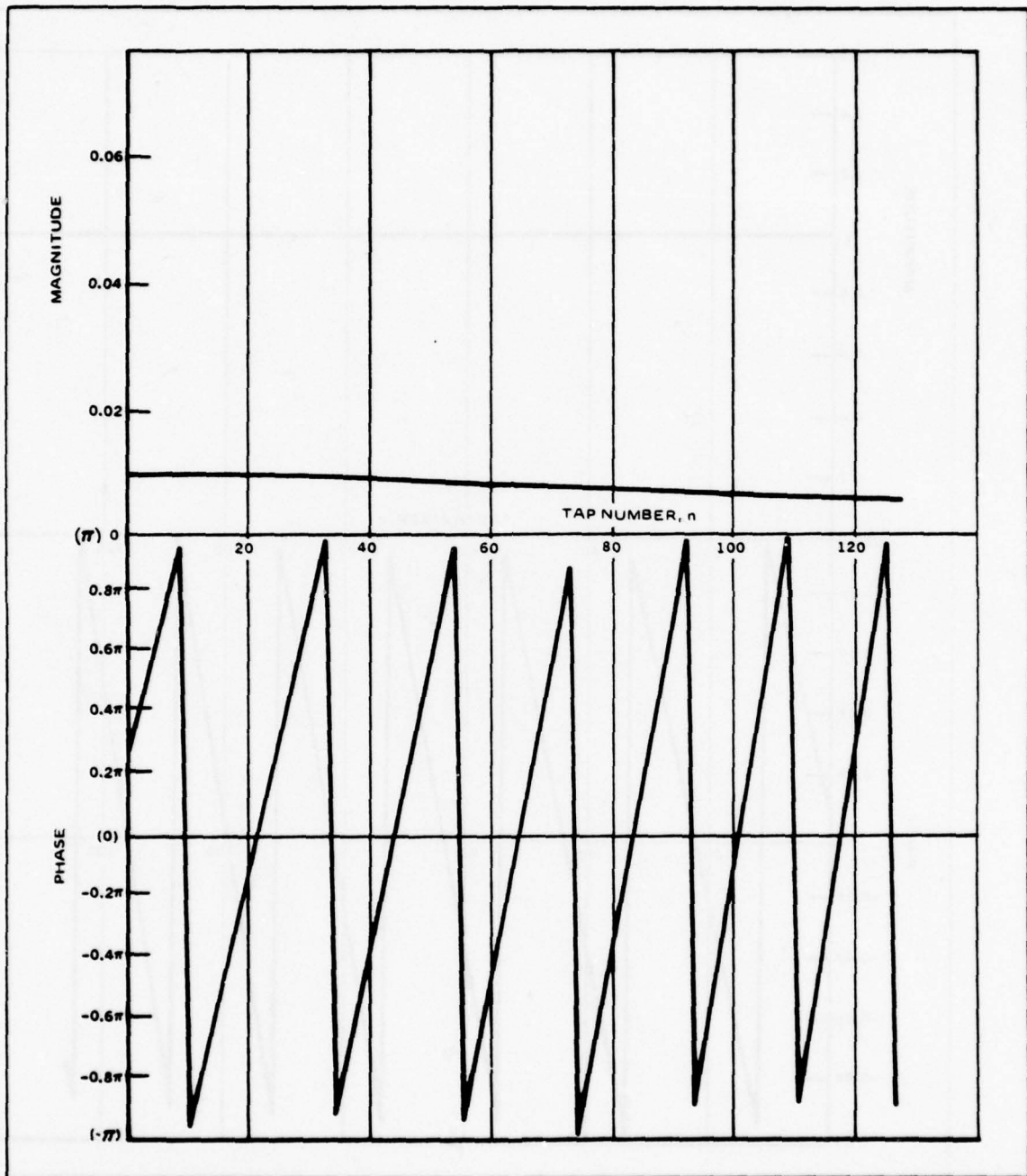


Figure 46. Steady State Weights with Dynamic Frequency $f = 1.25$ Hz/sec $\mu = 0.1$
No. of Taps = 128 SNR = 1

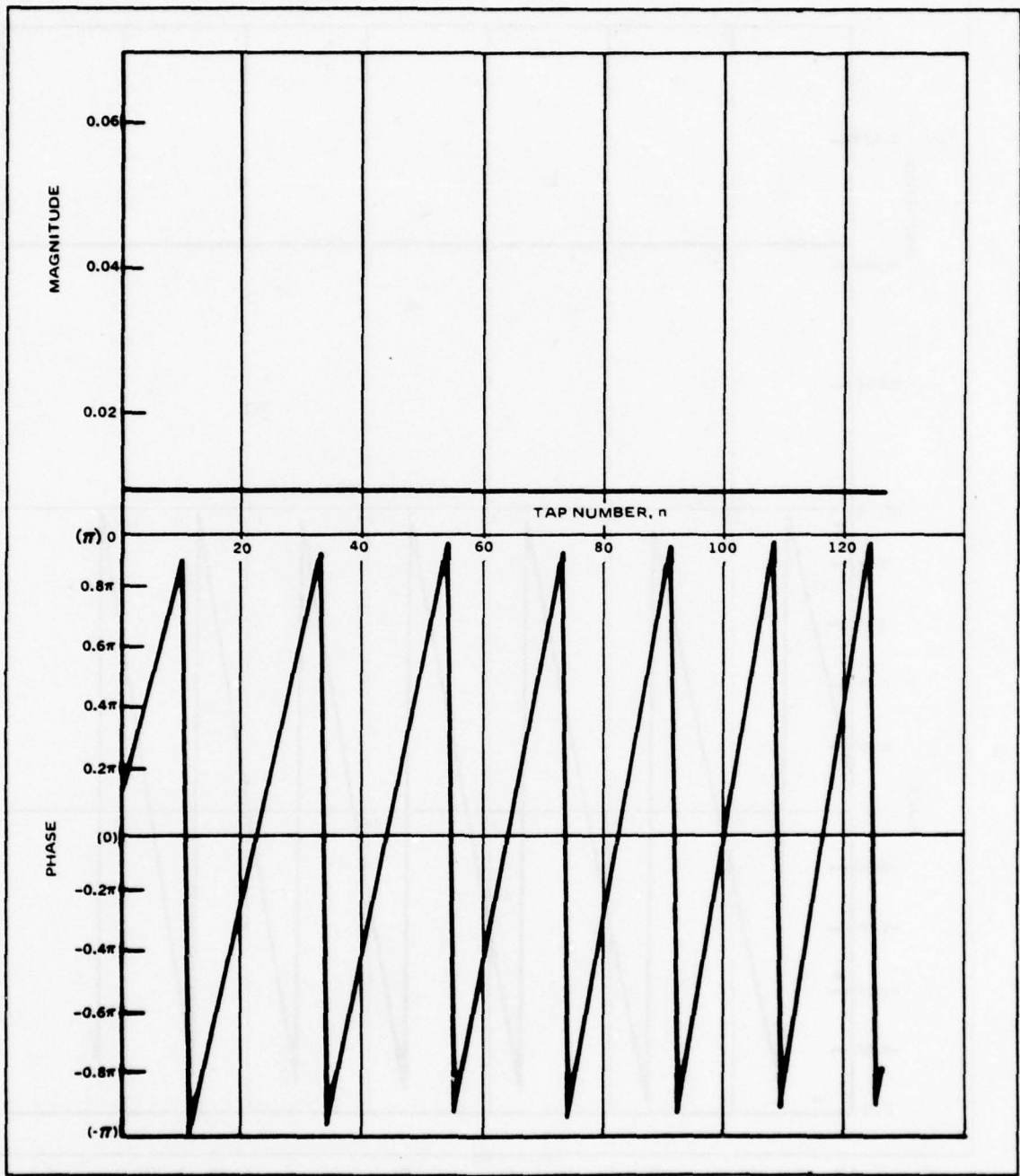


Figure 47. Steady State Weights with Dynamic Frequency $f = 1.25$ Hz/sec $\mu = 0.1$
No. of Taps = 128 SNR = 0.1

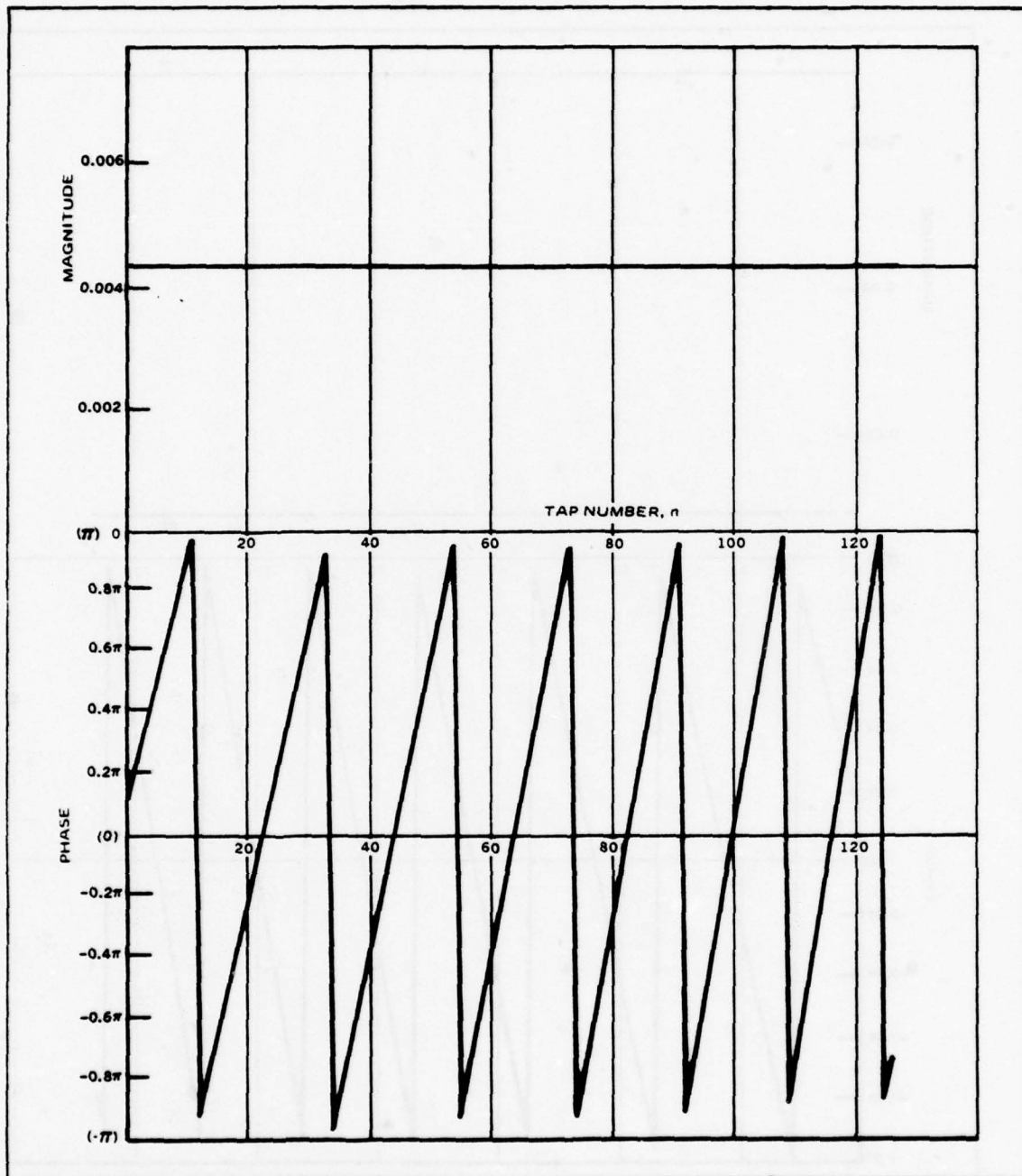


Figure 48. Steady State Weights with Dynamic Frequency $f = 1.25$ Hz/SEC $\mu = 0.1$
No. of Taps = 128 SNR = 0.01

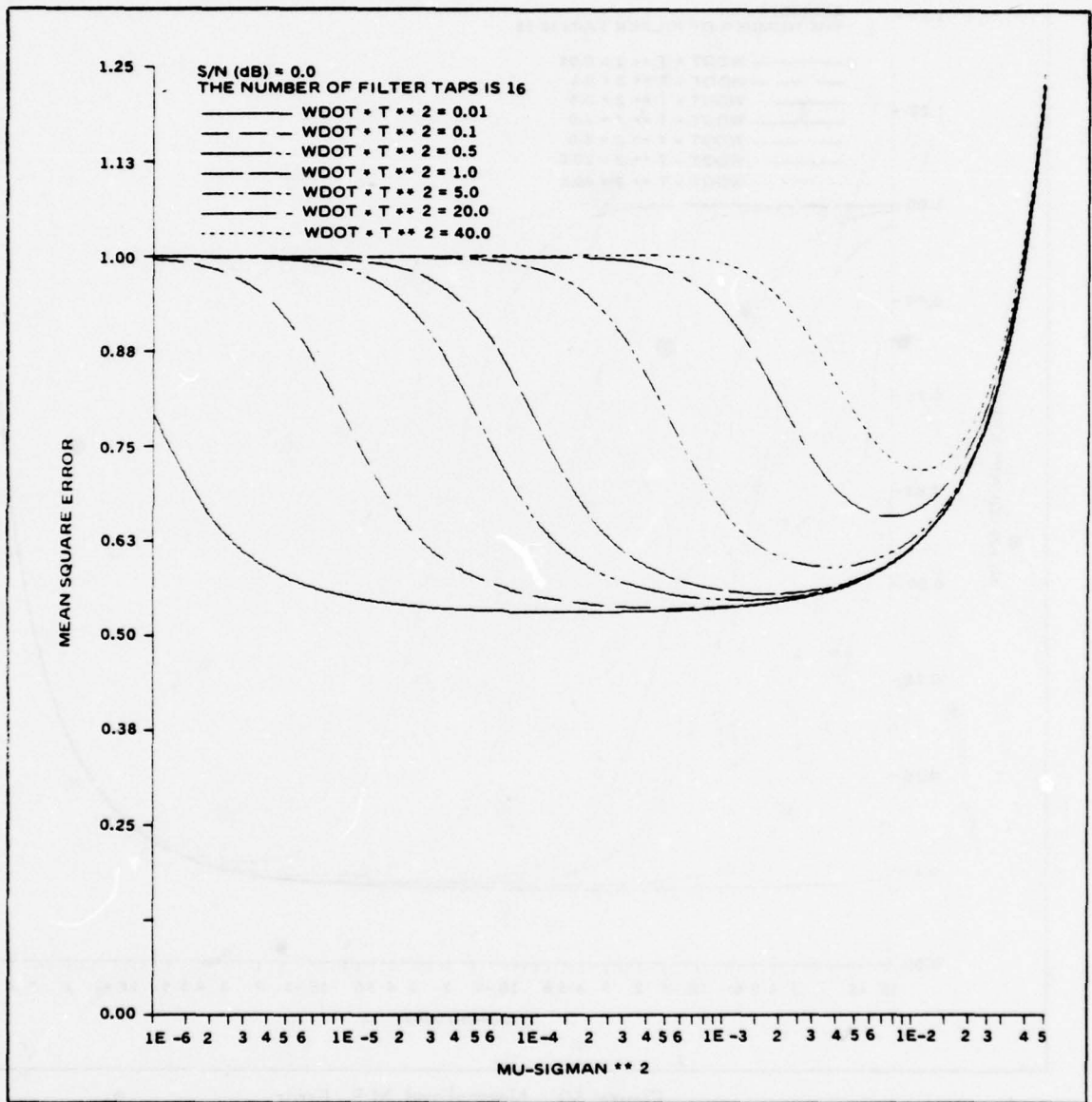


Figure 49. Normalized M.S. Error

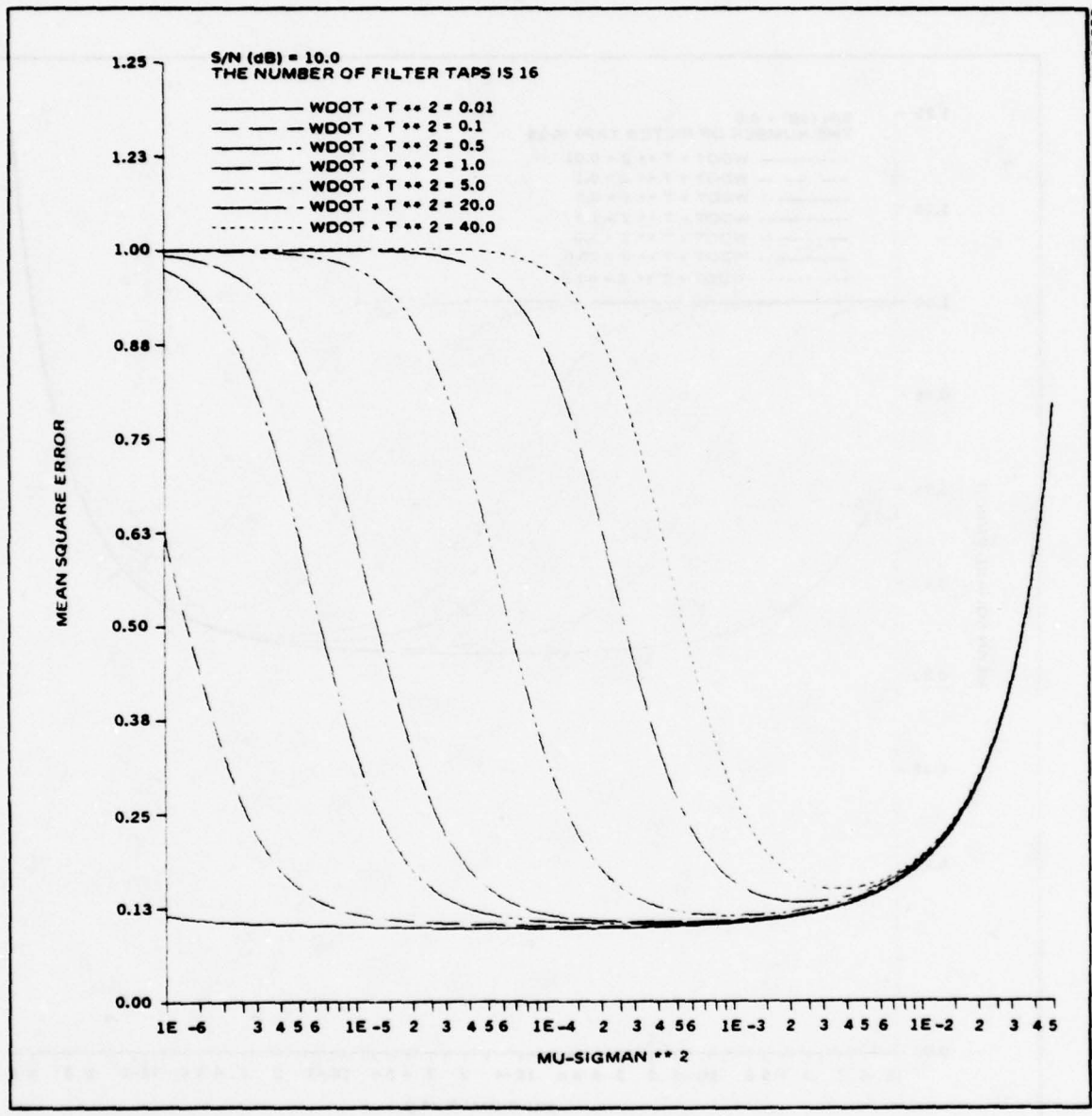
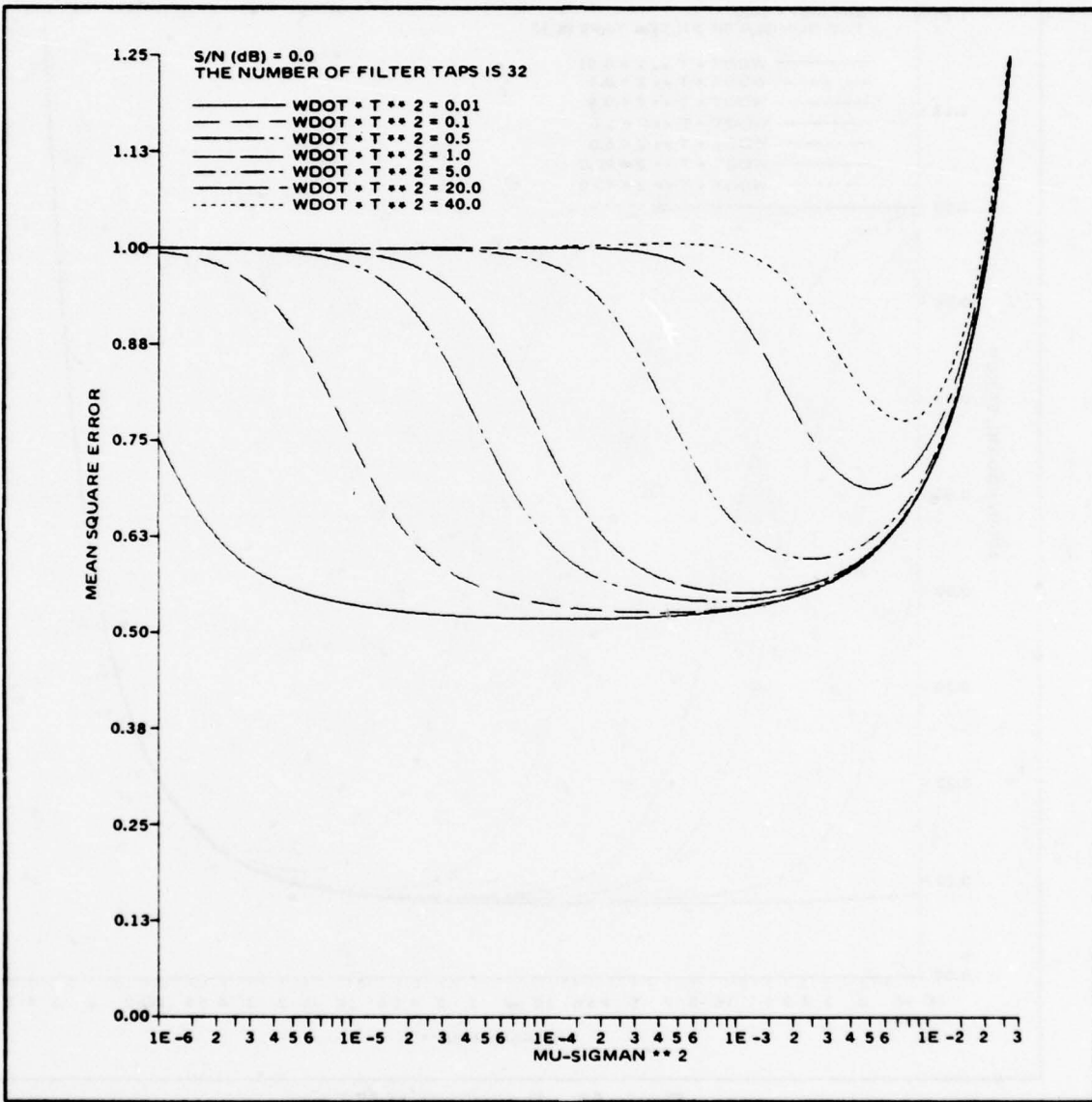


Figure 50. Normalized M.S. Error



81156-57

Figure 51. Normalized M.S. Error

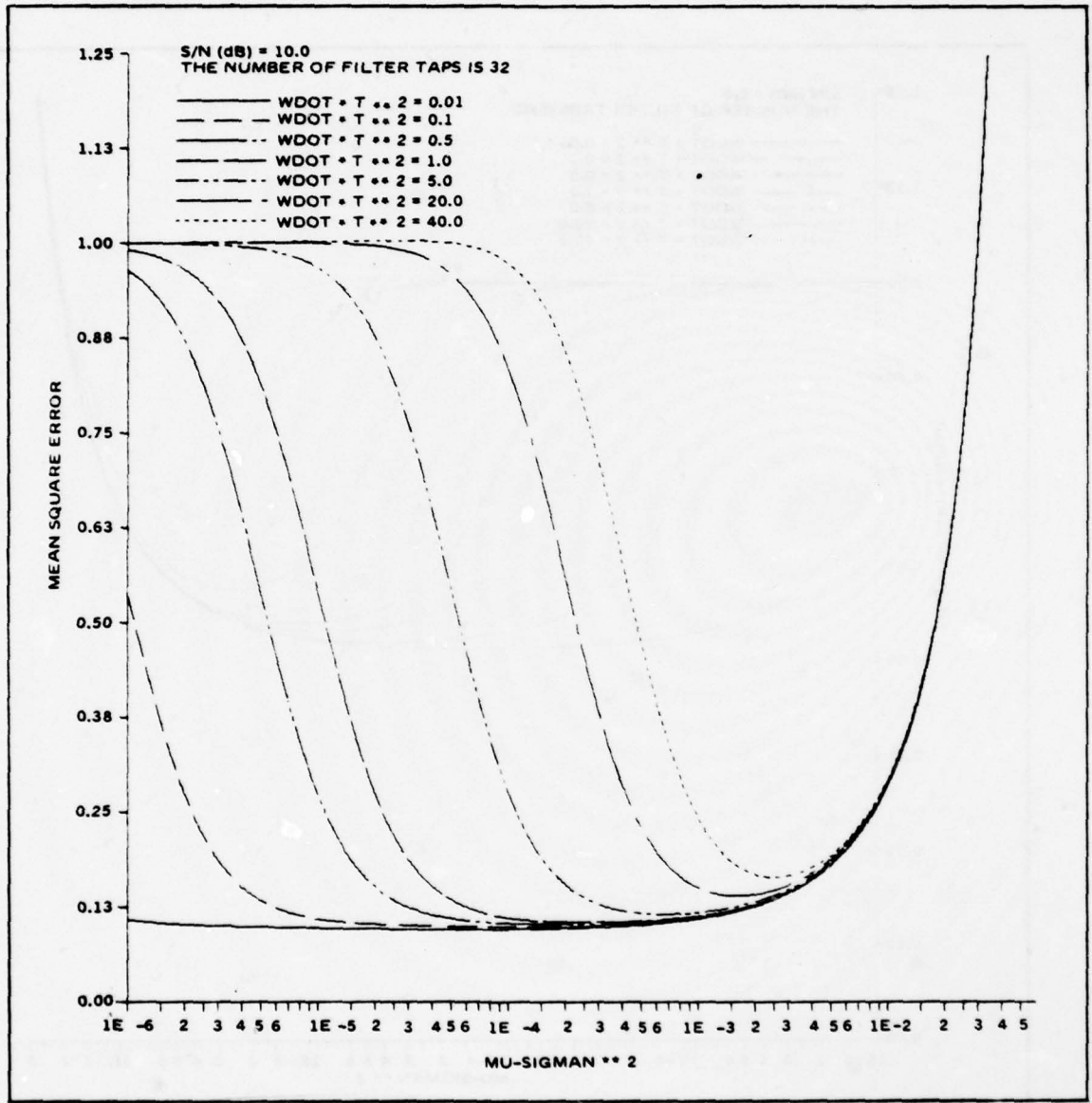


Figure 52. Normalized M.S. Error

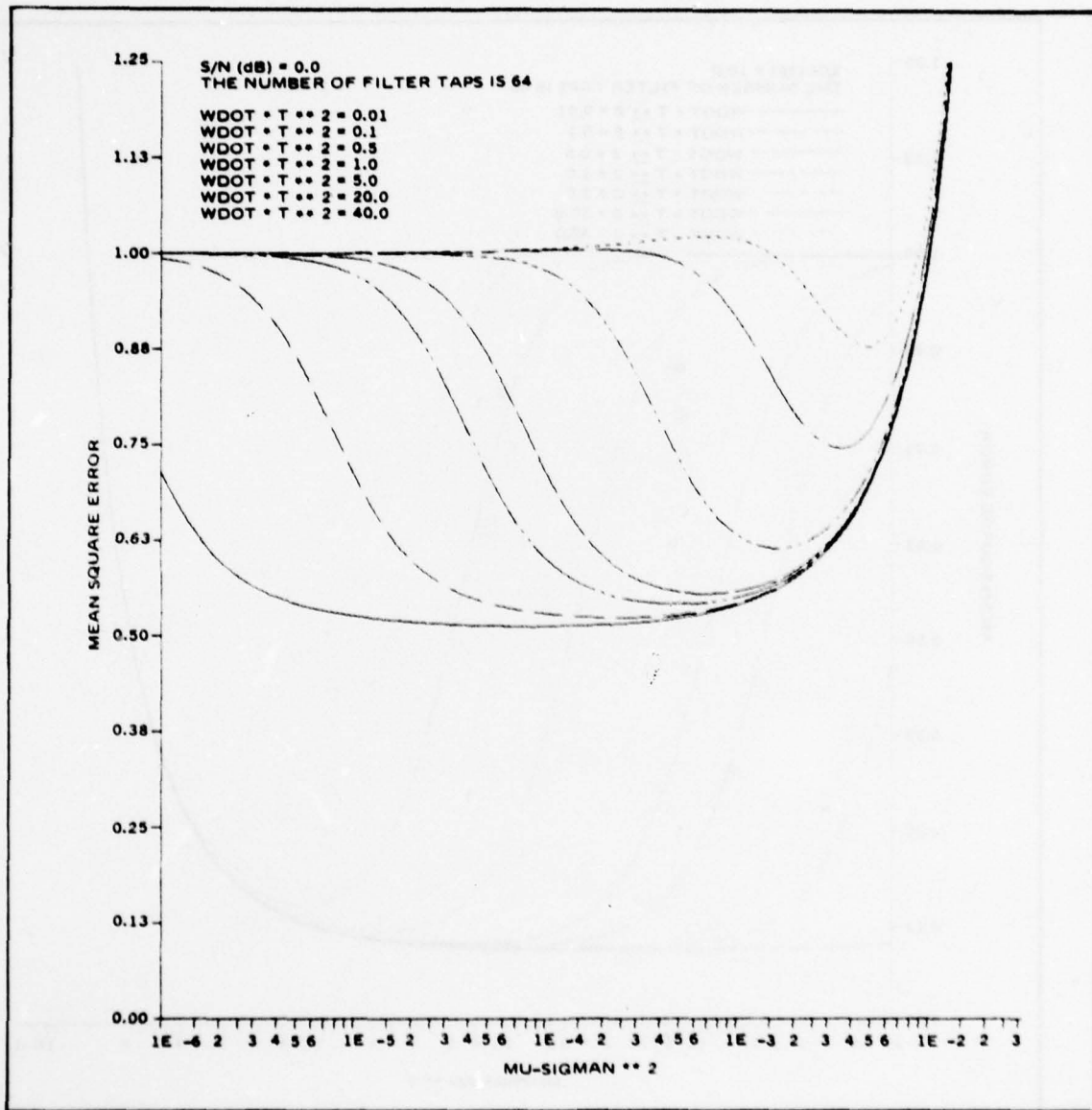
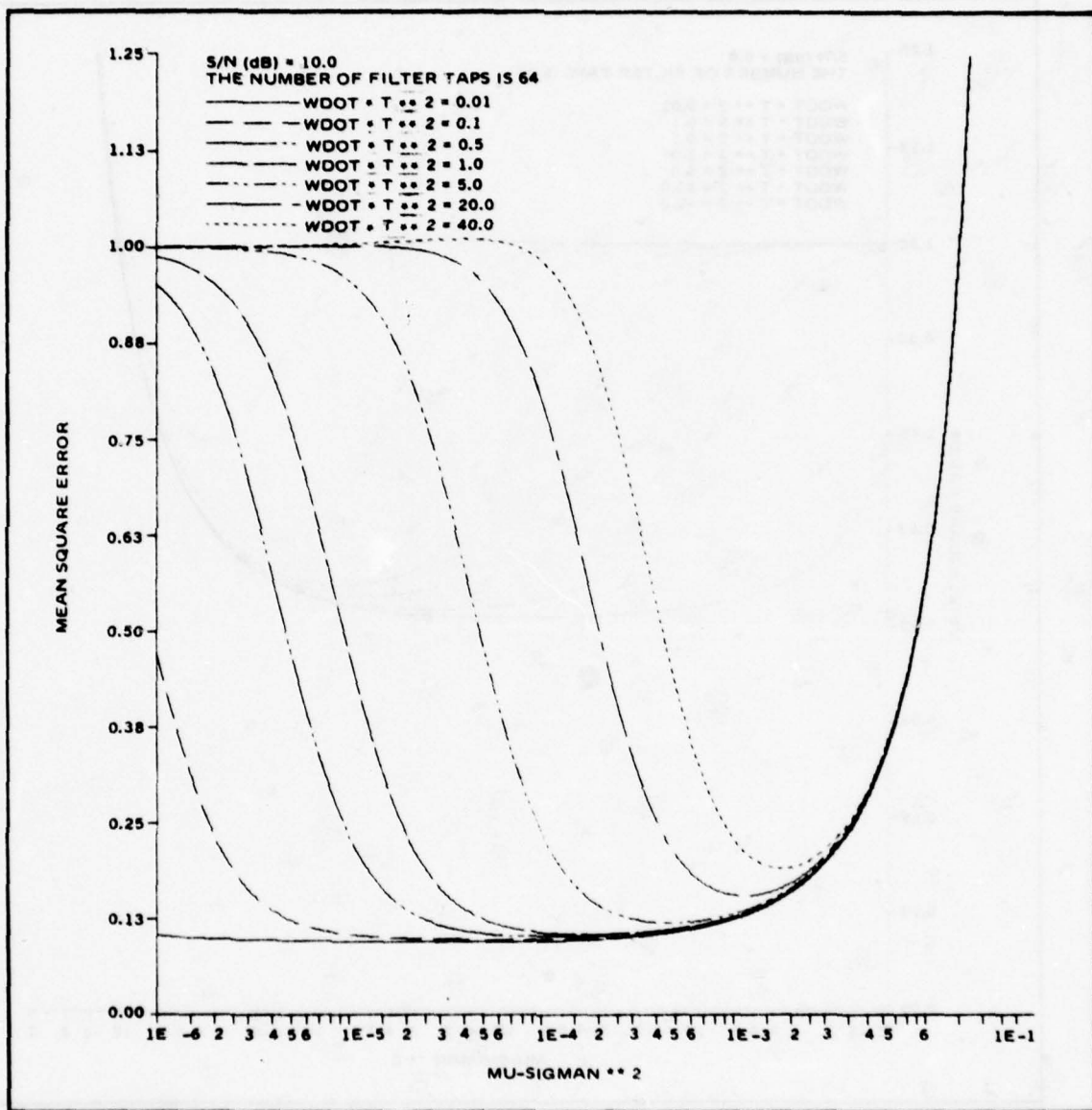
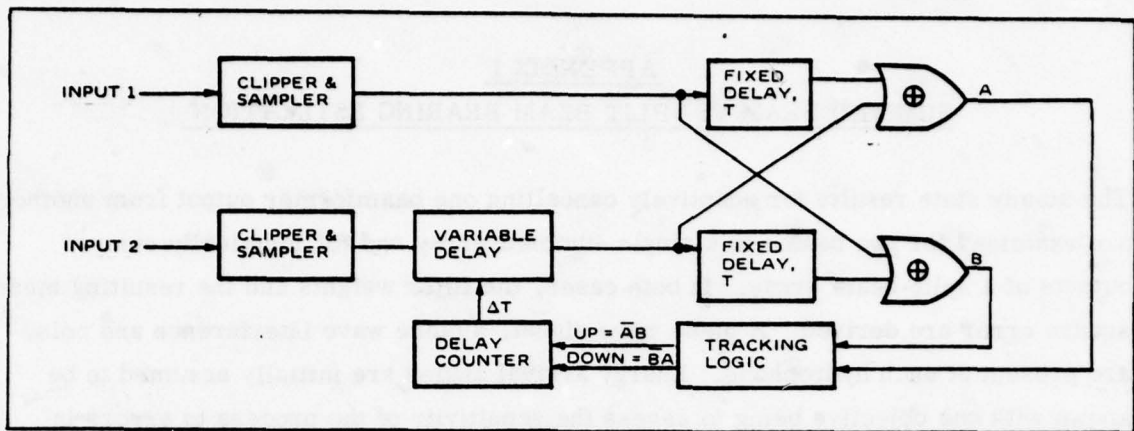


Figure 53. Normalized M.S. Error



81156-60

Figure 54. Normalized M.S. Error



81156-61

Figure 55. Two Point Correlator Tracker Block Diagram

APPENDIX I
SUMMED BEAM VS SPLIT BEAM BEARING ESTIMATION

The steady state results for adaptively cancelling one beamformer output from another are examined for two beams in a single summed array and for identically steered outputs of a split-beam array. In both cases, the filter weights and the resulting mean square error are derived. A plane wave signal, a plane wave interference and noise are present at each hydrophone. Energy arrival angles are initially assumed to be known with one objective being to assess the sensitivity of the process to errors in steering for use as a bearing tracker. The power spectra for all waveforms is kept completely general, but is assumed to be known a priori.

Summed Beam System

The situation being studied is shown in Figure 1. The signal, interference and noise spectra at the kth array element are denoted by $s(\omega)$, $i(\omega)$, and $n_k(\omega)$ respectively. The waveforms are zero mean and mutually uncorrelated. At any frequency, $\omega = 2\pi f$, the vectors of these waveforms at all the hydrophones can be expressed as follows:

$$\begin{aligned}
 I(\omega) &= \begin{pmatrix} e^{j\phi_I} \\ e^{j2\phi_I} \\ \vdots \\ e^{jM\phi_I} \end{pmatrix} & i(\omega) &= D_I(\omega) i(\omega) \\
 S(\omega) &= \begin{pmatrix} e^{j\phi_s} \\ e^{j2\phi_s} \\ \vdots \\ e^{jm\phi_s} \end{pmatrix} & s(\omega) &= D_s(\omega) s(\omega)
 \end{aligned}$$

$$N(\omega) = \begin{pmatrix} n_1(\omega) \\ n_2(\omega) \\ \cdot \\ \cdot \\ n_M(\omega) \end{pmatrix}$$

where

$$\phi_I = \omega \frac{d}{c} \sin \varphi_I$$

$$\phi_S = \omega \frac{d}{c} \sin \varphi_S$$

φ_I = interference energy arrival angle

φ_S = signal energy arrival angle

$i(\omega)$ = interference spectrum at frequency ω

$s(\omega)$ = signal spectrum at frequency ω

d = uniform element spacing

c = sound speed

The progressive delay vectors, $D_I(\omega)$ and $D_S(\omega)$, represent the propagation of the plane wave interference and signal along the uniformly spaced M element line array.

Two summed beams are formed using uniform shading. The steering vectors are $D_1(\omega)$ and $D_2(\omega)$, where

$$D_\ell(\omega) = \begin{pmatrix} e^{j\phi_\ell} \\ e^{j2\phi_\ell} \\ \cdot \\ \cdot \\ e^{jM\phi_\ell} \end{pmatrix}, \quad \ell = 1, 2$$

The beam steered in the neighborhood of the signal is the target beam, denoted by $d(\omega)$. The reference beam steered to the interference is the input to the adaptive filter, denoted by $x(\omega)$.

$$d(\omega) = D_1^+(\omega) D_I(\omega) i(\omega) + D_1^+(\omega) D_S(\omega) s(\omega) + D_1^+(\omega) N(\omega)$$

$$x(\omega) = D_2^+(\omega) D_I(\omega) i(\omega) + D_2^+(\omega) D_S(\omega) s(\omega) + D_2^+(\omega) N(\omega)$$

where the symbol + denotes the complex-conjugate transpose operation. To form the steady state complex weight at a single frequency requires calculating the cross-spectrum of d with x and the power spectrum of x . Thus,

$$E[d(\omega) x^*(\omega)] = D_1^+ [D_I D_I^+ P_I + D_S D_S^+ P_S + QP_n] D_2$$

$$E[x(\omega) x^*(\omega)] = D_2^+ [D_I D_I^+ P_I + D_S D_S^+ P_S + QP_n] D_2$$

where the frequency arguments on the D 's have been dropped for convenience, and where

$$E[NN^+] = QP_n$$

Q = normalized spatial covariance matrix of the noise

The complex weight, $B(\omega)$, is

$$B(\omega) = \frac{E[dx^*]}{E[xx^*]} = \frac{D_1^+ [D_I D_I^+ P_I + D_S D_S^+ P_S + QP_n] D_2}{D_2^+ [D_I D_I^+ P_I + D_S D_S^+ P_S + QP_n] D_2}$$

The error ϵ , is

$$\begin{aligned} \epsilon(\omega) &= d(\omega) - B(\omega) x(\omega) \\ &= [D_1^+ - BD_2^+] [D_I i(\omega) + D_S s(\omega) + N(\omega)] \end{aligned}$$

and the mean square error, $E[|\epsilon|^2]$, is

$$E[|\epsilon|^2] = (D_1^+ - BD_2^+) [D_1^+ D_I^+ P_I + D_S^+ D_S^+ P_S + QP_n] (D_1 - B^+ D_2)$$

To facilitate writing $E[|\epsilon|^2]$, let us define the following spatial responses.

$$\begin{aligned} \alpha_I &= D_1^+ D_I &&= \text{response of array steered to } \varphi_1, \text{ to energy arriving at } \varphi_I \\ \beta_I &= D_2^+ D_I &&= \text{response of array steered to } \varphi_2, \text{ to energy arriving at } \varphi_I \\ \alpha_S &= D_1^+ D_S &&= \text{response of array steered to } \varphi_1, \text{ to energy arriving at } \varphi_S \\ \beta_S &= D_2^+ D_S &&= \text{response of array steered to } \varphi_2, \text{ to energy arriving at } \varphi_S \\ \gamma &= D_1^+ D_2 &&= \text{response of array steered to } \varphi_1, \text{ to energy arriving at } \varphi_2 \end{aligned}$$

For a uniformly-shaded, uniformly-spaced line array.

$$\begin{aligned} \alpha_S &= e^{-j \left(\frac{M+1}{2}\right) (\phi_1 - \phi_S)} \frac{\sin \frac{M}{2} (\phi_1 - \phi_S)}{\sin 1/2 (\phi_1 - \phi_S)} \\ \beta_S &= e^{-j \left(\frac{M+1}{2}\right) (\phi_2 - \phi_S)} \frac{\sin \frac{M}{2} (\phi_2 - \phi_S)}{\sin 1/2 (\phi_2 - \phi_S)} \\ \gamma &= e^{-j \left(\frac{M+1}{2}\right) (\phi_1 - \phi_2)} \frac{\sin \frac{M}{2} (\phi_1 - \phi_2)}{\sin 1/2 (\phi_1 - \phi_2)} \end{aligned}$$

For α_I and β_I substitute ϕ_I for ϕ_S .

The mean square error can then be written as

$$\begin{aligned} E[|\epsilon|^2] &= |\alpha_I|^2 P_I + |\alpha_S|^2 P_S + D_1^+ Q D_1 P_n + |B|^2 \left[(\beta_I)^2 P_I + |\beta_S|^2 P_S \right. \\ &\quad \left. + D_2^+ Q D_2 P_n \right] - 2 \operatorname{Re} \left\{ B^+ (\alpha_I \beta_I^+ P_I + \alpha_S \beta_S^+ P_S + D_1^- Q D_2 P_n) \right\} \end{aligned}$$

where

$$B = \frac{\alpha_I \beta_I^* P_I + \alpha_s \beta_s^* P_s + D_1^* Q D_2 P_n}{|\beta_I|^2 P_I + |\beta_s|^2 P_s + D_2^* Q D_2 P_n}$$

For the special case where the noise is uncorrelated spatially from element-to-element, the matrix $Q=I$, the $M \times M$ identity, and the mean-square error is:

$$E[|\epsilon|^2] = \frac{\left\{ (M^2 - G_{12}^2) P_n^2 + P_s P_I (G_{1s} G_{2I} - G_{1I} G_{2s})^2 \right. \\ \left. + P_s P_n (M G_{1s}^2 + M G_{2s}^2 - 2 G_{1s} G_{2s} G_{12}) \right. \\ \left. + P_I P_n (M G_{2I}^2 + M G_{1I}^2 + 2 G_{1I} G_{2I} G_{12}) \right\}}{G_{2I}^2 P_I + G_{2s}^2 P_s + M P_n}$$

where

$$G_{ab} = \frac{\sin \frac{M}{2} (\phi_a - \phi_b)}{\sin 1/2 (\phi_a - \phi_b)}$$

and the complex weight, $B(\omega)$, is

$$B(\omega) = \frac{G_{1I} G_{2I} P_I + G_{1s} G_{2s} P_s + G_{12} P_n}{G_{2I}^2 P_I + G_{2s}^2 P_s + M P_n} e^{-j \left(\frac{M+1}{2} \right) (\phi_1 - \phi_2)}$$

An interesting example occurs for the case of correct steering, for which $\phi_1 = \phi_s$ and $\phi_2 = \phi_I$. For this case

$$G_{1s} = G_{2I} = M$$

$$G_{1I} = G_{2s} = G_{12}$$

and

$$E[|\epsilon|^2] = \frac{(M^2 - G_{12}^2) [P_n^2 + P_s P_I (M^2 - G_{12}^2) + M P_s P_n + M P_I P_n]}{M^2 P_I + G_{12}^2 P_s + M P_n}$$

Of additional interest is the case of a single plane wave broadband interference to be cancelled. This can be evaluated by setting $P_s = 0$ and examining the extent to which P_I is removed from the mean square error. Thus

$$B(\omega) = e^{-j \left(\frac{M+1}{2}\right) (\phi_1 - \phi_2)} \frac{G_{12}}{M}$$

and

$$E[|\epsilon|^2] = \frac{(M^2 - G_{12}^2) P_n}{M}$$

$$\left(\begin{array}{l} P_s = 0 \\ \phi_2 = \phi_1 \end{array} \right)$$

Note that for this case the interference is completely removed and the weight is independent of the interference power. The reason for this is that the noise at the two beam outputs has a deterministic correlation placed on it by the beamformer. This correlation is exactly the same as the correlation on the interference, which is the sidelobe gain. Thus, the filter weights due to the noise correlation are the same as the weights needed to cancel the interference. When interference is added to the acoustic field, it is cancelled regardless of the interference-to-noise ratio, because the filter weights do not have to change to accommodate the interference correlation. This will not be the case if the noises are correlated spatially or if the steering vectors are not precisely aligned to the energy arrival angles. Then the noise correlation on the beams are not exactly the same as the interference correlations and the adaptive filter will have to change to cancel the interference. For small interference-to-noise ratios, the filter would not change to cancel the interference because the resulting increase in noise power at the output would exceed the reduction in output power due to removing the interference.

The extent of the filter weights in time is twice the maximum time difference for propagation from the reference beam to the target beam. For example, when the two beams coincide, i. e. , $\sin \varphi_1 = \sin \varphi_2$, there exists just one weight at $t = 0$. If the reference is at forward endfire and the target is at aft endfire, then $\sin \varphi_1 - \sin \varphi_2 = 2$ and the total filter delay is $2M \frac{d}{c}$, which is twice the time for the wavefront to propagate across the aperture of the array.

It can be concluded that the correlation on the beams due to the noise is helping to cancel the interference. This is a desirable result when performing a post-beamformer interference cancellation (PIC), but it obscures the ability to identify signal correlation properties for tracking. The noises produce residual correlation on the beams, which the adaptive filter treats as a signal process. To decorrelate the noises one must form the beams from separate elements, so that the two inputs to the adaptive canceller are not linear combinations of the same set of processes. This motivates considering the split-beam processor, in the next section.

Split-Beam System

The split-beam configuration is shown in Figure 2. The $2M$ -array elements are divided equally and a beam is formed with both sub-arrays steered to the target. The objective is to subsequently process to get a refined estimate of the signal energy arrival angle and to automatically follow bearing and spectral changes.

The adaptive filter steady state impulse response is the inverse transform of the single frequency complex weights. The impulse response, which is approximated by the discrete filter weights, is

$$\begin{aligned}
 h(t) &= \int_{-\infty}^{\infty} B(\omega) e^{j\omega t} \frac{d\omega}{2\pi} \\
 &= \frac{1}{M} \int_{-\infty}^{\infty} e^{-j\left(\frac{M+1}{2}\right) \omega \frac{d}{c} (\sin \varphi_1 - \sin \varphi_2)} \frac{\sin \frac{M}{2} \omega \frac{d}{c} (\sin \varphi_1 - \sin \varphi_2)}{\sin \frac{1}{2} \omega \frac{d}{c} (\sin \varphi_1 - \sin \varphi_2)} e^{j\omega t} \frac{d\omega}{2\pi} \\
 &= \frac{1}{M} \int_{-\infty}^{\infty} e^{j\omega t} \sum_{k=1}^M e^{-j(\phi_1 - \phi_2) k} \frac{d\omega}{2\pi} \\
 &= \frac{1}{M} \sum_{k=1}^M \int_{-\infty}^{\infty} e^{j\omega t} e^{-j\omega \frac{d}{c} (\sin \varphi_1 - \sin \varphi_2) k} \frac{d\omega}{2\pi} \\
 &= \frac{1}{M} \sum_{k=1}^M \delta\left(t - k \frac{d}{c} (\sin \varphi_1 - \sin \varphi_2)\right)
 \end{aligned}$$

The filter weights are shown in Figure 7 for this special case.

The adaptive filter will converge to minimize the mean square error, i. e. to minimize the power in ϵ . This implies that implicit within the filter is estimation of the transformation to make the waveform x look as much as possible like d . If propagation delays or those shifts are the only differences between the half-array outputs, then one should be able to extract this information from the filter weights and the filter should be able to track reasonable dynamics.

Analysis of the steady-state performance in Figure 2 proceeds in the same way as the previous section. The signal energy arrival angle is ψ_s , from which a vector of propagation delays, $D_s(\omega)$, is formed. The steering direction, ψ , from which the vector $D(\omega)$ is formed, is close to but not exactly ψ_s . Thus

$$D_s(\omega) = \begin{pmatrix} e^{j\omega \frac{d}{c} \sin \psi_s} \\ e^{j\omega 2 \frac{d}{c} \sin \psi_s} \\ \vdots \\ e^{j\omega M \frac{d}{c} \sin \psi_s} \end{pmatrix}, \quad D(\omega) = \begin{pmatrix} e^{j\omega \frac{d}{c} \sin \psi} \\ \cdot \\ \cdot \\ \cdot \\ e^{j\omega M \frac{d}{c} \sin \psi} \end{pmatrix}$$

and just as before,

$$d(\omega) = D^+(\omega) D_s(\omega) s(\omega) + D^+ N_d(\omega)$$

$$x(\omega) = D^+(\omega) D_s(\omega) e^{jM\phi_s} s(\omega) + D^+ N_x(\omega)$$

where N_d and N_x are uncorrelated and all processes are zero mean. To form the complex filter weights one needs the cross correlation of d with x and the auto-correlation of x .

$$E [d(\omega) x^*(\omega)] = D^+ D_s D_s^+ D e^{-jM\phi_s} S(\omega)$$

$$E [x(\omega) x^*(\omega)] = D^+ D_s D_s^+ D S_s(\omega) + D^+ Q D S_n(\omega)$$

where $S_s(\omega)$ and $S_n(\omega)$ are the power spectra of $s(\omega)$ and $N_x(\omega)$, and where for convenience the frequency argument of the steering vectors has been dropped. The complex weight is

$$B(\omega) = \frac{E[d(\omega) x^*(\omega)]}{E[x(\omega) x^*(\omega)]} = \frac{|D^+ D_s|^2 e^{-jM\phi_s} S_s(\omega)}{|D^+ D_s|^2 S_s(\omega) + D^+ Q D S_n(\omega)}$$

For the case where the noise is uncorrelated spatially from element-to-element, the matrix $Q=L$. Also, let $\alpha(\omega)$ denote the spatial response of the array steered to ψ to energy arriving at ψ_s . Thus

$$\alpha(\omega) = D^+(\omega) D_s(\omega)$$

and

$$B(\omega) = \frac{|\alpha|^2 e^{-j M \omega \frac{d}{c} \sin \psi_s} S_s(\omega)}{|\alpha|^2 S_s(\omega) + M S_n(\omega)}$$

The resulting error power spectrum is

$$E[|\epsilon(\omega)|^2] = M S_n(\omega) \frac{2|\alpha(\omega)|^2 S_s(\omega) + M S_n(\omega)}{|\alpha(\omega)|^2 S_s(\omega) + M S_n(\omega)}$$

The filter transfer function, $h(t)$, is the inverse Fourier transform of $B(\omega)$. It is this function which the adaptive filter attempts to approximate with its finite taps.

$$\begin{aligned}
 h(t) &= \int_{-\infty}^{\infty} e^{j\omega t} B(\omega) \frac{d\omega}{2\pi} \\
 &= \int_{-\infty}^{\infty} e^{j\omega(t - M \frac{d}{c} \sin \psi_s)} \frac{S_s(\omega) |\alpha(\omega)|^2}{|\alpha(\omega)|^2 S_s(\omega) + M S_n(\omega)} \frac{d\omega}{2\pi}
 \end{aligned}$$

In the broadband case both $S_s(\omega)$ and $S_n(\omega)$ can initially be considered to be spectrally flat, i. e. independent of ω . Then

$$h(t) = \int_{-\infty}^{\infty} e^{j\omega(t - M \frac{d}{c} \sin \psi_s)} \frac{P_s |\alpha(\omega)|^2}{|\alpha(\omega)|^2 P_s + M P_n} \frac{d\omega}{2\pi}$$

Notice, that even with white input spectra, the power spectrum at the beamformer output is colored by the frequency dependence of the spatial response, $\alpha(\omega)$. Since

$$\alpha(\omega) = e^{-j \left(\frac{M+1}{2} \right) \omega \frac{d}{c} (\sin \psi - \sin \psi_s)} \frac{\sin \frac{M}{2} \omega \frac{d}{c} (\sin \psi - \sin \psi_s)}{\sin \frac{\omega d}{2c} (\sin \psi - \sin \psi_s)}$$

for a uniformly spaced and uniformly shaded line array, it can be seen that only for perfect steering, i. e. $\psi = \psi_s$ does $\alpha(\omega)$ not depend on frequency. For that special case,

$$\begin{aligned}
 h(t) \Big|_{\psi = \psi_s} &= \frac{M^2 P_s}{M(M P_s + P_n)} \int_{-\infty}^{\infty} e^{j\omega(t - \frac{M d}{c} \sin \psi_s)} \frac{d\omega}{2\pi} \\
 &= \frac{M^2 P_s}{M^2 P_s + M P_n} \delta\left(t - \frac{M d}{c} \sin \psi_s\right) \\
 &= \frac{M P_s / P_n}{1 + M P_s / P_n} \delta\left(t - \frac{M d}{c} \sin \psi_s\right)
 \end{aligned}$$

and the adaptive filter forms a single weight at the correct inter-phase center delay.

APPENDIX II
COMPARISON OF TIME AND FREQUENCY DOMAIN ADAPTIVE
TRACKERS WITH BROADBAND SIGNAL INPUTS

1. Steady State Equivalence of the Time and Frequency Domain Adaptive Trackers with Broadband Signal Inputs

This appendix considers the equivalence of the time domain and frequency domain implementations of the adaptive bearing estimator, shown in Figures 4 and 5, respectively. In the case of a broadband signal in noise, it is shown here that the two implementations converge to essentially the same steady state weight vector and mean square error if the FFT time window is long in comparison to the time delay difference between the signal at the adaptive tracker inputs.

For the broadband signal case, the time domain inputs to the tracker can be written as

$$\begin{aligned} x(t) &= s(t) + n_x(t) \\ d(t) &= s(t - \Delta T_s) + n_d(t) \end{aligned} \quad (1)$$

where $s(t)$, $n_x(t)$, and $n_d(t)$ are zero mean, stationary random processes, uncorrelated in time and independent of each other. Let the delay between the two inputs, Δ , be a multiple of the sampling interval, T_s . An FFT is performed on both $x(t)$ and $d(t)$ every RT_s seconds, so that each frequency domain filter iterates every RT_s seconds. With M the FFT size, $R = M$ corresponds to FFT processing without overlapping or gaps between time windows, $R < M$ corresponds to overlapping FFTs and $R > M$ indicates gap processing.

The i^{th} input to the adaptive filter in the k^{th} FFT bin is given by

$$X_k(i) = \sum_{n=0}^{M-1} \left\{ s[(n+iR)T_s] + n_x[(n+iR)T_s] \right\} e^{-j \frac{2\pi}{N} nk} \quad (2)$$

and

$$D_k(i) = \sum_{n=0}^{M-1} \left\{ S[(n+iR-\Delta)T_s] + n_d[(n+iR)T_s] \right\} e^{-j \frac{2\pi}{N} nk} \quad (3)$$

The adaptive filter in the k^{th} FFT bin has a single complex weight with a mean steady state value given by

$$W_k = R_{dx}^* / R_{xx}^* \quad (4)$$

where

$$R_{xx}^* = E [X_k(i) X_k^*(i)]$$

$$R_{dx}^* = E [D_k(i) X_k^*(i)] \quad (5)$$

For the particular case being considered here, the covariances are as follows.

$$R_{xx}^* = E \left[\sum_{n=0}^{M-1} \sum_{m=0}^{M-1} \left\{ S[(n+iR)T_s] + n_x[(n+iR)T_s] \right\} \left\{ S[(m+iR)T_s] + n_x[(m+iR)T_s] \right\} e^{-j \frac{2\pi}{m}(n-m)k} \right] = M\sigma_s^2 + M\sigma_n^2 \quad (6)$$

using the independence of $s(t)$ and $n_x(t)$, and the fact that both are uncorrelated in time. Also

$$R_{dx}^* = E \left[\sum_{n=0}^{M-1} \sum_{m=0}^{M-1} \left\{ S[(n+iR-\Delta)T_s] + n_d[(n+iR)T_s] \right\} \left\{ S[(m+iR)T_s] + n_x[(m+iR)T_s] \right\} e^{-j \frac{2\pi}{m}(n-m)k} \right] = (M-\Delta)\sigma_s^2 e^{-j \frac{2\pi}{m}\Delta k} \quad (7)$$

This results because $E \left\{ s[(n+ik)T_s] s^*[(m+iR+\Delta)T_s] \right\} = 0$ except when $m = n - \Delta$, and this occurs only $(M - \Delta)$ times over the range of the double summation.

Therefore the mean steady state weight in the kth frequency bin is

$$\bar{W}_k = \frac{(M-\Delta) \sigma_s^2}{M(\sigma_s^2 + \sigma_{nx}^2)} e^{-j \frac{2\pi}{M} \Delta k} \quad (8)$$

The error output for this weight is

$$\epsilon_k^{(i)} = D_k^{(i)} - \frac{(M-\Delta) \sigma_s^2}{M(\sigma_s^2 + \sigma_{nx}^2)} e^{-j \frac{2\pi}{M} \Delta k} X_k^{*(i)} \quad (9)$$

so the mean square error in the kth bin is

$$E[\epsilon_k^2(i)] = M \sigma_s^2 \left[1 - \left(\frac{M-\Delta}{M} \right)^2 \left(\frac{\sigma_s^2}{\sigma_s^2 + \sigma_n^2} \right) \right] + M \sigma_{nd}^2 \quad (10)$$

In order to compare the steady state results with that of the time domain filter, we need the inverse FFT of the vector of complex frequency domain weights. From (8), it can be seen that the nth time domain weight will be

$$\bar{a}_n = \frac{1}{M} \sum_{k=0}^{M-1} \bar{W}_k e^{j \frac{2\pi}{M} nk} = \begin{cases} 0, & n \neq \Delta, \\ \frac{(M-\Delta) \sigma_s^2}{M(\sigma_s^2 + \sigma_{nx}^2)}, & n = 0, 1, \dots, M-1 \end{cases} \quad (11)$$

The corresponding total mean square error is

$$E[\epsilon^2(i)] = \frac{1}{M^2} \sum_{k=0}^{M-1} E[\epsilon_k^2(i)] = \sigma_s^2 \left[1 - \left(\frac{M-\Delta}{M} \right)^2 \frac{\sigma_s^2}{\sigma_s^2 + \sigma_{nx}^2} \right] + \sigma_{nd}^2 \quad (12)$$

These are to be compared to values attained by the time domain weight vector,

$$\bar{b}_n = \begin{cases} 0 & , \quad n \neq \Delta, \\ \frac{\sigma_s^2}{\sigma_s^2 + \sigma_{n_x}^2} & , \quad n = \Delta, \end{cases} \quad n = 0, 1, \dots, M-1 \quad (13)$$

and mean square error,

$$E \left[\epsilon_t^2(i) \right] = \left[1 - \left(\frac{\sigma_s^2}{\sigma_s^2 + \sigma_n^2} \right) \right] \sigma_s^2 + \sigma_{n_d}^2 \quad (14)$$

Comparing (11), (12), (13), and (14), it can be seen that for $\Delta = 0$ the two filter implementations yield identical steady state results. Further, if the delay, Δ , is a small fraction of the FFT size, M , then

$$\frac{M - \Delta}{M} \approx 1$$

and the two implementations are essentially the same in steady state. This places a specification on the size of the FFTs to be used in the frequency implementation of an adaptive tracker. It is also interesting to observe that the steady state of the frequency domain implementation of the adaptive tracker does not depend upon R . This means that, at least with respect to steady state performance, use of overlapping or gap FFT processing will not affect the tracker performance.

2. Transient Comparison of the Time and Frequency Domain Implementations

The two implementations can be compared by examining the difference equations for the mean value of the weights in both cases using the inputs in the previous section. For the time domain, the difference equation for the m^{th} weight is

$$W_m(n+1) = W_m(n) + \mu \left[d(n) - \sum_p W_p(n) X_p(n) \right] X_m(n) \quad (15)$$

which when averaged is

$$E \left[W_m(n+1) \right] = E \left[W_m(n) \right] + \mu \left\{ E \left[d(n) X_m(n) \right] - E \left[X_m(n) \sum_p W_p(n) X_p(n) \right] \right\} \quad (16)$$

From the previous section,

$$E \left[d(n) X_m(n) \right] = E \left\{ \left[S(n-\Delta) + n_d(n) \right] \left[S(n-m) + n_x(n-m) \right] \right\} \\ = \begin{cases} \sigma_s^2 & \text{for } m = \Delta \\ 0 & \text{otherwise} \end{cases} \quad (17)$$

and

$$E \left[X_m(n) \sum_p W_p(n) X_p(n) \right] = E \left[W_m(n) \right] \left(\sigma_s^2 + \sigma_n^2 \right) \quad (18)$$

so that

$$E \left[W_m(n+1) \right] = E \left[W_m(n) \right] \left[1 - \mu (\sigma_s^2 + \sigma_n^2) \right] + \mu \sigma_s^2 \delta_{m\Delta}$$

where

$$\delta_{m \Delta} = \begin{cases} 1 & \text{if } m = \Delta \\ 0 & \text{otherwise} \end{cases} \quad (19)$$

In the frequency domain, the difference equation for the mean of the complex weight on the k^{th} FFT bin, is

$$\begin{aligned} E [W_k (n+1)] &= E [W_k (n)] + \mu E \left\{ [D_k (n) - W_k (n) X_k (n)] X_k^* (n) \right\} \\ &= E [W_k (n)] \left\{ 1 - \mu E [|X_k (n)|^2] \right\} + \mu E [D_k (n) X_k^* (n)] \end{aligned} \quad (20)$$

These terms were also evaluated in the previous section, where

$$E [X_k (n) X_k^* (n)] = M (\sigma_s^2 + \sigma_n^2)$$

and

$$E [D_k (n) X_k^* (n)] = (M - \Delta) \sigma_s^2 e^{-j \frac{2\pi}{M} \Delta k}$$

Thus

$$E [W_k (n+1)] = E [W_k (n)] \left\{ 1 - \mu M (\sigma_s^2 + \sigma_n^2) \right\} + \mu (M - \Delta) \sigma_s^2 e^{-j \frac{2\pi}{M} \Delta k} \quad (21)$$

This expression can be inverse transformed to return to a time domain weight vector for comparison with the time domain implementation. By transforming back,

$$E [W_m (n+1)] = E [W_m (n)] \left[1 - \mu M (\sigma_s^2 + \sigma_n^2) \right] + \mu (M - \Delta) \sigma_s^2 \delta_{m \Delta} \quad (22)$$

Equations (19) and (22) are now to be compared for transient response and weight fluctuations. This is most readily done for the $\Delta = 0$ case. If the feedback coefficients are distinguished from one another by letting μ_T and μ_F be the time and frequency domain coefficients respectively, then

$$\begin{aligned}\mu_T &= \mu \\ \mu_F &= M\mu\end{aligned}\tag{23}$$

to equate the two difference equations. The steady-state results then agree exactly, where for $\Delta = 0$ the windowing effects are neglected.

The time constant for the adaptive algorithm is $T_c = \frac{1}{2\mu P_{in}}$. The input power, P_{in} , is larger in the time domain by a factor of M , which is precisely the factor by which μ_F is larger than μ_T . Thus the μP_{in} product is the same for both systems and therefore the time responses are equal.

The fluctuations of the weights can be compared using results derived in the second quarter report. For the time domain filter with uncorrelated inputs

$$\lim_{n \rightarrow \infty} \text{Var} [W_m(n) | H_0] = \frac{\mu_T \sigma_{n,T}^2}{2 - (m+2)\mu_T \sigma_{n,T}^2}$$

and for the frequency domain

$$\lim_{n \rightarrow \infty} \text{Var} [W_k(n)] = \frac{\mu_F \sigma_{n,F}^2}{2 - 2\mu_F \sigma_{n,F}^2}$$

Again, for the time domain implementation, $\sigma_{n,T}^2$ is in the full band, whereas for the frequency domain $\sigma_{n,F}^2$ is in the FFT bin, so that

$$\sigma_{n,T}^2 = M \sigma_{n,F}^2$$

Thus for the frequency domain

$$\lim_{n \rightarrow \infty} \text{Var} [W_k(n) | H_0] = \frac{\mu_F \sigma_n^2 / M}{2 - 2\mu_F \frac{\sigma_n^2}{M}} = \frac{\mu \sigma_n^2 / M}{2 - 2\mu \sigma_n^2 / M}$$

and for the time domain

$$\lim_{n \rightarrow \infty} \text{Var} [W_m(n)] = \frac{\mu_T \sigma_n^2}{2 - (M+2)\mu_T \sigma_n^2} = \frac{\mu \sigma_n^2 / M}{2 - \frac{(M+2)\mu \sigma_n^2}{M}}$$

The variances differ by the ratio

$$\frac{2 - 2\frac{\mu}{M}\sigma_n^2}{2 - \frac{(M+2)}{M}\mu\sigma_n^2}$$

which is approximately unity for $\mu\sigma_n^2$ small.

It is thus concluded that for all practical purposes, the frequency domain adaptive filter model is equivalent to the time domain adaptive filter.

APPENDIX III
MEAN AND VARIANCE OF A SINGLE COMPLEX TAP WEIGHT
WITH SIGNAL AND NOISE INPUTS

In narrow bands at the FFT output, the adaptive filter is a single complex weight. The weight update equations are given by

$$W(n+1) = W(n) + \mu \epsilon(n) x^*(n)$$

$$\epsilon(n) = d(n) - y(n) = \text{error (cancelled) waveform}$$

$$y(n) = W(n) x(n) = \text{filter output}$$

$$d(n) = \text{reference waveform}$$

$$x(n) = \text{input data sequence}$$

$$W(n) = \text{complex weight}$$

$$\mu = \text{feedback coefficient.}$$

Thus the filter is described here at the n th time iteration on the data sequence of a particular FFT bin. One such device operates on each of the FFT bins spanning the signal bandwidth.

Consider again the structure in Figure 5, where the common plane wave component is denoted by $I(n)$. Then

$$d(n) = \alpha I(n) + n_1(n)$$

$$x(n) = I(n) + n_2(n)$$

where α is the complex coefficient for the inter-array phase shift.

It is assumed that the input sequences are zero mean, gaussian, independent of one another, and uncorrelated in time.

The error sequence $\epsilon(n)$ is

$$\epsilon(n) = \alpha I(n) - W(n)I(n) + n_1(n) - W(n) n_2(n)$$

The mean square error is

$$E[|\epsilon(n)|^2] = E\left\{|\alpha I(n) - W(n)I(n)|^2 + \left[|n_1(n)|^2 + |n_2(n)W(n)|^2\right]\right\}$$

The variance of the weight, $\text{Var}[W(n)]$, is needed to compute the output power. The weight variance is computed as follows. The weight update equation is rewritten as

$$W(n+1) = W(n) \left[1 - \mu |x(n)|^2\right] + \mu d(n)x^*(n)$$

The solution to this difference equation is given by

$$W(n+1) = W(0) \prod_{k=0}^n (1 - \mu |x(k)|^2) + \mu \sum_{m=0}^n d(m) x^*(m) \prod_{k=m+1}^n [1 - \mu |x(k)|^2]$$

where

$$\prod_{k=n+1}^n () \triangleq 1$$

The initial weight $W(0)$ can be set to zero.

Let

$$F(m) = d(m)x^*(m) \prod_{k=m+1}^n [1 - \mu |x(k)|^2]$$

Averaging to obtain the mean weight yields

$$\begin{aligned} E[W(n+1)] &= \mu \sum_{m=0}^n E[F(m)] = \mu \sum_{m=0}^n E[d(m)x^*(m)] \prod_{k=m+1}^n E[1 - \mu |x(k)|^2] \\ &= \mu \sum_{m=0}^n \sigma_1^2 [1 - \mu \sigma_2^2]^{n-m} \end{aligned}$$

where it is assumed that

$$E[d(m)x^*(m)] = \sigma_1^2$$

$$E[|x(m)|^2] = \sigma_2^2$$

For $d(m) = \alpha I(m) + n_1(m)$

and $x(m) = I(m) + n_2(m)$

where n_1 and n_2 are independent,

$$\sigma_1^2 = \alpha \sigma_I^2$$

and

$$\sigma_2^2 = \sigma_I^2 + \sigma_n^2$$

The summation can be expressed in closed form as

$$E[W(n+1)] = \frac{\alpha \sigma_I^2}{\sigma_I^2 + \sigma_n^2} \left\{ 1 - \left[1 - \mu (\sigma_I^2 + \sigma_n^2) \right]^{n+1} \right\}$$

In steady state,

$$\lim_{n \rightarrow \infty} E[W(n+1)] = \frac{\alpha \sigma_I^2}{\sigma_I^2 + \sigma_n^2}$$

To obtain the variance the mean squared weight is needed.

$$E[|W(n+1)|^2] = \mu^2 \sum_{m=0}^n \sum_{q=0}^n E[F(m)F^*(q)] = \mu^2 \sum_{m=0}^n E[|F(m)|^2] \\ + 2\mu^2 \sum_{m=0}^n \sum_{q=0}^{m-1} E[F(m)F^*(q)]$$

The single sum is treated first.

$$E[|F(m)|^2] = E \left\{ |d(m)x(m)|^2 \prod_{p=m+1}^n \prod_{q=m+1}^n \left[1 - \mu |x(p)|^2 \right] \left[1 - \mu |x(q)|^2 \right] \right\} \\ = E \left[|d(m)x(m)|^2 \prod_{p=m+1}^n E \left\{ \left[1 - \mu |x(p)|^2 \right]^2 \right\} \right]$$

The expectation separates because the terms in the product involve inputs at later times, which are uncorrelated. Using the gaussian assumption,

$$E \left[|d(m)x(m)|^2 \right] = \left(|\alpha|^2 \sigma_I^2 + \sigma_n^2 \right) \left(\sigma_I^2 + \sigma_n^2 \right) + 2|\alpha|^2 \sigma_I^4 \\ E \left\{ \left[1 - \mu |x(p)|^2 \right]^2 \right\} = 1 - 2\mu \left(\sigma_I^2 + \sigma_n^2 \right) + 2\mu^2 \left(\sigma_I^2 + \sigma_n^2 \right)^2$$

Thus

$$\mu^2 \sum_{m=0}^n E[|F(m)|^2] = \frac{\mu \left\{ |\alpha|^2 \sigma_I^2 + \sigma_n^2 \right\} \left[\sigma_I^2 + \sigma_n^2 \right] + 2|\alpha|^2 \sigma_1^4}{\left(\sigma_n^2 + \sigma_I^2 \right) \left[2 - 2\mu \left(\sigma_n^2 + \sigma_I^2 \right) \right]} \cdot \left[1 - \left(1 - 2\mu \left(\sigma_n^2 + \sigma_I^2 \right) + 2\mu^2 \left(\sigma_n^2 + \sigma_I^2 \right)^2 \right)^{n+1} \right]$$

The double sum term in $E[W^2(n+1)]$ involves $E[F(m)F(q)]$ which is treated as follows

$$E[F(m)F^*(q)] = E \left\{ d(m)x^*(m)d(q)x^*(q) \prod_{p=m+1}^n \prod_{v=q+1}^n \left[1 - \mu |x(p)|^2 \right] \left[1 - \mu |x(v)|^2 \right] \right\}$$

In the double sum, $q < m$, so that

$$\prod_{p=m+1}^n \prod_{v=q+1}^n (\quad) = \prod_{p=m+1}^n \prod_{v=m+1}^n \prod_{v=q+1}^m (\quad) .$$

Thus, since both p and v range over indices that are greater than m and q ,

$$E[F(m)F^*(q)] = E \left\{ \prod_{p=m+1}^n \prod_{v=m+1}^n \left[1 - \mu |x(p)|^2 \right] \left[1 - \mu |x(v)|^2 \right] \right\} \cdot E \left\{ d(m)x^*(m)d(q)x^*(q) \prod_{v=q+1}^m \left[1 - \mu |x(v)|^2 \right] \right\}$$

The first expectation is identical to $E[F^2(m)]$, evaluated previously. The second expectation, since q is always less than m , is

$$E \left\{ d(m)x^*(m)d(q)x^*(q) \prod_{v=q+1}^m \left[1 - \mu |x(v)|^2 \right] \right\} = E[d(q)x^*(q)] E \left\{ d(m)x^*(m) \left[1 - \mu |x(m)|^2 \right] \right\}$$

$$\prod_{v=q+1}^{m-1} E \left[1 - \mu |x(v)|^2 \right]$$

The expectation in the center is

$$E\left\{d(m)x^*(m) - \mu d(m)x^3(m)\right\} = \alpha \sigma_I^2 - 2\mu \alpha \sigma_I^2 (\sigma_I^2 + \sigma_n^2)$$

Combining the above,

$$E[F(m)F^*(q)] = \left[1 - 2\mu (\sigma_I^2 + \sigma_n^2) + 2\mu^2 (\sigma_I^2 + \sigma_n^2)^2 \right]^{n-m} \\ \cdot \left[1 - \mu (\sigma_I^2 + \sigma_n^2) \right]^{m-q-1} |\alpha|^2 \sigma_I^4 \left[1 - 2\mu (\sigma_I^2 + \sigma_n^2) \right]$$

The double sum term is then

$$r^2 \sum_{m=0}^n \sum_{q=0}^{m-1} E[F(m)F^*(q)] = \mu^2 |\alpha|^2 \sigma_I^4 \left[1 - 2\mu (\sigma_I^2 + \sigma_n^2) \right] \\ \cdot \sum_{m=0}^n \left[1 - 2\mu (\sigma_I^2 + \sigma_n^2) + 2\mu^2 (\sigma_I^2 + \sigma_n^2)^2 \right]^{n-m} \\ \cdot \sum_{q=0}^{m-1} \left[1 - \mu (\sigma_I^2 + \sigma_n^2) \right]^{m-q-1} \\ = \mu^2 |\alpha|^2 \sigma_I^4 \left[1 - 2\mu (\sigma_I^2 + \sigma_n^2) \right] \\ \cdot \sum_{m=0}^n \left[1 - 2\mu (\sigma_I^2 + \sigma_n^2) + 2\mu^2 (\sigma_I^2 + \sigma_n^2)^2 \right]^{n-m} \\ \cdot \left(\frac{1 - \left[1 - \mu (\sigma_I^2 + \sigma_n^2) \right]^m}{\mu (\sigma_I^2 + \sigma_n^2)} \right)$$

AD-A063 392

HUGHES AIRCRAFT CO FULLERTON CALIF GROUND SYSTEMS GROUP
ADAPTIVE TRACKING SYSTEM STUDY.(U)

F/6 17/1

OCT 78 P L FEINTUCH, F A REED, N J BERSHAD
FR78-11-1345

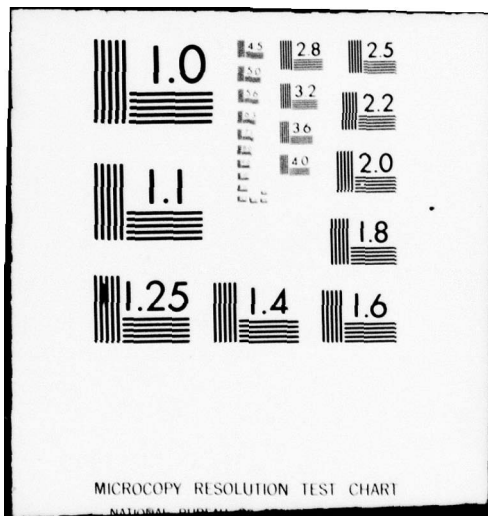
N00024-77-C-6251
NL

UNCLASSIFIED

2 of 2
AD
A063 392



END
DATE
FILMED
3-79
DDC



MICROCOPY RESOLUTION TEST CHART

NATIONAL BUREAU OF STANDARDS-1963-A

$$r^2 \sum_{m=0}^n \sum_{q=0}^{m-1} E[F(m)F^*(q)] = \mu^2 |\alpha|^2 \sigma_I^4 \left[1 - 2\mu(\sigma_I^2 + \sigma_n^2) \right]$$

$$\left\{ \sum_{m=0}^n \frac{\left[1 - 2\mu(\sigma_I^2 + \sigma_n^2) + 2\mu^2(\sigma_I^2 + \sigma_n^2)^2 \right]^{n-m}}{\mu(\sigma_I^2 + \sigma_n^2)} \right.$$

$$\left. - \sum_{m=0}^n \frac{\left[1 - 2\mu(\sigma_I^2 + \sigma_n^2) + 2\mu^2(\sigma_I^2 + \sigma_n^2)^2 \right]^{n-m} \left[1 - \mu(\sigma_I^2 + \sigma_n^2) \right]^n}{\mu(\sigma_I^2 + \sigma_n^2) \left[1 - \mu(\sigma_I^2 + \sigma_n^2) \right]^{n-m}} \right\}$$

$$= \frac{\mu |\alpha|^2 \sigma_I^4}{\sigma_I^2 + \sigma_n^2} \left[1 - 2\mu(\sigma_I^2 + \sigma_n^2) \right] \left\{ \frac{1 - \left[1 - 2\mu(\sigma_I^2 + \sigma_n^2) + 2\mu^2(\sigma_I^2 + \sigma_n^2)^2 \right]^{n+1}}{\mu(\sigma_I^2 + \sigma_n^2) \left[2 - 2\mu(\sigma_I^2 + \sigma_n^2) \right]} \right.$$

$$\left. - \left[1 - \mu(\sigma_I^2 + \sigma_n^2) \right]^n \frac{\left(1 - \frac{\left[1 - 2\mu(\sigma_I^2 - \sigma_n^2) + 2\mu^2(\sigma_I^2 + \sigma_n^2)^2 \right]^{n+1}}{1 - \mu(\sigma_I^2 + \sigma_n^2)} \right)}{1 - \frac{\left[1 - 2\mu(\sigma_I^2 + \sigma_n^2) + 2\mu^2(\sigma_I^2 + \sigma_n^2)^2 \right]}{1 - \mu(\sigma_I^2 + \sigma_n^2)}} \right\}$$

$$= \left(\frac{|\alpha| \sigma_I^2}{\sigma_I^2 + \sigma_n^2} \right)^2 \left[1 - 2\mu(\sigma_I^2 + \sigma_n^2) \right] \left\{ \frac{1 - \left[1 - 2\mu(\sigma_I^2 + \sigma_n^2) + 2\mu^2(\sigma_I^2 + \sigma_n^2)^2 \right]^{n+1}}{2 - 2\mu(\sigma_I^2 + \sigma_n^2)} \right.$$

$$\left. - \frac{\left[1 - \mu(\sigma_I^2 + \sigma_n^2) \right]^{n+1} - \left[1 - 2\mu(\sigma_I^2 + \sigma_n^2) + 2\mu^2(\sigma_I^2 + \sigma_n^2)^2 \right]^{n+1}}{1 - 2\mu(\sigma_I^2 + \sigma_n^2)} \right\}$$

Thus in steady-state,

$$\lim_{n \rightarrow \infty} E\left[|W(n+1)|^2\right] = \frac{\mu \left\{ \left[\frac{|\alpha|^2 \sigma_I^2 + \sigma_n^2}{\sigma_I^2 + \sigma_n^2} \right] \left[\sigma_I^2 + \sigma_n^2 \right] + 2|\alpha|^2 \sigma_I^4 \right\}}{(\sigma_I^2 + \sigma_n^2) \left[2 - 3\mu(\sigma_I^2 + \sigma_n^2) \right]}$$

$$+ 2 \left(\frac{|\alpha| \sigma_I^2}{\sigma_I^2 + \sigma_n^2} \right)^2 \frac{\left[1 - 2\mu(\sigma_I^2 + \sigma_n^2) \right]}{2 - 2\mu(\sigma_I^2 + \sigma_n^2)}$$

To obtain the variance, subtract the mean steady-state weight squared, with the result that

$$\text{Var}[W(\infty)] = \frac{\mu \sigma_n^2 \left[(|\alpha|^2 + 1) \sigma_I^2 + \sigma_n^2 \right]}{(\sigma_I^2 + \sigma_n^2) \left[2 - 2\mu(\sigma_I^2 + \sigma_n^2) \right]}$$

For a special case, if $\sigma_I^2 \gg \sigma_n^2$

$$\text{Var}[W(\infty)] \approx \frac{\mu \sigma_n^2 (|\alpha|^2 + 1)}{2 - 2\mu \sigma_I^2}$$

To determine the cancellation level, the above result is used in the evaluation of the mean squared error, i.e., the power in the canceller output.

$$E\left[|\epsilon(n)|^2\right] = E\left\{ \left| \alpha I(n) + n_1(n) - W(n) \left[I(n) + n_2(n) \right] \right|^2 \right\}$$

$$E \left[|\epsilon(n)|^2 \right] = E \left\{ |\alpha - W(n)|^2 \right\} \sigma_I^2 + \sigma_n^2 \left\{ 1 + E \left[W^2(n) \right] \right\}$$

$$= \sigma_I^2 \left\{ |\alpha|^2 - 2\alpha E[W(n)] + \text{Var} [W(n)] + E^2 [W(n)] \right\} + \sigma_n^2 \left\{ 1 + \text{Var} [W(n)] + E^2 [W(n)] \right\}$$

In steady-state

$$E \left[|\epsilon(\infty)|^2 \right] = \sigma_I^2 \left\{ \left(\frac{|\alpha| \sigma_n^2}{\sigma_I^2 + \sigma_n^2} \right)^2 + \frac{\mu \sigma_n^2 (\alpha^2 + 1)}{2 - 2\mu \sigma_I^2} \right\} + \sigma_n^2 \left\{ 1 + \frac{\mu \sigma_n^2 (\alpha^2 + 1)}{2 - 2\mu \sigma_I^2} \right\}$$

$$+ \left(\frac{|\alpha| \sigma_I^2}{\sigma_I^2 + \sigma_n^2} \right)^2 \left\{ \right.$$

For the special case where $\sigma_I^2 \gg \sigma_n^2$

$$E \left[|\epsilon(\infty)|^2 \right] \approx (1 + |\alpha|^2) \frac{\sigma_n^2 (1 - \mu \sigma_I^2)}{2 - 2\mu \sigma_I^2}$$

If, in addition, $\mu \sigma_I^2 \ll 1$, then

$$E \left[|\epsilon(\infty)|^2 \right] \approx (1 + |\alpha|^2) \sigma_n^2$$

and the common waveform has been cancelled down to the uncorrelated noise flow.

For the tracking problem, the low signal-to-noise ratio case is more critical.

For $\sigma_n^2 \gg \sigma_I^2$,

$$E \left[|\epsilon(\infty)|^2 \right] \approx \sigma_n^2 \left(1 + \mu \sigma_n^2 \frac{|\alpha|^2 + 1}{2} \right) + |\alpha|^2 \sigma_I^2$$

The time response is given by the time constant, τ_c , for the LMS algorithm (1) which can be approximated by

$$\tau_c \approx \frac{\Delta}{2\mu P_{in}}$$

where

Δ = time between iterations

P_{in} = total input power.

These results can now be used to evaluate tracker performance in Appendix IV.

APPENDIX IV
VARIANCE OF THE SPLIT BEAM ADAPTIVE BEARING ESTIMATOR
AND COMPARISON TO CRLB

With reference to Figure 6, for the continuous adaptive filter, it is assumed that

$$X_L(t) = s(t - \frac{d}{c} \sin \theta) + n_L(t)$$

$$X_R(t) = s(t) + n_R(t)$$

where $s(t)$, $n_L(t)$, and $n_R(t)$ are zero mean, white random processes on $[\omega_L, \omega_U]$ with power P_S , P_N , and P_N , respectively.

Also

d = distance between phase centers of half arrays

c = speed of sound

θ = angle between plane wavefront and axis of phase centers

The length of the adaptive filter is assumed to be long in comparison to the correlation times of the random processes involved.

Let the steady-state impulse response of the filter be $h(t)$ and the transfer function $H(\omega)$. The mean value of the impulse response is the Wiener filter, so, from Appendix III, the corresponding mean transfer function is

$$E[H(\omega)] = \frac{P_S}{P_S + P_N} e^{-j\omega \frac{d}{c} \sin \theta}$$

and the correlation of the transfer function is

$$E[H(\omega_1)H^*(\omega_2)] = \frac{2\pi \mu P_N [2P_S + P_N]}{(P_S + P_N) [2 - 2\mu(P_S + P_N)]} \delta(\omega_1 - \omega_2) + \left(\frac{P_S}{P_S + P_N}\right)^2 e^{-j(\omega_1 - \omega_2) \frac{d}{c} \sin \theta}$$

The angle, θ , is to be estimated by determining the value of τ for which the impulse response, $h(\tau)$, is a maximum. This is an estimate of the delay between arrivals of the signal wavefront at the half array phase centers, and can be converted to a bearing estimate, $\hat{\theta}$, using

$$\tau = \frac{d}{c} \sin \theta.$$

The value of $\hat{\theta}$ for which $h(\tau)$ is peaked corresponds to the value for which the derivative of $h(\tau)$ with respect to θ is zero. In the neighborhood of the zero crossing the derivative of the impulse response is approximately linear. The fluctuations in the derivative of the transfer function then map through the linear function to provide an estimate of the mean square error in the angle estimate. Thus the mean value of the derivative of the transfer function, the standard deviation of the derivative of the transfer function, and the slope of the mean of the derivative of the transfer function are required, at the point where $\hat{\theta} = \theta$. Then the errors in the transfer function can be mapped into the errors in one's ability to extract the peak of the transfer function as follows:

$$\text{Var}^{1/2} [\hat{\theta}] = \frac{\text{Var}^{1/2} \left[\frac{\partial h(\tau)}{\partial \tau} \right]}{\frac{\partial E \left[\frac{\partial h(\tau)}{\partial \tau} \right]}{\partial \theta}} \bigg|_{\tau = \frac{d}{c} \sin \theta}$$

This approach is motivated by the treatment of BDI split beam trackers by MacDonald and Schultheiss in Reference [1]. The derivative of the impulse response and its statistics are

$$\begin{aligned} \frac{d}{d\tau} h(\tau) &= \frac{1}{2\pi} \int_{-\infty}^{\infty} j\omega H(\omega) e^{j\omega\tau} d\omega \\ E \left[\frac{d h(\tau)}{d\tau} \right] &= \frac{1}{2\pi} \int_{-\infty}^{\infty} j\omega \frac{P_S}{P_S + P_N} e^{-j\omega \frac{d}{c} \sin \theta} e^{j\omega\tau} d\omega \\ &= \frac{1}{\pi} \frac{P_S}{P_S + P_N} \int_{\omega_L}^{\omega_V} d\omega \omega \sin \left[\omega \left(\tau - \frac{d}{c} \sin \theta \right) \right] \end{aligned}$$

where the band is assumed to be limited to (ω_L, ω_U) . The mean value of the derivative passes through zero when $\tau = d/c \sin \theta$, so that determination of the zero crossing provides an unbiased estimate of θ . The variance of the derivative is needed as well.

$$\text{Var} \left[\frac{dh(\tau)}{d\tau} \right] = E \left[\left(\frac{dh(\tau)}{d\tau} \right)^2 \right] - E^2 \left[\frac{dh(\tau)}{d\tau} \right]$$

Note that the mean value of the derivative is zero when $\hat{\theta} = \theta$ so that the variance is the mean square value at this point.

$$\text{Var} \left[\frac{dh(\tau)}{d\tau} \right] = \frac{1}{(2\pi)^2} \int_{-\infty}^{\infty} \int_{-\infty}^{\infty} \omega_1 \omega_2 E \left[H(\omega_1) H^*(\omega_2) \right] e^{j\nu(\omega_1 - \omega_2)} d\omega_1 d\omega_2$$

where $\nu = \tau - d/c \sin \theta$. Using the correlation of the transfer function, the variance is

$$\begin{aligned} \text{Var} \left[\frac{dh(\tau)}{d\tau} \right] &= \frac{1}{(2\pi)^2} \int_{-\infty}^{\infty} \int_{-\infty}^{\infty} K_1 \omega_1 \omega_2 e^{j\nu(\omega_1 - \omega_2)} (2\pi) (\omega_1 - \omega_2) d\omega_1 d\omega_2 \\ &\quad + \frac{1}{(2\pi)^2} \int_{-\infty}^{\infty} \int_{-\infty}^{\infty} K_2 \omega_1 \omega_2 e^{j\nu(\omega_1 - \omega_2)} d\omega_1 d\omega_2 \end{aligned}$$

where

$$K_1 = \frac{\mu P_N [2P_S + P_N]}{(P_S + P_N) [2 - 2\mu (P_S + P_N)]}$$

$$K_2 = \left(\frac{P_S}{P_S + P_N} \right)^2$$

The second integral is zero, when $\nu = 0$, and the delta function reduces the first double integral to a single integral, with the result that

$$\text{Var} \left[\frac{dh(\tau)}{d\tau} \right] = \frac{2}{(2\pi)^2} \frac{(2\pi) \mu P_N [2P_S + P_N]}{(P_S + P_N) [2 - 2\mu (P_S + P_N)]} \left[\frac{\omega_U^3 - \omega_L^3}{3} \right]$$

where again the processes are band limited to (ω_L, ω_U) . Since $\tau = d/c \sin \theta$,

$$\frac{\partial h(\tau)}{\partial \theta} = \frac{\partial h(\tau)}{\partial \tau} \frac{\partial \tau}{\partial \theta} = \frac{d}{c} \cos \theta \frac{dh(\tau)}{d\tau}.$$

The denominator of the expression for $\text{Var } [\theta]$ is

$$\begin{aligned} \frac{\partial E \left[\frac{\partial h(\tau)}{\partial t} \right]}{\partial \theta} &= \frac{d \cos \theta}{c} \frac{d}{d\tau} E \left[\frac{dh(\tau)}{d\tau} \right] \\ \tau &= \frac{d}{c} \sin \theta \\ &= \frac{d \cos \theta}{c} \frac{d}{d\tau} \left\{ \frac{1}{\pi} \frac{P_S}{P_S + P_N} \int_{\omega_L}^{\omega_U} d\omega \omega^2 \cos \left[\omega \left(\tau - \frac{d}{c} \sin \theta \right) \right] \right\} \\ &= \frac{d \cos \theta}{c} \frac{1}{\pi} \frac{P_S}{P_S + P_N} \left[\frac{\omega_U^3 - \omega_L^3}{3} \right] \end{aligned}$$

Thus,

$$\text{Var}^{1/2} [\hat{\theta}] = \frac{c \sqrt{2\pi}}{\sqrt{2} d \cos \theta} \left[\frac{\mu P_N}{P_S^2} \frac{(P_S + P_N)(2P_S + P_N)}{2 - 2\mu(P_S + P_N)} \right]^{1/2} \left[\frac{\omega_U^3 - \omega_L^3}{3} \right]^{-1/2}$$

The behavior with extreme cases of signal-to-noise ratio is of interest. For $P_S \gg P_N$,

$$\text{Var}^{1/2} [\hat{\theta}] \approx \frac{c \sqrt{2\pi}}{\sqrt{2} d \cos \theta} [\mu P_N]^{1/2} \left[\frac{\omega_U^3 - \omega_L^3}{3} \right]^{1/2}$$

and for $P_S \ll P_N$,

$$\text{Var}^{1/2} [\hat{\theta}] \approx \frac{c \sqrt{2\pi}}{2d \cos \theta} \frac{P_N}{P_S} (\mu P_N)^{1/2} \left[\frac{\omega_U^3 - \omega_L^3}{3} \right]^{-1/2}$$

The critical concern is the behavior of the variance at low signal-to-noise ratios.

The objective therefore is to compare the above expression with a performance measure which is invariant with processor structure. The Cramer-Rao Lower Bound (CRLB) is such a measure. The last equation in this section is therefore related to the CRLB in the next section.

COMPARISON WITH THE CRLB

The Cramer-Rao Lower Bound (CRLB) provides a lower bound on the variance attainable by any unbiased estimate of a parameter. It is computed in Reference [1] and repeated here for comparison with the variance obtained by the adaptive filter bearing estimator. From equation (19) of [1].

$$\text{Var}^{1/2} [\theta] \geq \frac{\sqrt{\pi} c}{d \cos \theta \sqrt{T}} \left[\frac{P_S^2 / P_N^2}{1 + 2 P_S / P_N} \right]^{-1/2} \left[\frac{\omega_U^3 - \omega_L^3}{3} \right]^{-1/2}$$

For small signal-to-noise ratios, i. e., $P_S \ll P_N$,

$$\text{Var}^{1/2} [\theta] \geq \frac{\sqrt{\pi} c}{d \cos \theta \sqrt{T}} \frac{P_N}{P_S} \left[\frac{\omega_U^3 - \omega_L^3}{3} \right]^{-1/2}$$

where a total observation time of T seconds is assumed, P_S/P_N is the signal-to-noise ratio at the split array output, and d is the distance between half array phase centers.

Since μP_N applies to the discrete version of the adaptive filter and the CRLB uses continuous data we must relate the discrete adaptive filter weight updates to a continuous process. Let μ_d and μ_c correspond to the feedback coefficients in the discrete and continuous versions respectively. In discrete form

$$W((n+1)\Delta) = W(n\Delta) + \mu_d \epsilon(n\Delta) x(n\Delta)$$

or

$$\frac{W((n+1)\Delta) - W(n\Delta)}{\Delta} = \frac{\mu_d \epsilon(n\Delta) x(n\Delta)}{\Delta}$$

Taking appropriate limits provides the differential equation form, i. e. ,

$$\frac{dw(t)}{dt} = \mu_c \epsilon(t) x(t)$$

Thus for the continuous case $\mu_c = \mu_d/\Delta$. This can also be interpreted as though the power spectrum in the continuous case is the discrete power spectrum times Δ , with μ fixed in both.

One other term must be reconciled for the two expressions to be compared, the relation between μP_N and the value of $E[H(\omega)]$ at $t = \tau$. Previously it was assumed that the mean transfer function $E[H(\omega)]$ had reached a steady state value when determining $\text{Var}^{1/2}[\hat{\theta}]$ above. Actually $E[H(\omega)]$ is a function of t and the expression for $E[H(\omega)]$ used in computing $\text{Var}^{1/2}[\hat{\theta}]$ above is $E[H(j\omega, \infty)]$. We desire $E[H(\omega, t)]$ where $t = 0$ is when the filter is turned on. It is easy to show that the continuous time approximation to $E[H(\omega, t)]$ is

$$\begin{aligned} E[H(\omega, t)] &= \left(\frac{P_S}{P_S + P_N} \right) e^{-j\omega \frac{d}{c} \sin\theta} \left[1 - e^{-t/T_c} \right] \\ &= E[H(\omega, \infty)] \left[1 - e^{-t/T_c} \right] \end{aligned}$$

where T_c is the time constant associated with the mean weights.

Furthermore we assume that the variance of the weights has already reached steady-state so that no correction for a transient variance term is required. From Appendix III, it can be seen that the time constant of the variance is approximately half as large as the time constant of the mean for $\mu(\sigma_I^2 + \sigma_n^2) \ll 1$.

Thus, taking into account the transient mean weight, for the continuous comparison, the variance of the adaptive filter bearing estimate becomes

$$\text{Var}^{1/2}[\hat{\theta}] = \frac{c \sqrt{2\pi}}{2d \cos\theta} \frac{P_N}{P_S} \left(\frac{\mu P_N}{\Delta} \right)^{1/2} \left[\frac{\omega_u^3 - \omega_L^3}{3} \right]^{-1/2} \left[1 - e^{-t/T_c} \right]^{-1}$$

The convergence time for the adaptive process, i. e., the time for the root-mean-square-error learning curve to decay by $1/e$ of its initial value, is

$$T_c = \frac{\Delta}{\mu P_N}$$

so that

$$\text{Var}^{1/2} [\hat{\theta}] = \frac{c \sqrt{2\pi}}{2 d \cos \theta \sqrt{T_c}} \frac{P_N}{P_S} \left[\frac{\omega_U^3 - \omega_L^3}{3} \right]^{-1/2} \left[1 - e^{-t/T_c} \right]^{-1}$$

Comparison with the CRLB at low signal-to-noise ratios results in the following ratio

$$\frac{\text{Var}^{1/2} [\hat{\theta}]}{\text{CRLB}} = \frac{1}{\sqrt{2}} \sqrt{\frac{T}{T_c}} \left[1 - e^{-T/T_c} \right]^{-1}$$

The optimum selection of T_c involves the trade-off between weight vector noise and mean value. Table 10 shows the ratio for various T/T_c . The minimum is at approximately $T/T_c = 1$ and is 1.13. Hence, the split-beam adaptive bearing tracker is only about 0.5 dB degraded from the CRLB.

It can thus be concluded that the adaptive filter can be used to estimate bearing in close proximity to the theoretical limits in performance. Although its performance degrades at low signal-to-noise ratios, so does that of all processors. Indeed, the split beam adaptive filter tracker behaves just as the CRLB, throughout the entire range of signal-to-noise ratios and bandwidths.

REFERENCES

1. V. H. MacDonald and P. M. Schultheiss, "Optimum Passive Bearing Estimation in a Spatially Incoherent Noise Environment," J. Acoustical Soc. of Am, Vol 46, No. 1, 1969.

TABLE 10 $\text{Var}^{1/2} [\hat{\theta}]/\text{CRLB}$ VS. T/T_c

| T/T_c | $\text{Var}^{1/2} [\hat{\theta}]/\text{CRLB}$ |
|---------|---|
| 0.49 | 1.25 |
| 1.00 | 1.13 |
| 2.00 | 1.16 |
| 4.00 | 1.43 |

APPENDIX V
DELAY ESTIMATION WITH A DISCRETE ADAPTIVE TRACKER

In the preceding section, an expression for the variance of the bearing estimate of a continuous adaptive filter configured as an adaptive tracker was developed. The estimate is based upon determination of the peak of the continuous impulse response of the adaptive filter. In practice, however, the adaptive filter is discrete in time and of finite length, and the peak of the impulse response must be determined by interpolating between the discrete sample points. The interpolation process increases the variance of the bearing estimate with respect to that of the continuous case. This section describes a numerical method of determining the peak of an interpolated impulse response, and develops an expression for the variance of the estimate using this method.

Let the discrete adaptive filter weights be denoted $h(mT_s)$ for $m = 0, 1, \dots, M-1$, with T_s the sample interval and M the number of taps in the time domain adaptive filter. The value of the weight vector at some time, t , between filter taps can be interpolated as

$$h_I(t) = \sum_{m=0}^{m-1} h(mT_s) \frac{\sin 2 B(t-mT_s)}{2 B(t-mT_s)} \quad (1)$$

This is a truncated expansion of the discrete samples in series of orthonormal functions. If the $h(mT_s)$ are samples of a perfectly bandlimited impulse response, $h(t)$, then (1) can be considered as a finite approximation to the sampling theorem.

In the adaptive tracking system, we are only interested in the location of the peak of $h_I(t)$, not in the entire function, so a numerical method is used to locate the peak. The peak of $h_I(t)$ will be in the vicinity of the $h(mT_s)$ with the largest value, so if the largest weight occurs for $m = q$, then the initial guess for the location of the peak is

$$t_0 = qT_s$$

The slope of $h_I(t)$ will be zero at the maximum, so a bisection technique is used to find the zero crossing of

$$h'_I(t) = \sum_{m=0}^{M-1} h(mT_s) \left[\frac{\cos 2 B(t-mT_s)}{t - mT_s} - \frac{\sin 2 B(t-mT_s)}{2 B(t-mT_s)^2} \right] \quad (2)$$

By observing the sign of $h'_I(t)$, at the current estimate, t_i , a new estimate is computed as

$$t_{i+1} = t_i + I \left[h'_I(t_i) \right] \delta_i \quad (3)$$

where

δ_i = current step size

and

$$I \left[h'_I(t_i) \right] = \begin{cases} +1 & \text{if } h'_I(t_i) > 0 \\ -1 & \text{if } h'_I(t_i) < 0 \end{cases}$$

Each time $h'_I(t_{i+1})$ and $h'_I(t_i)$ have opposite sign, the zero crossing has been passed, and the step size is divided by some $F > 1$. The procedure stops when

$$-\epsilon \leq h'_I(t_j) \leq \epsilon \quad (4)$$

in which case t_j is the estimated location of the zero crossing, and hence, the estimated delay between the tracker inputs.

The variance of this estimate can be determined in the same way as that using the continuous adaptive tracker in the preceding section. When the tracker is implemented in the frequency domain, as shown in Figure 5, the mean and variance of the complex weight in the k th frequency bin has been shown, neglecting windowing effects, which are unique to the frequency domain implementation, to be

$$E \left[W_k \right] = \frac{P_S}{P_S + P_N} e^{-j \frac{2\pi}{m} \Delta k} \quad (5)$$

and

$$\text{Var}^{1/2} \left[W_k \right] = \left[\frac{\mu M P_N (2P_S + P_N)}{(P_S + P_N) (2 - 2\mu M (P_S + P_N))} \right]^{1/2} \quad (6)$$

We let $H(k) = W_k$, so that the time domain weights can be written as

$$h(mT_s) = \frac{1}{M} \sum_{k=0}^{M-1} H(k) e^{j \frac{2\pi}{M} mk} \quad (7)$$

Now, consider an interpolated impulse response, $h_I(t)$, using a general interpolation function, $f(t)$, that is

$$\begin{aligned} h_I(t) &= \sum_{m=0}^{M-1} h(mT_s) f(t-mT_s) \\ &= \frac{1}{M} \sum_{m=0}^{M-1} \sum_{k=0}^{M-1} H(k) f(t-mT_s) e^{j \frac{2\pi}{M} mk} \end{aligned} \quad (8)$$

Following the method described for the variance of the estimate with the continuous adaptive filter, the variance in the determination of the peak of $h_I(t)$ can be computed as

$$\text{Var}^{1/2} \left[\hat{t}_z \right] = \frac{\text{Var}^{1/2} \left[\frac{\partial h_I(t)}{\partial t} \right]}{\frac{\partial E \left[\frac{\partial h_I(t)}{\partial t} \right]}{\partial t}} \bigg|_{t=t_z} \quad (9)$$

Now, assume that the inputs to the adaptive filter are bandlimited to some bandwidth, B_S , so that

$$H(k) = 0 \text{ for } k > (J-1) = \left\lfloor B_S T_S \right\rfloor \frac{M}{2} \quad (10)$$

where $\lfloor X \rfloor$ is the largest integer less than or equal to X . Further, in order for $h(mT_s)$ to be real, we require

$$H(k) = H^*(M-k) \quad (11)$$

Using (8), it can readily be verified that

$$\text{Var}^{1/2} [h'_I(t)] = \frac{1}{M^2} \sum_{k=0}^{M-1} \text{Var} [H(k)] \sum_{m_1=0}^{M-1} \sum_{m_2=0}^{M-1} f'(t-m_1 T_s) f'(t-m_2 T_s) e^{j \frac{2\pi}{M} (m_1 - m_2) k} \quad (12)$$

and

$$\frac{\partial E [h'_I(t)]}{\partial t} = \frac{1}{M} \sum_{k=0}^{M-1} E [H(k)] \sum_{m=0}^{M-1} f''(t-m T_s) e^{j \frac{2\pi}{M} m k} \quad (13)$$

We want the mean and variance of the weights in (5) and (6) to meet the constraints of (10) and (11). This leads to

$$E [H(k)] = \begin{cases} \frac{P_S}{P_S + P_N} e^{-j \frac{2\pi}{M} \Delta k} & , 0 \leq k \leq J-1 \\ 0 & , J-1 < k < M-J \\ \frac{P_S}{P_S + P_N} e^{-j \frac{2\pi}{M} \Delta (M-k)} & , M-J \leq k \leq M-1 \end{cases} \quad (14)$$

and

$$\text{Var} [H(k)] = \begin{cases} \frac{\mu M P_N (2P_S + P_N)}{(P_S + P_N) (2 - 2\mu M (P_S + P_N))} & , 0 \leq k \leq J-1 \text{ or } M-J \leq k \leq M-1 \\ 0 & , J-1 < k < M-J \end{cases} \quad (15)$$

Using this in (12) and (13), we obtain

$$\text{Var}^{1/2} \left[\hat{t}_z \right] = \left[\frac{\mu P_N}{P_S^2} \frac{(2P_S + P_N)(P_S + P_N)}{2 - 2\mu M(P_S + P_N)} \right]^{1/2}$$

$$\cdot \frac{\left[\sum_{m_1=0}^{M-1} \sum_{m_2=0}^{M-1} f'(t_z - m_1 T_S) f'(t_z - m_2 T_S) \left[2 \text{Re} \left(\sum_{K=0}^{J-1} e^{j \frac{2\pi}{M} (m_1 - m_2) k} \right) \right] \right]^{1/2}}{\sum_{m=0}^{M-1} f''(t_z - m T_S) \left[2 \text{Re} \left(\sum_{K=0}^{J-1} e^{j \frac{2\pi}{M} (m - \Delta) k} \right) \right]^{1/2}}$$

$$= \frac{1}{\sqrt{2}} \left[\frac{\mu P_N}{P_S^2} \frac{(2P_S + P_N)(P_S + P_N)}{2 - 2\mu M(P_S + P_N)} \right]^{1/2} K_I \quad (16)$$

Note that K_I depends upon the input bandwidth, and the choice of interpolator function, $f(t)$, but not on the signal to noise ratio. This is analogous to the term

$$\left[\frac{\omega_u^3 - \omega_L^3}{3} \right]^{-1/2}$$

in the expression for the variance using a continuous adaptive filter. Equation (16) can be further simplified by writing the summations on k in closed form as

$$\text{Re} \left[\sum_{K=0}^{J-1} e^{j \frac{2\pi}{M} (m_1 - m_2) k} \right] = \frac{\sin \left[\frac{\pi J}{M} (m_1 - m_2) \right]}{\sin \left[\frac{\pi}{M} (m_1 - m_2) \right]} \cos \left[\left(\frac{J-1}{M} \right) \pi (m_1 - m_2) \right] \quad (17)$$

and

$$\text{Re} \left[\sum e^{j \frac{2\pi}{M} (\Delta - m) k} \right] = \frac{\sin \left[\frac{\pi J}{M} (\Delta - m) \right]}{\sin \left[\frac{\pi}{M} (\Delta - m) \right]} \cos \left[\left(\frac{J-1}{M} \right) \pi (\Delta - m) \right] \quad (18)$$

This gives

$$K_I = \frac{\left[\sum_{m_1=0}^{M-1} \sum_{m_2=0}^{M-1} f'(t_z - m_1 T_s) f'(t_z - m_2 T_s) \left\{ \frac{\sin \left[\frac{\pi J}{M} (m_1 - m_2) \right]}{\sin \left[\frac{\pi}{M} (m_1 - m_2) \right]} \cos \left[\left(\frac{J-1}{M} \right) \pi (m_1 - m_2) \right] \right\} \right]^{1/2}}{\sum_{m=0}^{M-1} f''(t_z - m T_s) \left\{ \frac{\sin \left[\frac{\pi J}{M} (\Delta - m) \right]}{\sin \left[\frac{\pi}{M} (\Delta - m) \right]} \cos \left[\left(\frac{J-1}{M} \right) \pi (\Delta - m) \right] \right\}}$$

(19)

For the interpolation function used here, (1), we have

$$f'(t_z - m T_s) = \frac{\cos 2\pi B(t_z - m T_s)}{(t_z - m T_s)} - \frac{\sin 2\pi B(t_z - m T_s)}{2\pi B(t_z - m T_s)^2}$$

(20)

$$f'(0) = 0$$

$$f''(t_z - m T_s) = \frac{2 \sin 2\pi B(t_z - m T_s)}{2\pi B(t_z - m T_s)^3} - \frac{2 \cos 2\pi B(t_z - m T_s)}{(t_z - m T_s)^2} - \frac{2\pi B \sin 2\pi B(t_z - m T_s)}{(t_z - m T_s)}$$

(21)

$$f''(0) = -\frac{(2\pi B)^2}{3}$$

Using (19), (20), and (21), K_I can be evaluated numerically on the computer for any choice of signal bandwidth, B_s , interpolator bandwidth, B , filter size, M , and sample interval, T_s . The computed value of K_I can then be used to compute the variance of the delay estimate, \hat{t}_z , from (16), for selected signal-to-noise ratio and μ . Note that for typical values of μ , M , and $(P_S + P_N)$, the factor

$$\frac{1}{\sqrt{2}} \left[\frac{\mu P_N}{P_S^2} \frac{(2P_S + P_N)(P_S + P_N)}{2 - 2\mu M(P_S + P_N)} \right]$$

in (16) is essentially independent of M , the filter length.

It must be noted here that this result applies only when the variance of $h_1(t)$ falls in the linear portion of $h'_1(t)$ near the peak of $E[h_1(t)]$. This is equivalent to saying that the largest of the discrete weights must be in the vicinity of the true peak. This will be true when the mean of the largest weight is large in comparison to the variance of the weights. For a particular input signal to noise ratio, this can be assured by selecting the feedback coefficient, μ , sufficiently small.

A number of simulations of an adaptive tracker using this interpolation scheme have been performed using the configuration shown in Figure 13. Using the results in this section, the estimation performance has been calculated on the computer, and is shown in the graph of Figure 11 as a function of SNR and for several values of μ . Also shown are sample variances of the estimates derived from the computer simulations described in section 6. It can be seen that when μ is sufficiently small, the theoretical predictions and simulation results agree quite well. However, when μ is not small enough to be consistent with the assumptions of this section, the variance of the estimate is much larger. This is because fluctuations in the weight vector cause the largest weight to appear in a bin other than the peak of the mean weight vector.

In order to select μ sufficiently small to achieve the predicted results, we want μ such that the mean of the largest weight is large in comparison to the weight variance. Figure 12 shows the ratio

$$R = \frac{E[W_{\max}]}{\text{Var}^{1/2} W}$$

as a function of SNR for several values of μ , and for the configuration simulated above. Comparison with results of the simulations indicates that R must be nominally 1.5 to give the predicted results. Then, for example, if performance were required down to -20 dB for the simulation, $\mu \leq 2^{-17}$ would be required.

In order to give some feel for the meaning of these results in terms of bearing estimation, Figure 11 also shows predicted variance of a bearing estimate for a broadside target for two arrays, a small tactical array with 11.46 feet between split array phase centers, and a towed array with 114.6 feet between phase centers.

APPENDIX VI

TRACKING BEHAVIOR OF THE MEAN WEIGHTS FOR VARIOUS SIGNAL MODELS AND A LINEARLY-TIME-VARYING DELAY

1. Tracking Behavior of an Adaptive Filter Tracker for Single Frequency Inputs with Linearly Time-Varying Bearing in Uncorrelated Noise

An LMS adaptive filter is configured as a canceller between two half array beamformed outputs to perform split beam bearing tracking. The tracking performance is analyzed for a narrowband signal that is moving such that the delay between split array phase centers is linearly changing with time. The time varying mean weights are derived in both transient and steady state conditions and compared with previous results.

The LMS adaptive filter is configured as a bearing tracker in Figure 2. The objective is for the adaptive algorithm to properly estimate and track changes in the propagation time between split arrays and map that time estimate into an estimate of signal energy arrival angle. The narrowband signal case in uncorrelated noise is treated herein. It is assumed that $\Theta(t)$ is such that the delay, $\tau(t)$, between array phase centers is linear with time. Since

$$\tau(t) = \frac{d}{C_0} \sin \Theta(t)$$

for a split array aperture of d meters in a sound speed of C_0 meters/sec, the assumption of linear $\tau(t)$ corresponds to assuming small linear $\Theta(t)$, such that $\sin \Theta(t) \approx \Theta(t)$ and

$$\tau(t) \cong \frac{d}{C_0} \Theta(t) = ct.$$

The model for the moving case is as follows. The output of the upper beamformer in Figure 2 produces the reference waveform, $d(t)$, where

$$d(t) = A \cos (\omega_0 t + \phi) + n_1(t)$$

The filter input is the lower beamformer output

$$\begin{aligned} x(t) &= A \cos (\omega_0 t - \tau(t) + \phi) + n_2(t) \\ &= A \cos \left(\omega_0 t - \frac{\omega_0 d}{C_0} \sin \Theta(t) + \phi \right) + n_2(t) \\ &= A \cos \psi(t) + n_2(t) \end{aligned}$$

where $\psi(t)$ is the total signal phase. The frequency of the signal portion of $x(t)$ is the time derivative of $\psi(t)$, so that

$$2\pi f(t) = \frac{d\psi(t)}{dt} = \omega_0 \left(1 - \frac{d}{C_0} \cos \Theta(t) \frac{d\Theta(t)}{dt} \right).$$

Thus the effect of the moving plane wave signal is to introduce a frequency shift on the sine wave. The ability of the adaptive filter to track this moving frequency shift will now be analyzed.

ANALYSIS

The algorithm for changing the complex weights in the adaptive filter is given by

$$\begin{aligned} W(n+1) &= W(n) + \mu [d(n) - X^T(n)W(n)] X^*(n) \\ &= W(n) + \mu [d(n) X^*(n) - X^*(n)X^T(n)W(n)] \end{aligned} \quad (1)$$

where

$W(n)$ = filter weight vector at time sample n

$d(n)$ = desired signal at time sample n

$X(n)$ = observed data vector of samples within the tapped delay line

and where the symbols * and T denote complex conjugate and vector transpose respectively. Figure 8 shows the data vector X(n) in the tapped delay line. The scalar d(n) is

$$d(n) = \sigma_S e^{j\omega_0 n\Delta t} + n_1(n\Delta t) \quad (2)$$

and the vector X(n) is

$$X(n) = \sigma_S \begin{pmatrix} e^{j\omega_0 (n\Delta t - \tau(n\Delta t))} \\ e^{j\omega_0 (n\Delta t - \delta - \tau(n\Delta t - \delta))} \\ e^{j\omega_0 (n\Delta t - 2\delta - \tau(n\Delta t - 2\delta))} \\ \cdot \\ \cdot \\ \cdot \\ e^{j\omega_0 (n\Delta t - M\delta - \tau(n\Delta t - M\delta))} \end{pmatrix} + N_2 \quad (3)$$

where

δ = time delay between taps

Δt = algorithm sampling time (usually $\Delta t = \delta$)

M = number of taps.

The equation of the mean weight vector is obtained by averaging (1) and assuming that the data sequence X(n) is independent over time.

$$E[W(n+1)] = E[W(n)] + \mu \left\{ R_{dx}(n) - R_{xx}(n) E[W(n)] \right\} \quad (4)$$

Using the inputs in (2) and (3), R_{dx} and R_{xx} are calculated as follows:

$$R_{dx}(n) = E[d(n) X^*(n)] = \sigma_S^2 \begin{pmatrix} e^{j\omega_0 \tau(n\Delta t)} \\ e^{j\omega_0 [\tau(n\Delta t - \delta) + \delta]} \\ \cdot \\ \cdot \\ \cdot \\ e^{j\omega_0 [\tau(n\Delta t - M\delta) + M\delta]} \end{pmatrix} \quad (5)$$

$$R_{xx}(n) = E[X(n) X^*T(n)] = \sigma_S^2 \left\{ e^{j\omega_0 [\tau(n\Delta t - k\delta) - \tau(n\Delta t - l\delta) + (k-l)\delta]} \right\} + \sigma_n^2 I \quad (6)$$

where k and l range from 0 to M and I is the $M \times M$ identity matrix for the covariance of the uncorrelated noise.

Note that both second order statistics are dependent on $n\Delta t$, reflecting the non-stationarity of the input processes. Define the matrix $D(n)$ as follows:

$$D(n) = \begin{pmatrix} e^{j\omega_0 \tau(n\Delta t)} \\ e^{j\omega_0 [\tau(n\Delta t - \delta) + \delta]} \\ \cdot \\ \cdot \\ \cdot \\ e^{j\omega_0 [\tau(n\Delta t - M\delta) + M\delta]} \end{pmatrix} \quad (7)$$

Then

$$R_{dx}(n) = \sigma_S^2 D(n) \quad (8)$$

$$R_{xx}(n) = \sigma_S^2 D(n) D^{*T}(n) + \sigma_n^2 I \quad (9)$$

If $\tau(t) = ct$, as assumed at the outset, then

$$D(n) = e^{j\omega_0 c n \Delta t} \begin{pmatrix} 1 \\ j\omega_0 (1-c)\delta \\ \cdot \\ \cdot \\ j\omega_0 (1-c) M\delta \\ c \end{pmatrix} = e^{j\omega_0 c n \Delta t} D(0) \quad (10)$$

and

$$R_{dx}(n) = \sigma_S^2 e^{j\omega_0 c n \Delta t} D(0) \quad (11)$$

$$R_{xx}(n) = \sigma_S^2 D(0) D(0)^{*T} + \sigma_n^2 I \quad (12)$$

Using (11) and (12) in (4), the mean weights are

$$E[W(n+1)] = \left\{ I - \mu \left[\sigma_n^2 I + \sigma_S^2 D(0) D(0)^{*T} \right] \right\} E[W(n)] + \mu \sigma_S^2 e^{j\omega_0 c n \Delta t} D(0) \quad (13)$$

The difference equation (13) can be solved explicitly for $E[W(n)]$. Assuming that

$E[W(0)] = 0$, i. e. zero initial conditions,

$$E[W(n)] = \mu \sigma_S^2 e^{j\omega_0 c (n+1) \Delta t} [I-A]^{-1} [I-A^n] D(0) \quad (14)$$

where

$$A = e^{-j\omega_0 c \Delta t} \left[I - \mu \left(\sigma_n^2 I + \sigma_S^2 D(0) D(0)^{*T} \right) \right] \quad (15)$$

Let

$$\alpha = e^{-j\omega_0 c \Delta t} \quad (16)$$

$$\beta = \frac{\mu \sigma_S^2 \alpha}{1 - \alpha (1 - \mu \sigma_n^2)} \quad (17)$$

$$D = D(0) \quad (18)$$

Then

$$(I-A)^{-1} = \left[1 - \alpha (1 - \mu \sigma_n^2) \right]^{-1} \left[I - \frac{\beta DD^*T}{1 + M\beta} \right] \quad (19)$$

and

$$A^n D = \left[\alpha (1 - \mu (\sigma_n^2 + M\sigma_S^2)) \right]^n D \quad (20)$$

Thus

$$E[W(n)] = \frac{\mu \sigma_S^2 \alpha^{-n}}{1 - \alpha (1 - \mu \sigma_n^2)} \left[I - \frac{\beta}{1 + M\beta} DD^*T \right] \left\{ 1 - \left[\alpha (1 - \mu (\sigma_n^2 + M\sigma_S^2)) \right]^n \right\} D$$

$$E[W(n)] = \alpha^{-(n+1)} \frac{\beta}{1 + M\beta} \left[1 - \alpha^n (1 - \mu (\sigma_n^2 + M\sigma_S^2))^n \right] D \quad (21)$$

Equation (21) is the transient behavior of the mean value of the weight vector. Note that it is time varying, even in steady state, since the phase term $\alpha^{-(n+1)}$ does not decay as $n \rightarrow \infty$. In steady state, if

$$\mu (\sigma_n^2 + M\sigma_S^2) < 1$$

then

$$\lim_{n \rightarrow \infty} E[W(n)] = \alpha^{-(n+1)} \frac{\beta}{1+M\beta} \begin{pmatrix} e^{j\omega_0 (1-c)\delta} \\ \cdot \\ \cdot \\ \cdot \\ e^{j\omega_0 (1-c)M\delta} \end{pmatrix} \quad (22)$$

The weights are all of magnitude

$$\frac{\beta}{1+M\beta} = \frac{\mu \sigma_S^2 \alpha}{1 - \alpha + \alpha \mu (\sigma_n^2 + M\sigma_S^2)} \quad (23)$$

but have a phase that is precessing across the tapped delay line as time progresses. The weights may be viewed as a sinusoid at the shifted frequency of the input, $\omega_0 (1-c)$, with a phase that is "barber polling" along the delay line. The weights are shown in Figure 9 as time changes.

In the static case, $c = 0$, $\alpha = 1$, $\beta = \sigma_S^2 / \sigma_n^2$, and

$$E[W(\infty)] = \frac{\sigma_S^2 / \sigma_n^2}{1 + M \sigma_S^2 / \sigma_n^2} \begin{pmatrix} e^{j\omega_0 \delta} \\ \cdot \\ \cdot \\ \cdot \\ e^{j\omega_0 M\delta} \end{pmatrix} \quad (24)$$

which agrees precisely with previously derived results for the LMS algorithm in steady state with a stationary sine wave input in uncorrelated noise.

Conclusions

The transient and steady state tracking behavior of the mean value of the LMS adaptive filter tracker weights has been derived. The filter corrects a frequency shift and doppler precession due to the angular movement of the target in bearing.

2. Tracking Behavior of an Adaptive Filter Tracker for a Broadband White Signal with Linearly Time-Varying Bearing in Uncorrelated Noise

The adaptive filter split-beam bearing tracker analysis is now extended to include a broadband spectrally white input signal that is moving in bearing. The time varying mean weights are derived in both transient and steady state conditions.

The LMS adaptive filter is configured as a bearing tracker in Figure 8. The objective is for the adaptive algorithm to properly estimate and track changes in the propagation time between split arrays and map that time estimate into an estimate of signal energy arrival angle, $\theta(t)$. It is assumed that $\theta(t)$ is such that the delay, $\tau(t)$, between array phase centers is linear with time. Since

$$\tau(t) = \frac{d}{C_0} \sin \theta(t)$$

for a split array aperture of d meters in a sound speed of C_0 meters/sec, the assumption of linear $\tau(t)$ corresponds to assuming small linear $\theta(t)$, such that $\sin \theta(t) \approx \theta(t)$ and

$$\tau(t) \cong \frac{d}{C_0} \theta(t) = ct.$$

The input signal, $s(t)$, in this case is a zero mean Gaussian random process that is spectrally white over the band corresponding to the sampling frequency. The total signal power is σ_s^2 and the total uncorrelated noise power is σ_n^2 . As in the prior analysis, one split array output, $d(n)$, is the desired signal for the adaptive process, and the other is the input, $x(n)$, to the adaptive filter. The ability of the adaptive filter to track the bearing changes in the broadband plane wave signal process is analyzed in the next section.

Analysis

The algorithm for changing the complex weights in the adaptive filter is given by

$$\begin{aligned} W(n+1) &= W(n) + \mu [d(n) - X^T(n)W(n)] X^*(n) \\ &= W(n) + \mu [d(n) X^*(n) - X^*(n)X^T(n)W(n)] \end{aligned} \quad (1)$$

where

$W(n)$ = filter weight vector at time sample n

$d(n)$ = desired signal at time sample n

$X(n)$ = observed data vector of samples within the tapped delay line

and where the symbols $*$ and T denote complex conjugate and vector transpose respectively. Figure 11 shows the data vector $X(n)$ in the tapped line. The scalar $d(n)$ is

$$d(n) = s(n\Delta t - \tau(n\Delta t)) + n_1(n\Delta t) \quad (2)$$

and the vector $X(n)$ is

$$X(n) = \begin{pmatrix} s(n\Delta t) \\ s(n\Delta t - \delta) \\ s(n\Delta t - 2\delta) \\ \vdots \\ s(n\Delta t - M\delta) \end{pmatrix} + N_2(n\Delta t) \quad (3)$$

where

δ = time delay between taps

Δt = algorithm sampling time (usually $\Delta t = \delta$)

M = number of taps.

It is assumed that $\tau(t) = ct$ and that the signal is white, so that

$$E [s(n) s(m)] = \sigma_s^2 \Delta(n-m) \quad (4)$$

where

$$\Delta(n-m) = \begin{cases} 1 & \text{if } n=m \\ 0 & \text{otherwise} \end{cases}$$

The difference equation for the mean of the adaptive filter weight is:

$$E[W(n+1)] = [I - \mu R_{XX}(n)] E[W(n)] + \mu R_{dX}(n) \quad (5)$$

where

$$\begin{aligned} \mu &= \text{feedback coefficient} \\ I &= M \times M \text{ identity matrix} \\ R_{dX}(n) &= E[d(n) X^*(n)] \\ R_{XX}(n) &= E[X(n) X^{*T}(n)] \end{aligned}$$

If $R_{XX}(n)$ is independent of n , and if the initial mean weight $E[W(0)] = 0$, then equation (5) can be re-written as

$$E[W(n)] = \mu \sum_{k=0}^{n-1} [I - \mu R_{XX}]^{n-k-1} R_{dX}(k) \quad (6)$$

The second order statistics can be calculated from the input waveforms, as follows:

$$R_{XX}(n) = (\sigma_s^2 + \sigma_n^2) I \quad (7)$$

$$R_{dX}(n) = \sigma_s^2 \begin{pmatrix} \Delta(cn\Delta t) \\ \Delta(cn\Delta t - \delta) \\ \Delta(cn\Delta t - 2\delta) \\ \vdots \\ \Delta(cn\Delta t - M\delta) \end{pmatrix} \quad (8)$$

Using (6), the mean weight vector at the n th iteration is given by

$$E[W(n)] = \mu \sigma_s^2 \sum_{k=0}^{n-1} [1 - \mu (\sigma_s^2 + \sigma_n^2)]^{n-k-1} \begin{pmatrix} \Delta(ck\Delta t) \\ \Delta(ck\Delta t - \delta) \\ \vdots \\ \Delta(ck\Delta t - M\delta) \end{pmatrix} \quad (9)$$

In the static case, $c = 0$ and only the first weight is non-zero, with mean value

$$E [W_o(n)] = \frac{\sigma_s^2}{\sigma_s^2 + \sigma_n^2} [1 - (1 - \mu(\sigma_s^2 + \sigma_n^2))^n] \quad (10)$$

which converges to the Wiener Filter for the broadband stationary case as $n \rightarrow \infty$.

In the dynamic case, the weights are a moving set of spikes that are changing with amplitude as the signal moves and as the weights converge. The total weight vector is the sum of the vectors in (9). The weights can be viewed as a sliding window of exponentially growing responses, or as a moving weight at the leading edge that leaves behind it an exponentially decaying wake.

This can be seen by examining the weight at the leading edge of the response. In (9), the leading edge will occur at the latest time. If the filter is sufficiently long so that the response still falls within the tapped delay line, i.e., $M > n$, then the amplitude and location of the leading weight are found by examining the term in the summation for which $k = n - 1$. The amplitude of the leading edge is $\mu\sigma_s^2$ and its location is at tap number $c(n-1)$ (assuming that $\Delta t = \delta$). If $c = 1$ then the signal moves one tap per iteration and the adaptive filter tracks the movement. If the signal changes more slowly, then $c < 1$ and the leading edge moves more slowly than the iteration rate.

For the special case where $c = 1$ the weight vector in (9) can be readily expanded, as follows, letting $r = 1 - \mu(\sigma_s^2 + \sigma_n^2)$.

$$E[W(n)] = \mu\sigma_s^2 \left[\begin{array}{c} r^{n-1} \\ 0 \\ 0 \\ \vdots \\ \vdots \\ \vdots \\ \vdots \\ 0 \end{array} \right] + \left[\begin{array}{c} 0 \\ r^{n-2} \\ 0 \\ \vdots \\ \vdots \\ \vdots \\ \vdots \\ 0 \end{array} \right] + \left[\begin{array}{c} 0 \\ 0 \\ r^{n-3} \\ 0 \\ \vdots \\ \vdots \\ \vdots \\ 0 \end{array} \right] + \left[\begin{array}{c} 0 \\ \cdot \\ \cdot \\ \cdot \\ 0 \\ r^1 \\ 0 \\ \cdot \\ 0 \end{array} \right] + \left[\begin{array}{c} 0 \\ 0 \\ \cdot \\ \cdot \\ \cdot \\ 1 \\ 0 \\ 0 \\ 0 \end{array} \right] \quad (11)$$

$$= \mu\sigma_s^2 \left[\begin{array}{c} r^{n-1} \\ r^{n-2} \\ \cdot \\ \cdot \\ \cdot \\ r^1 \\ 1 \\ 0 \\ \cdot \\ 0 \end{array} \right] \quad (12)$$

Equation (12) shows the decaying wake behind the leading weight which shifts along the delay line as n increases. Figure 10 shows this effect.

For $c < 1$ the weights move more slowly and the basic model herein tends to become less realistic. The signal sequence used is totally uncorrelated in time. In general this is not the case. The impact of this assumption is to have weights respond only at the exact correct alignment of input delays and tap delay values. In the band limited, non-white signal case, correlation will exist even at non-integer delay shifts, and larger weight responses should be expected at the leading edge for slower moving signals. It is shown in the next section that the amplitude of the leading edge decreases monotonically with c from $\sigma_s^2 / (\sigma_s^2 + \sigma_n^2)$, (the value for $c = 0$), to $\mu\sigma_s^2$, (the value for which movement is so fast that the signal samples decorrelate totally at each time sample). The extent of the wake and the height of the leading edge will depend on signal dynamics.

Conclusions

The transient and steady state tracking behavior of the mean value of the LMS adaptive filter tracker weights has been derived for a spectrally white process with linear time varying bearing dynamics. The filter weights are a moving tap which leaves behind it an exponentially decreasing wake. Tracking the bearing involves estimating the delay location of the leading edge of the weights.

3. Tracking Behavior for Band-Limited Broadband (Correlated) Signal with Linearly Time-Varying Bearing in Un-Correlated Noise for Small Signal-to-Noise Ratios

The adaptive filter split-beam bearing tracker analysis is now extended to include band-limited broadband (correlated) signals that are moving in bearing. The time-varying mean weights are derived from the transient and steady-state conditions for low signal-to-noise ratios.

The conditions of the previous section hold with one extension. The signal spectrum is no longer white. Equations 2 and 3 of the previous section are still valid. However, $R_{dx}(n)$ and $R_{xx}(n)$ (Equations 7 and 8 of the previous section) are now given by

$$R_{dx}(n) = \begin{pmatrix} R_s(cn\Delta t) \\ R_s(cn\Delta t - \delta) \\ \vdots \\ R_s(cn\Delta t - M\delta) \end{pmatrix} = \sigma_s^2 \begin{pmatrix} \rho|cn\Delta t| \\ \rho|cn\Delta t - \delta| \\ \rho|cn\Delta t - 2\delta| \\ \vdots \\ \rho|cn\Delta t - M\delta| \end{pmatrix}$$

$$R_{xx}(n) = \sigma_n^2 I + \begin{pmatrix} \sigma_s^2 R_s(\delta) \dots R_s(M\delta) \\ \text{SYM} \\ \sigma_s^2 \end{pmatrix} = \sigma_n^2 I + \sigma_s^2 \Lambda$$

where

$$\Lambda = \begin{pmatrix} 1 & \rho^\delta & \rho^{2\delta} & \dots & \rho^{M\delta} \\ \text{SYM} & & & & \end{pmatrix}$$

Since $R_{xx}(n)$ is independent of n , for $[E W(0)] = 0$

$$E W(n) = \mu \sum_{k=0}^{n-1} [I - \mu R_{xx}]^{n-k-1} R_{dx}(k)$$

let

$$R = (1 - \mu\sigma_n^2) I - \mu\sigma_s^2 \Lambda$$

and

$$D(k) = \begin{pmatrix} \rho|ck\Delta t| \\ \rho|ck\Delta t - \delta| \\ \vdots \\ \rho|ck\Delta t - M\delta| \end{pmatrix}$$

then

$$E[W(n)] = \mu \sigma_s^2 \sum_{k=0}^{n-1} R^{n-k-1} D(k)$$

Assume small signal-to-noise ratio, i.e., $\sigma_s^2 \ll \sigma_n^2$.

Then

$$R_{XX}(n) \approx \sigma_n^2 I$$

$$R \approx (1 - \mu \sigma_n^2) I$$

If we select $\Delta t = \delta$, i.e., iterate at the sample rate, then the mean weight for small signal-to-noise ratio is approximately

$$E[W_j(n)] \approx \mu \sigma_s^2 \sum_{k=0}^{n-1} (1 - \mu \sigma_n^2)^{n-k-1} \begin{pmatrix} \rho^{ck\delta} \\ \rho^{|ck-1|\delta} \\ \rho^{|ck-2|\delta} \\ \vdots \\ \rho^{|ck-M|\delta} \end{pmatrix}$$

The jth weight:

$$E[W(n)] \approx \mu \sigma_s^2 \sum_{k=0}^{n-1} (1 - \mu \sigma_n^2)^{n-k-1} \rho^{|ck-j|\delta}$$

Assume that the filter is long enough so that $M = n-1$, and let $j = Mc$ so that we are at the end of the filter. For $r = 1 - \mu \sigma_n^2$

$$E[W_{Mc}(n)] = \mu \sigma_s^2 r^M \sum_{k=0}^M r^{-k} \rho^{-(k-M)c\delta}$$

$$= \mu \sigma_s^2 r^M \rho^{Mc\delta} \sum_{k=0}^M (r \rho^{c\delta})^{-k}$$

$$\begin{aligned}
&= \mu \sigma_s^2 r^M \rho^{M\delta c} \frac{1 - (r\rho^{c\delta})^{-M-1}}{1 - (r\rho^{c\delta})^{-1}} \\
&= \mu \sigma_s^2 r^M \rho^{Mc\delta} \frac{r\rho^{c\delta} - (r\rho^{c\delta})^{-M}}{r\rho^{c\delta} - 1} \\
&= \mu \sigma_s^2 \frac{r^M \rho^{(M+1)c\delta} - 1}{r\rho^{c\delta} - 1}
\end{aligned}$$

This is the transient behavior of the mean weight for small signal-to-noise ratios. In steady-state, i. e., M arbitrarily large, one can readily see the relationships between signal correlation, ρ , signal dynamics, c , and algorithm dynamics, μ .

$$\begin{aligned}
\lim_{M \rightarrow \infty} E W_{Mc}^{(M)} &= \frac{\mu \sigma_s^2}{1 - r\rho^{c\delta}} \\
&= \frac{\mu \sigma_s^2}{1 - [1 - \mu \sigma_n^2] \rho^{c\delta}}
\end{aligned}$$

There are several cases of interest. If $\rho = 1$, then the signal is totally correlated from tap to tap, regardless of signal dynamics. For this case

$$E W_{Mc} = \frac{\sigma_s^2}{\sigma_n^2}$$

which is a small signal-to-noise ratio approximation to

$$\frac{\sigma_s^2}{\sigma_n^2 + \sigma_s^2}$$

which is what one would expect in the static case.

If $\rho = 0$, the signal is totally un-correlated and again signal dynamics should not affect the result. For this case,

$$E(W_{Mc}) = \mu \sigma_s^2$$

which agrees with the results of the previous section (Equation 12) where dynamics tended to de-correlate the signal.

If there are no signal dynamics, i. e., $c = 0$, then

$$E W_{Mc}(\infty) = \frac{\sigma_s^2}{\sigma_n^2}$$

independent of ρ , which is again the expected small signal-to-noise ratio static result.

The tradeoff between dynamics and signal correlation can be seen by examining the term $\rho^{c\delta}$ in the expression for $E[W_{Mc}(\infty)]$. As c decreases $\rho^{c\delta}$ looks more like unity and signal looks more correlated. As c increases ρ (which is less than one) is raised to a higher power and the signal has become less correlated.

APPENDIX VII

Transient behavior of the LMS Adaptive Filter response to variable
frequency spectral lines.

ABSTRACT

The transient behavior of the LMS adaptive filter is studied when configured as a canceller operating in the presence of a fixed or variable complex frequency sine-wave signal buried in white noise. For a fixed frequency signal, the mean weights are shown to respond to signal more rapidly than to noise alone. For a chirped signal, a fixed parameter matrix first-order difference equation is derived for the mean weights and a closed-form steady-state solution obtained. The transient response is obtained as a function of the eigenvectors and eigenvalues of the input covariance matrix. Sufficient conditions for the stability of the transient response are derived and an upper bound on the eigenvalues obtained. Finally, the mean-square error is evaluated when responding to a chirped signal. The gain coefficient of the LMS algorithm is determined that minimizes the mean-square error for chirped signals as a function of chirp rate and signal and noise powers.

INTRODUCTION

The LMS adaptive filter has been proposed and used in situations where the statistics of the input processes are unknown or partially known^[1-3]. The structure of the LMS algorithm for adjusting the weights of the adaptive filter requires quadratic operations on stochastic input data which, in general, are difficult to analyze. Under the assumption of statistically independent data samples, the mean weight vector and the covariance of the weight fluctuations have been obtained for a variety of stationary input data statistics^[1-11]. Special configurations of the LMS algorithm, such as noise cancelling^[4] line enhancing^[4,6,8,9,11], spectral analysis,^[5,12] and single frequency line detection^[7-10], have been studied in considerable detail. The special characteristics of the LMS filter configuration have been used to aid in the analysis of the behavior of the algorithm.

The purpose of this paper is to present some exact analytical results for the LMS algorithm configured as an adaptive noise canceller when the input process consists of a chirped sine wave in additive stationary white noise. Although some previous work on LMS algorithm behavior in a non-stationary environment has been published^[13-16], only one^[16] has investigated the response of the LMS algorithm to chirped sinusoids in white noise. The analysis is performed by assuming the chirping is slow enough so that a quasi-stationary model for the mean weights can be used. In this paper, exact analytical results are obtained for the chirped sinusoidal signal with arbitrary chirp rate. Since the adaptive cancelling of dynamic signals is a key element in cancelling, line enhancing and frequency tracking, the analytical results for the above model have wide applicability.

Two principal results of this paper are

1. A closed form analytical expression for the LMS mean weights in a dynamic signal environment.
2. Explicit trade-off results between filter parameters, weight variances, mean-square-error, and input signal dynamics.

The latter result is of special interest since it shows explicitly the compromise between fast adaptation in order to respond to variations in the input statistics and slow adaptation to reduce the fluctuations in the adaptation process itself.

For the narrowband signal in white-noise case, the configuration shown in Figure 40 can be used to model the above LMS algorithm functions.

With reference to Figure 40,

$$d(n) = \sigma_s e^{j(\omega_0 n\Delta t + \dot{\omega}(n\Delta t)^2/2 + \phi)} + n_1(n\Delta t)$$

Δ is chosen so that $n_1(n\Delta t)$ and $n_1(n\Delta t - \Delta)$ are un-correlated. On the other hand, because the desired signal is a chirped sine-wave, it decorrelates more slowly than the noise.

DYNAMIC MODEL FOR THE INPUTS

The algorithm for changing the complex weights of the adaptive filter is given by ^[17],

$$\begin{aligned} W(n+1) &= W(n) + \mu [d(n) - X^T(n) W(n)] X^*(n) \\ &= W(n) + \mu [d(n) X^*(n) - X^*(n) X^T(n) W(n)] \end{aligned} \quad (1)$$

where $W(n)$ = filter weight vector at time n , $d(n)$ = desired signal, $X(n)$ = observed data vector at time n , and where $*$ and T denote complex conjugate and vector transpose respectively.

Averaging equation (1) and assuming 1) the data sequence $X(n)$ is statistically independent over time ^[1-4] and 2) the present weight vector and the present data vector are statistically independent ^[11], yields

$$E\{W(n+1)\} = E\{W(n)\} + \mu [R_{dx}(n) - R_{xx}(n) E\{W(n)\}] \quad (2)$$

where $R_{dx}(n) = E\{d(n)X^*(n)\}$, $R_{xx}(n) = E\{X^*(n)X^T(n)\}$.

In practice the algorithm sampling interval (Δt) is usually chosen to correspond to the delay δ between the taps of the adaptive filter. Furthermore (Δt) is usually chosen to correspond to independent samples of the noisy data. Hence the delay is chosen to be integer multiples of (Δt) in order for the noises in the two inputs to be un-correlated. On the other hand, the longer that Δ is chosen, the less correlated is the signal component. Thus choice of $\Delta = \delta$ is the best that can be accomplished.

When the input consists of a complex sine-wave with linearly-varying frequency in additive noise,

$$d(t) = \sigma_s e^{j(\omega_0 t + \dot{\omega} t^2 / 2 + \phi)} + n(t) \quad (3)$$

*Other integer values of δ for the bulk delay Δ can be studied using the subsequent analysis and the results show that $\Delta = \delta$ yields the best filter performance.

where σ_s^2 = signal power, ω_o = signal frequency, $\dot{\omega}$ = rate of change of signal frequency, ϕ = random phase of signal and the noise is independent of the signal with noise power σ_n^2 and normalized covariance matrix G, then

$$R_{xx}(n) = \sigma_n^2 G + \sigma_s^2 D(n) D^*(n)^T \quad (4)$$

$$R_{dx}(n) = \sigma_s^2 D(n) \quad (5)$$

where

$$D^T(n) = e^{j\omega_o \Delta} \left(e^{j\omega_o \delta^2 n} - e^{j\delta^2 \dot{\omega}/2}, \dots \right. \\ \left. e^{j\omega_o m \delta} e^{j\dot{\omega} m \delta^2 n} - e^{j m^2 \delta^2 \dot{\omega}/2}, \dots \right. \\ \left. e^{j\omega_o M \delta} e^{j\dot{\omega} M \delta^2 n} - e^{j M^2 \delta^2 \dot{\omega}/2} \right) \quad (6)$$

with M = number of complex weights.

Using Eqs. (4) and (5) in Eq. (2) yields

$$E[W(n+1)] = \left[I - \mu (\sigma_n^2 G + \sigma_s^2 D(n) D^*(n)^T) \right] E[W(n)] + \mu \sigma_s^2 D(n) \quad (7)$$

For white noise, $G = I$. Define

$$M(n) = I + \frac{\sigma_s^2}{\sigma_n^2} D(n) D^*(n)^T \quad (8)$$

For any n, the eigenvectors of M(n) are the vector D(n) and any set of (M-1) vectors orthogonal to D(n). The associated eigenvalues are

$$\lambda_1 = 1 + M \frac{\sigma_s^2}{\sigma_n^2}$$

$$\lambda_2 = \lambda_3 = \dots = \lambda_M = 1 \quad (9)$$

Note that the eigenvalues are independent of time. All the time variations in $M(n)$ are contained in the eigenvectors. This special property of $M(n)$ is exploited to obtain closed form solutions for Eq. (7).

SOLUTION OF EQ (7) FOR THE MEAN WEIGHT BEHAVIOR

Since $M(n)$ is Hermitian, there exists a unitary transformation $P(n)$ which diagonalizes $M(n)$ for each n ,

$$P(n) M(n) P^{-1}(n) = \lambda = \text{Diag} (\lambda_1, \lambda_2 \dots \lambda_m) \quad (10)$$

The λ_i are not functions of n . Due to the special form of $D(n)$,

$$D^T(n) = e^{j\omega_0 \Delta} V^n D^T(0) \quad (11)$$

where

$$V = \text{Diag} (a, a^2, \dots, a^M), \quad a = e^{j\omega_0 J^2}$$

Also $P(n)$ can be written in terms of the eigenvectors of $M(n)$,

$$P^+(n) = \frac{1}{\sqrt{M}} [D(n), R_1(n), \dots, R_{m-1}(n)] \quad (12)$$

where $^+$ = conjugate transpose and $R_1, R_2 \dots R_{M-1}$ are $M-1$ mutually ortho-normal vectors, also orthogonal to $D(n)$ for each n . Using Eq. (11),

$$P(n) = P(0) (V^*)^n \quad (13)$$

Using Eqs. (8), (11) and (13) and defining $Z(n) = P(n) E[w(n)]$, Eq. (7) can be written in terms of Z only as

$$Z(n+1) = P(0) V^* P^{-1}(0) [I - \mu \sigma_n^2 \lambda] Z(n) + \mu \sigma_s^2 P(0) V^* D(0) \quad (14)$$

Since Eq. (14) is a constant coefficient linear difference equation, with $P(0) = P_0$, it follows that

$$Z(n) = \left\{ P_0 V^* P_0^{-1} [I - \mu \sigma_n^2 \lambda] \right\}^n Z(0) + \mu \sigma_s^2 \sum_{m=1}^n \left\{ P_0 V^* P_0^{-1} [I - \mu \sigma_n^2 \lambda] \right\}^{m-1} P_0 V^* D(0) \quad (15)$$

Before investigating the general case of Eq. (15), consider the fixed frequency sinusoid signal case when $V = I$ and Eq. (15) simplifies to

$$Z(n) = [I - \mu \sigma_n^2 \lambda]^n Z(0) + \mu \sigma_s^2 \sum_{m=1}^n [I - \mu \sigma_n^2 \lambda]^{m-1} S \quad (16)$$

where $S^T = (\sqrt{M}, 0, 0, \dots, 0)$. Expressing the matrix sum in closed form

$$Z(n) = [I - \mu \sigma_n^2 \lambda] Z(0) + \frac{\sigma_s^2}{\sigma_n^2} \lambda^{-1} S [I - (I - \mu \sigma_n^2 \lambda)^n] \quad (17)$$

Thus, using Eq. (9), the components of $Z(n)$ are given by

$$z_1(n) = \left[1 - \mu (\sigma_n^2 + M \sigma_s^2) \right]^n z_1(0) + \frac{\sqrt{M} \sigma_s^2 / \sigma_n^2}{1 + M \sigma_s^2 / \sigma_n^2} \left\{ 1 - \left[1 - \mu (\sigma_n^2 + M \sigma_s^2) \right]^n \right\}$$

$$z_j(n) = \left[1 - \mu \sigma_n^2 \right]^n z_j(0) \quad (18)$$

$$j = 2, 3, \dots, M$$

Hence, for $\mu(\sigma_n^2 + M\sigma_s^2) < 1$, the response of the weights to the signal frequency is more rapid than to any other frequency. If $z_j(0) = 0$, $j = 1, 2, \dots, M$, then $z_1(n)$ is the only response,

$$z_1(n) = \frac{\sqrt{M}\sigma_s^2 / \sigma_n^2}{1 + M\sigma_s^2 / \sigma_n^2} \left\{ 1 - \left[1 - \mu(\sigma_n^2 + M\sigma_s^2) \right]^n \right\} \quad (19)$$

Transforming back to the original coordinate system,

$$E[W(n)] = P_0^{-1} Z(n) = \frac{\sigma_s^2 / \sigma_s^2}{1 + M\sigma_s^2 / \sigma_n^2} \left\{ 1 - \left[1 - \mu(\sigma_n^2 + M\sigma_s^2) \right]^n \right\} D(0) \quad (20)$$

Hence, the mean weights are scaled versions of the desired signal response. From Eq. (18), note that the time it takes the filter to adapt from zero initial conditions and learn the signal is less than the time required to forget the signal if it disappears. That is, from Eq (19), if $z_j(0) = 0$, $j = 1, 2, \dots, M$, signal response time is proportional to $1 - \mu(\sigma_n^2 + M\sigma_s^2)$. If the signal suddenly disappears so that $z_1(0) \neq 0$, then from Eq. (17) with $\sigma_s^2 = 0$, the decay time towards $z_1(n) = 0$, is proportional to $1 - \mu\sigma_n^2$.

STEADY-STATE WEIGHT BEHAVIOR

The explicit solution of Eq. (14) requires evaluation of the eigenvalues and eigenvectors of the matrix operator in brackets in Eq. (15) (see Appendix). However, the steady-state solution to Eq. (14) is obtainable without knowledge of the eigenvalues. In Eq. (15), set $Z(0) = 0$ (zero initial conditions) without loss of generality. Let Q be the matrix of eigenvectors of the matrix $P_o V^0 P_o^{-1} \left[I - \mu \sigma_n^2 \lambda \right]$ and $\Lambda = \text{Diag} (\Lambda_1, \Lambda_2 \dots \Lambda_m)$ be the matrix of eigenvalues. Thus

$$\begin{aligned} Z(n) &= \mu \sigma_s^2 \sum_{m=1}^n [Q \Lambda Q^{-1}]^{m-1} P_o V^* D(o) \\ &= \mu \sigma_s^2 Q \left(\sum_{m=0}^{n-1} \Lambda^m \right) Q^{-1} P_o V^* D(o) \end{aligned} \quad (21)$$

But

$$\sum_{m=0}^{n-1} \Lambda^m = \text{Diag} \left[\frac{1 - \Lambda_1^n}{1 - \Lambda_1}, \frac{1 - \Lambda_2^n}{1 - \Lambda_2}, \dots, \frac{1 - \Lambda_m^n}{1 - \Lambda_m} \right] \quad (22)$$

for $|\Lambda_i| < 1$ for all i , and

$$\lim_{n \rightarrow \infty} \sum_{m=0}^{n-1} \Lambda^m = (I - \Lambda)^{-1} \quad (23)$$

In Appendix I, it is shown that $|\Lambda_i| < 1$, for all i if $0 < \mu(\sigma_n^2 + M\sigma_s^2) < 2$. Let $Z_{ss} = \lim_{n \rightarrow \infty} Z(n)$. Then, using Eq. (23), Eq. (21) becomes

$$Z_{ss} = \mu\sigma_s^2 Q(I-\Lambda)^{-1} Q^{-1} P_o V^* D(0)$$

$$= \frac{\mu\sigma_s^2 P_o [V - (1 - \mu\sigma_n^2) I]^{-1} D(0)}{1 + \mu\sigma_s^2 D_o + [V - (1 - \mu\sigma_n^2) I]^{-1} D(0)} \quad (24)$$

The steady-state weights are the quantities of interest. Note that they will be time varying, even though the adaptive filter is in steady-state. Here, steady-state implies that the adaptive filter has converged, interpreted as the convergence of the transformed weight vector $Z(n)$. However, the filter has converged to a time-varying solution to follow the time-varying, non-stationary input signal. Thus, when Z_{ss} is inverse transformed back to the mean value of the weights, the transform is via the eigenvectors of the input covariance matrix, which are time-varying. Let $E[W_{ss}(n)]$ denote the mean value of the steady-state weights at time n .

$$E[W_{ss}(n)] = P^{-1}(n) Z_{ss}$$

$$= \frac{\mu\sigma_s^2 [V - (1 - \mu\sigma_n^2) I]^{-1} D(n)}{1 + \mu\sigma_s^2 \sum_{k=1}^M \frac{1}{e^{j\hat{\omega}k\delta^2} - (1 - \mu\sigma_n^2)}} \quad (25)$$

As a check, Eq. (25) can be compared with the steady-state value of the weights in the stationary case, i. e., with $\hat{\omega} = 0$. For that case $V = I$, $D(n) = D(0)$ and

$$E[W_{ss}(n)]_{\hat{\omega}=0} = \frac{\frac{\sigma_s^2 / \sigma_n^2}{1 + M \frac{\sigma_s^2}{\sigma_n^2}} D(0)}{1 + M \frac{\sigma_s^2}{\sigma_n^2}} \quad (26)$$

which agrees with Eq. (20) when $n \rightarrow \infty$.

Computer evaluation of the steady-state mean weights in Eq. (25) is presented in Figures 41-44 for $f = 5 \text{ Hz/sec}^2$ and in Figures 45-48 for $f = 1.25 \text{ Hz/sec}^2$. In all cases, the filter has 128 taps with $\mu = .1$. The signal-to-noise ratios are varied from unity to 10^{-2} . The figures display the magnitude and phase of the weights across the filter. Three interesting phenomena are displayed in these figures:

1. As the signal-to-noise ratio decreases, the adaptive filter uses more of the taps but at lower amplitudes,
2. The tap phases follow the movement of the linearly varying frequency input,
3. As f increases, the taps at the far end of the line contribute relatively less to the filter output than those taps at the beginning of the line.

These phenomena can be explained as follows:

1. The two sources of randomness that contribute to the filter output mean-square-error, are input noise and algorithm noise (weight misadjustment). The contribution of the input noise to the mean square error decreases linearly with the number of taps whereas the algorithm noise increases linearly with the number of taps. Thus, at high input signal-to-noise ratios, the algorithm noise is the limiting factor and few taps are needed. At low input signal-to-noise ratios, input noise is the limiting factor and a large number of taps are needed in order to reject the input noise. Eventually algorithm noise becomes the significant factor.
2. The figures show only the mean values of the steady-state weights at a particular instant of time after the filter has converged. Hence, there should be a quadratic phase shift with the tap number in accordance with $D(n)$ in Eq. (6). Comparison of Figures 42-44 with Figure 41 and Figures 46-48 with Figure 45 shows that the steady-state weights do display this behavior.
3. The filter trades off coherent integration (proportional to the number of significantly non-zero weights) against the phase changes required at each tap to follow the chirped signal. Since the phase change required at each iteration for each tap grows linearly with tap number (entries in V), weights at the far end of the line must make large phase changes in comparison to those at the beginning of the line. Note that the quadratic phase correction along the line, $D(o)$, is independent of time. Hence,

once the filter estimates f_0 and \hat{f} , it knows $D(\omega)$ and can introduce these phase corrections statically. On the other hand, the filter must change phase by the entries in V at each iteration. Large phase changes are most easily made when the magnitude of the weights are small. In Figures 42-44, $\Delta\phi = \omega\delta^2 = 2/10M$ radians and in Figures 46-48, $\Delta\phi = 2/40M$ radians. Hence the M^{th} weight has to change by $\pi/5$ and $\pi/20$ radians, respectively. In order to accommodate these large phase changes for the same algorithm step size, the weights of the far end of the line must be smaller than those at the beginning of the line. As \hat{f} decreases, the difference in phase changes at the two ends of the line decreases and the filter can make use of significant values for the weights at the far end of the line.

THE MEAN SQUARE ERROR IN STEADY-STATE

The error, $\epsilon(n)$, is the difference between $d(n)$ and the filter output, $W^T(n) X(n)$. Its mean square value is given by

$$\begin{aligned} E[|\epsilon(n)|^2] &= E\left\{ [d(n) - W^T(n) X(n)] [d^*(n) - W^+(n) X^*(n)] \right\} \\ &= E[d(n) d(n)^*] - E[W^T(n) X(n) d^*(n)] - E[d(n) W^+(n) X^*(n)] \\ &\quad + E[W^T(n) X(n) W^+(n) X^*(n)] \end{aligned}$$

Using the assumptions preceding Eq. (2),

$$E[|\epsilon(n)|^2] = \left(\sigma_s^2 + \sigma_n^2 \right) - \sigma_s^2 2 \operatorname{Re} \left\{ E [W(n)]^+ D(n) \right\} + E[W^T(n) X(n) W^+(n) X^*(n)] \quad (28)$$

The middle term in brackets in Eq. (28) can be evaluated using Eq. (25) and is given by

$$E[W_{ss}(n)]^+ D(n) = \frac{\mu \sigma_s^2 \sum_{k=1}^M \left(e^{j\omega k \delta^2} (1 - \mu \sigma_n^2) \right)^{-1}}{1 + \mu \sigma_s^2 \sum_{k=1}^M \left(e^{j\omega k \delta^2} (1 - \mu \sigma_n^2) \right)^{-1}} \quad (29)$$

The last term in Eq. (28) can be evaluated as follows. Let the weight vector be written as a mean value plus a zero-mean fluctuation process.

$$W(n) = E\{W(n)\} + \zeta(n) \quad (30)$$

Then

$$\begin{aligned} E\left[W^T(n) X(n) W^+(n) X^*(n)\right] &= E\left[W^+(n)\right] E\left[X^*(n) X^T(n)\right] E\left[W(n)\right] \\ &+ E\left[\zeta^+(n) X^*(n) X^T(n) \zeta(n)\right] \end{aligned} \quad (31)$$

The first term in Eq. (31) is known. The second term in Eq. (31) is

$$\begin{aligned} E\left[\zeta^+(n) X^*(n) X^T(n) \zeta(n)\right] &= E\left[\zeta^+(n) E\left[X^*(n) X^T(n)\right] \zeta(n)\right] \\ &= \left(\sigma_s^2 + \sigma_n^2\right) E\left[\zeta^+(n) \zeta(n)\right] \\ &= \left(\sigma_s^2 + \sigma_n^2\right) M \sigma_w^2, \end{aligned} \quad (32)$$

assuming the weight fluctuations are stationary, uncorrelated from tap-to-tap, and have the same variance σ_w^2 for each individual weight. Thus, using Eqs. (31) and (32) in Eq. (28) yields

$$\begin{aligned} E\left[|\epsilon(n)|^2\right] &= \sigma_s^2 \left|1 - E\left[W(n)\right]^+ D(n)\right|^2 + \sigma_n^2 \left[1 + E\left[W(n)\right]^+ E\left[W(n)\right]\right] \\ &+ M \left(\sigma_s^2 + \sigma_n^2\right) \left[\frac{\mu \sigma_n^2}{2 - (M+1) \mu \sigma_n^2}\right] \end{aligned} \quad (33)$$

where σ_w^2 has been approximated by the weight fluctuations under noise alone^[4, 5, 7]. The first term in Eq. (33) represents the error in estimating the chirped complex exponential signal. The second term is the sum of the noise power in the reference channel and the noise power passed by the mean weights of the adaptive filter. The last term represents the weight misadjustment variance multiplied by the total input power.

Eq. (33) normalized by the total input power, has been evaluated as a function of $\mu \sigma_n^2$ for $M = 16, 32, 64$, signal-to-noise ratios of 0 and +10 dB and various $\omega \zeta^2$. In Figures 49-54, the trade-off can be seen between static and dynamic contributions to

total mean-square error. In each case, there is an optimum selection of $\mu\sigma_n^2$ which minimizes the deleterious effects of signal errors, input noise and weight misadjustment noise. Comparison of the filter performance for increasing input signal-to-noise ratios verifies improved system performance. On the other hand, for sufficiently large $\dot{\omega}\xi^2$ and SNR = 10 dB, it is seen that the normalized mean square error increases as M increases. This effect is due to the weight mis-adjustment noise exceeding the longer coherent integration gain obtained with larger filters. As $\dot{\omega}\xi^2$ decreases, a point is reached where sufficient smoothing time is available (small $\mu\sigma_n^2$) to reduce the weight misadjustment noise to a level so that improved performance is obtained for longer filters (e.g. $\dot{\omega}\xi^2 = 4 \times 10^{-5}$).

It can be seen from Figures 49-54 that the optimum selection of $\mu\sigma_n^2$, for a given filter length M and signal-to-noise ratio, varies in the same manner as $\dot{\omega}\xi^2$. As $\dot{\omega}\xi^2$ increases, a larger value of $\mu\sigma_n^2$ is required to achieve the minimum mean-square error. However this minimum mean-square error increases as $\dot{\omega}\xi^2$. The filter has less time to learn the statistics of the signal and hence must make a larger mean-square-error as the price for tracking a faster moving signal. It is somewhat difficult to determine the point where the LMS algorithm loses track of the signal since mean-square error is not a good measure of tracking performance.

CONCLUSIONS

A mathematical model of the mean weight behavior for the LMS adaptive filter has been presented when the filter is operating as a single frequency line enhancer and line follower. For a fixed frequency complex sine wave input, the LMS filter weights have been shown to respond to signal and noise more rapidly than to noise alone. This implies that the filter learns more quickly that a line has appeared than it is able to forget that the line is turned off.

When the signal frequency is changing linearly with time, the mathematical model predicts a time-varying behavior of the filter mean weights necessary to respond to the changing signal frequency. As the chirp rate increases, the filter reduces the relative amplitudes of the weights so as to adjust the effective filter length to optimally match the properties of the signal. That is, for example, suppose the filter designer selects a filter of length $M = M_1$. However, the chirp rate is sufficiently large so that the change in signal frequency, between algorithm iterations, is greater than the bandwidth of the filter. Then, the LMS algorithm will automatically scale the amplitude of its weights to have an effective length M_2 , $M_2 < M_1$, such that the signal remains inside the adaptive filter between iterations. As long as the signal frequency lies within the LMS filter bandwidth, the LMS filter algorithm can track the changing frequency since there is sufficient correlation between the two inputs to drive the LMS algorithm in the correct direction.

The mathematical model of the mean weight behavior has been used for selecting μ , the adaptation coefficient of the algorithm, for a wide variety of signal and noise parameters. The criteria of optimality was that of minimizing the filter output mean square error, since the error is the driving term in the weight adjustment algorithm. (An alternate criteria, based on a signal detection model using the filter output, could also be a candidate for optimization.) A set of curves of normalized mean-square error as a function of signal-to-noise ratio and chirp rate were obtained. From these curves, the following observations can be made:

1. For a given signal-to-noise ratio and chirp rate $\omega\delta^2$, there exists an optimum selection of μ that minimizes the overall mean square error.
2. For slowly changing signal frequency, the mean square error exhibits a relatively broad minimum. This is because a large range of $\mu\sigma_n^2$ will follow the slowly changing signal frequency yet allow sufficient smoothing

CONCLUSIONS

so as to keep the weight misadjustment noise below a certain minimum. On the other hand, for a rapidly moving signal frequency, mismatch in selection of $\mu\sigma_n^2$ can cause a significant increase in mean-square error as compared to the optimum selection of $\mu\sigma_n^2$.

3. As a system designer, one would choose a $\mu\sigma_n^2$ that would be optimum for the fastest chirp rate expected. The mean square error would always be upperbounded by the mean square error for the fastest chirp rate.

REFERENCES

1. B. Widrow, P. Mantey, L. Griffiths and B. Goode "Adaptive Antenna Systems," Proc. IEEE, Vol. 55 pp. 2143-2159, Dec. 1967.
2. B. Widrow "Adaptive Filters" in Aspects of Network and System Theory, R. Kalman and N. DeClaris Eds, New York: Holt, Rinehart and Winston, 1971, pp. 563-587.
3. L.J. Griffiths "A Simple Algorithm for Real-Time Processing in Antenna Arrays," Proc. IEEE, Vol. 56 pp. 1696-1704, Oct. 1969.
4. B. Widrow et al., "Adaptive Noise Cancelling Principles and Applications," Proc. IEEE Vol. 63 pp. 1692-1716, Dec. 1975.
5. L.J. Griffiths "Rapid Measurement of a Digital Instantaneous Frequency," IEEE Trans. Acoust. Speech, Signal Processing ASSP-23, pp. 207-222, Apr. 1975.
6. J.R. Zeidler and D.M. Chabries "An Analysis of the LMS Adaptive Filter used as a Spectral Line Enhancer," TN 1476 Feb. 1975, Naval Undersea Center, San Diego, California.
7. P.L. Feintuch and N.J. Bershad "Signal Detection Using Adaptive Filters," 1976 IEEE Int. Symp. on Inform. Th., June 21-24, 1976, Ronneby, Sweden.
8. L. Griffiths, J. Keeler and R. Medaugh "Detection and Convergence Results Relating to the Performance of an Adaptive Line Enhancer", Dept. of Electrical Engr., University of Colorado, Boulder, Colorado, Dec. 1976.
9. S. T. Alexander, J. R. Zeidler and P. M. Reeves "An Analysis of ROC Performance Evaluation of the Adaptive Line Enhancer," Tech. Rpt. Naval Ocean Systems Center, San Diego, Calif.
10. S. T. Alexander, J. R. Zeidler, M. Shensa and R. Medaugh "Detection of Sinusoids in White Noise Using Adaptive Linear Prediction Filtering," May, 1978 (submitted for publication).
11. J. T. Rickard and J. R. Zeidler "Second Order Output Statistics of the Adaptive Line Enhancer," NOSC Tech. Rpt. 202, 1 Dec 1977, Naval Ocean Systems Center, San Diego, Calif.
12. D.W. Tufts, L.J. Griffiths, B. Widrow, J. Glover, J. McCool and J. Treichler "Adaptive Line Enhancement and Spectrum Analysis," Proc IEEE, Vol. 65, No. 1, pp. 169-173.

13. T. P. Daniell and J. E. Brown III "Adaptation in Non-Stationary Applications," in Proc 1970 IEEE Symp. Adaptive Processes (9th) Austin, Texas, Paper No. XXIV-4, Dec. 1970.
14. Y. T. Chien, K. S. Fu "Learning in Non-Stationary Environment Using Dynamic Stochastic Approximation," in Proc. 5th Allerton Conf. on Circuits and Systems Theory, pp. 337-345, 1967.
15. B. Widrow, J. M. McCool, M. G. Larimore, and C. R. Johnson Jr., "Stationary and Non-Stationary Learning Characteristics of the LMS Adaptive Filter," Proc. IEEE Vol. 64, No. 8, pp. 1151-1162, Aug 1976.
16. J. R. Treichler, "The Spectral Line Enhancer - The Concept, an Implementation and an Application," PhD Thesis, Dept. of Electrical Engineering, Stanford University, May 1977.
17. B. Widrow, J. McCool and M. Ball "The Complex LMS Algorithm," IEEE Proc. April 1975, pp. 719-720.
18. L. A. Zadeh and C. A. Desoer "Linear System Theory - A State Space Approach," pp. 575-576, McGraw Hill, New York 1963.

APPENDIX. EIGENVALUES OF TRANSFORMATION MATRIX

In order to easily evaluate the m^{th} power of a matrix, the eigenvalues of the matrix are needed. The matrix in brackets in Eq. (15) is

$$\begin{aligned} P_0 V^* P_0^{-1} [I - \mu \sigma_n^2 \lambda] &= P_0 V^* [P_0^{-1} - \mu \sigma_n^2 P_0^{-1} \lambda] \\ &= P_0 V^* [I - \mu \sigma_n^2 M(0)] P_0^{-1} \end{aligned} \quad (I-1)$$

Since P_0 premultiplies and P_0^{-1} post-multiplies $R = V^* [I - \mu \sigma_n^2 M(0)]$, it is only necessary to find the eigenvalues, λ , of R . The eigenvalues of R satisfy:

$$\left| V^* \left[I - \mu \left(\sigma_n^2 I + \sigma_s^2 D_0 D_0^+ \right) \right] - \lambda I \right| = \left| (1 - \mu \sigma_n^2) I - \lambda V - \mu \sigma_s^2 D_0 D_0^+ \right| = 0 \quad (I-2)$$

where

$D_0 = D(0)$ and $||$ denotes the determinant.

Because of the simple structure to R , an expression for the eigenvalues can be found. Given a matrix of the form $B = A + a_1 b_1^+$ where a and b are column vectors,

$$|B| = |A| \left[1 + b_1^+ A^{-1} a_1 \right] \quad (I-3)$$

Thus, with $A = (1 - \mu\sigma_n^2) I - \Lambda V$, $a_1 = D_0 = b_1$,

$$\begin{aligned} \left| (1 - \mu\sigma_n^2) I - \Lambda V - \mu\sigma_s^2 D_0 D_0^+ \right| &= \left| (1 - \mu\sigma_n^2) I - \Lambda V \right| \left\{ I - \mu\sigma_s^2 D_0^+ \right. \\ &\quad \left. \text{Diag} \left(\frac{a}{(1 - \mu\sigma_n^2)^{a-\Lambda}}, \frac{a^2}{(1 - \mu\sigma_n^2)^{a^2-\Lambda}}, \dots, \frac{a^M}{(1 - \mu\sigma_n^2)^{a^M-\Lambda}} \right) D_0 \right\} \\ &= \left[1 - \mu\sigma_n^2 \right]^M \left| I - \frac{V}{1 - \mu\sigma_n^2} \right| \left\{ 1 - \mu\sigma_s^2 \sum_{m=1}^M \frac{a^m}{(1 - \mu\sigma_n^2)^{a^m-\Lambda}} \right\} = 0 \end{aligned} \quad (I-4)$$

The term in brackets yields an M 'th order polynomial in Λ for which there is no general analytic solution. Eq. (I-4) must be programmed on a digital computer for various μ , σ_s^2 , σ_n^2 and a .

Although explicit values of Λ are not obtainable, a simple upper bound on the eigenvalues of Λ and hence on the transient behavior of Eq. (21) are obtainable. This upper bound on the eigenvalues is useful since it is an indication of the slowest possible response of the system.

Let \underline{u} be an eigenvector of the matrix in Eq. (I-1) with associated eigenvalue, Λ_i . Then, with $\underline{u} + \underline{u} = 1$, and $\underline{u}^T = [u_1 u_2 \dots u_m]$

$$\Lambda_i \underline{u} = P_0 V^* P_0^{-1} (I - \mu\sigma_n^2 \lambda) \underline{u} \quad (I-5)$$

Now,

$$\begin{aligned} \Lambda_i^* \underline{u}^+ \underline{u} \Lambda_i &= \left| \Lambda_i \right|^2 = \underline{u}^+ (I - \mu\sigma_n^2 \lambda)^+ P_0^{-1+} V^{*+} P_0^+ P_0 V^* P_0^{-1} \\ &\quad (I - \mu\sigma_n^2 \lambda) \underline{u} \end{aligned} \quad (I-6)$$

Using $P_o^{-1} = P_o^+$ and $V^+ = V^{-1}$

$$\begin{aligned} |\Lambda_i|^2 &= \sum_{j=1}^M |u_j|^2 |1 - \mu \sigma_n^2 \lambda_j|^2 \\ &= |u_1|^2 \left| 1 - \mu (\sigma_n^2 + M \sigma_s^2) \right|^2 + |1 - \mu \sigma_n^2|^2 \sum_{j=2}^M |u_j|^2 \end{aligned} \quad (I-7)$$

Let $q = \sum_{i=2}^M |u_i|^2 \leq 1$ and $p = 1 - q = |u_1|^2 \leq 1$. Then

$$\begin{aligned} |\Lambda_i|^2 &= (1-q) \left| 1 - \mu (\sigma_n^2 + M \sigma_s^2) \right|^2 + q \left| 1 - \mu \sigma_n^2 \right|^2 \\ &= \left| 1 - \mu (\sigma_n^2 + M \sigma_s^2) \right|^2 + q \left(\left| 1 - \mu \sigma_n^2 \right|^2 - \left| 1 - \mu (\sigma_n^2 + M \sigma_s^2) \right|^2 \right) \\ &\leq \left| 1 - \mu \sigma_n^2 \right|^2 \text{ for } \left| 1 - \mu \sigma_n^2 \right| \geq \left| 1 - \mu (\sigma_n^2 + M \sigma_s^2) \right| \end{aligned} \quad (I-8)$$

Similarly

$$\begin{aligned} |\Lambda_i|^2 &= p \left| 1 - \mu (\sigma_n^2 + M \sigma_s^2) \right|^2 + (1-p) \left| 1 - \mu \sigma_n^2 \right|^2 \leq \left| 1 - \mu (\sigma_n^2 + M \sigma_s^2) \right|^2 \\ &\text{for } \left| 1 - \mu (\sigma_n^2 + M \sigma_s^2) \right| \geq \left| 1 - \mu \sigma_n^2 \right| \end{aligned} \quad (I-9)$$

Eqs. (I-8) and (I-9) lead to the following bounds:

① If $\mu (\sigma_n^2 + M \sigma_s^2) \leq 1$, assuming $\sigma_n^2 \neq 0$

$$|\Lambda_i|^2 \leq \left| 1 - \mu \sigma_n^2 \right|^2 < 1 \quad (I-10)$$

② If $\mu(\sigma_n^2 + M\sigma_s^2) > 1$ but $\mu\sigma_n^2 \leq 1$, then for $\sigma_n^2 \neq 0$

$$|\Lambda_i|^2 \leq |1 - \mu\sigma_n^2|^2 < 1 \quad \text{for } \mu M\sigma_s^2 \leq 2(1 - \mu\sigma_n^2)$$

and

$$|\Lambda_i|^2 \leq |1 - \mu(\sigma_n^2 + M\sigma_s^2)|^2 \quad \text{for } \mu M\sigma_s^2 > 2(1 - \mu\sigma_n^2) \quad (I-11)$$

In the latter case, $|\Lambda_i|^2 < 1$ if $\mu(\sigma_n^2 + M\sigma_s^2) < 2$

③ If $\mu\sigma_n^2 > 1$ then

$$|\Lambda_i|^2 \leq |1 - \mu(\sigma_n^2 + M\sigma_s^2)|^2 \quad (I-12)$$

and

$$|\Lambda_i|^2 < 1 \quad \text{if } \mu(\sigma_n^2 + M\sigma_s^2) < 2$$

Combining these, it can be seen that $|\Lambda_i| < 1$ if $\mu(\sigma_n^2 + M\sigma_s^2) < 2$. Since $|\Lambda_i| < 1$ is the condition for existence of a steady state mean weight vector, $\mu(\sigma_n^2 + M\sigma_s^2) < 2$ is a sufficient condition for a steady state solution. It is interesting to note that the bound on $|\Lambda_i|^2$ in each case is just the magnitude of the largest eigenvalue in the stationary frequency case, with σ_n^2 , σ_s^2 , μ and M unchanged. Further

$$\mu(\sigma_n^2 + M\sigma_s^2) < 2$$

is the condition for the convergence of the adaptive canceller in the fixed sinusoid case. This leads to the surprising conclusion that if the mean weight vector achieves a steady state value in the stationary case for given σ_s^2 , σ_n^2 , M and μ , then a steady state solution will exist for those parameter values regardless of the rate of change of frequency.

A more direct result for convergence can be obtained as shown below. This latter approach does not bound the eigenvalues however.

From the discussion following Eq. (I-1) it is seen that R is similar to Q and therefore has the same eigenvalues. From ^[18],

$$\lim_{n \rightarrow \infty} \sum_{m=1}^n A^{m-1} = (I - A)^{-1} \quad (I-13)$$

if the L_2 norm of A is less than unity, i. e., $\|A\| < 1$. In our case, $R = A$ and

$$\|R\| = \|V^* [I - \mu \sigma_n^2 (\lambda)]\| \leq \|V^*\| \|I - \mu \sigma_n^2 \lambda\| \quad (I-14)$$

But $\|V^*\| = 1$ and $\|I - \mu \sigma_n^2 \lambda\|$ can be evaluated explicitly as the square root of the largest eigenvalue of the matrix $[I - \mu \sigma_n^2 \lambda]^* [I - \mu \sigma_n^2 \lambda]$.

But $[I - \mu \sigma_n^2 \lambda]$ is self-adjoint and has only two distinct eigenvalues.

$$\Lambda_1 = 1 - \mu (\sigma_n^2 + M \sigma_s^2)$$

$$\Lambda_2 = \Lambda_3 = \lambda_M = 1 - \mu \sigma_n^2 \quad (I-15)$$

Hence $\left| 1 - \mu (\sigma_n^2 + M \sigma_s^2) \right| < 1$

and

$$\left| 1 - \mu \sigma_n^2 \right| < 1$$

which implies $|\Lambda_i| < 1$ if

$$0 < \mu(\sigma_n^2 + M\sigma_s^2) < 2 \quad (I-16)$$

in agreement with the discussion following Eq. (I-12).

APPENDIX VIII
 COMPARISON OF ADAPTIVE TRACKER PERFORMANCE
 WITH AN EXISTING AUTOMATIC TRACKER

It is of interest to compare the performance of the adaptive tracker with a non-adaptive tracking system. For this purpose, the automatic tracking system described in reference [1] will be used. Figure 55 shows a block diagram of the tracker to be considered. The input signals from the left and right half beams are hard clipped and sampled, with the clipped signal for one side subjected to a variable delay, τ . This delayed signal and the other clipped input are processed by a two point correlator, as shown, which computes the correlation, $\phi(\tau)$, of the clipped signal at $\tau - T$. The value of $\phi(\tau)$ is either +1 or -1 for the clipped inputs. The contents of the delay register, which determines the value of the adjustable delay, is increased by $\Delta\tau$ when +1 occurs on input 2 and -1 on input 1. It is decreased by $\Delta\tau$ when +1 occurs on input 1 and -1 on input 2, with no change in count when the two agree. The tracker is in steady state when $\phi(\tau - T)$ and $\phi(\tau + T)$ are equal (both +1 or both -1). Assuming that the correlation function of the input is symmetrical, this means that the value of t is equal to the delay between the two split beam inputs.

The performance of this tracker has been analyzed in reference [1]. The analyzer is in excellent agreement with both computer simulations and at-sea tests of the device. For a broadband stationary target, the variance of the delay estimate was shown to be

$$\sigma_{\hat{\tau}}^2 = \frac{\Delta\tau}{(8/\pi) \left(\frac{\sigma_s^2}{\sigma_s^2 + \sigma_n^2} \right) (-\phi'_{ss}(T))} \quad (1)$$

where

$\Delta\tau$ = adjustable delay step size

σ_s^2 = signal power

σ_n^2 = noise power

$\phi'_{ss}(T)$ = value of the derivative of the normalized autocorrelation function of the signal at $\tau = T$

and T = fixed bulk delay used in the correlator.

This result is valid when the value of α_T is small in comparison to the width of $\phi_{ss}(\tau)$.

The structure of this tracker is considerably different than that of the adaptive tracker. Typically, the delay step size, $\Delta\tau$, is set much finer than the time between taps in the adaptive filter. This very high sample rate is tolerable, however, because the system uses one bit representations of the input, so hardware is minimal. The adaptive tracker replaces a high sampling rate with multibit processing and interpolation between coarser delays. In spite of the differences, the comparison of the two is interesting in light of the wide application of trackers similar to the clipped system.

In order to compare realizations of the two tracking schemes that are in some sense equivalent, the time constants of the two will be made equal. For low signal-to-noise ratio the time constant for convergence of the weight vector of the adaptive filter, both in mean and variance is in seconds

$$\tau_{at} = \left[\mu(\sigma_s^2 + \sigma_n^2) \right]^{-1} T_{at} \quad (2)$$

where T_{at} is the adaptive tracker sample interval.

Reference [1] has shown the time constant of the clipped tracker of Figure 55 to be

$$\tau_{ct} = \frac{(\pi/2)}{F_{ct} \Delta\tau \left(\frac{\sigma_s^2}{\sigma_s^2 + \sigma_n^2} \right) (-\phi'_{ss}(T))} \quad (3)$$

where F_{ct} is the clipped tracker sampling rate.

It is now necessary to set $\Delta\tau$ such that $\tau_{ct} = \tau_{ct}$. In practice, the input to the adaptive tracker is normalized such that

$$\sigma_s^2 + \sigma_n^2 = 1$$

This normalization will also be applied to the input of the clipped tracker. Then, setting (2) equal to (3) yields

$$\Delta\tau = \frac{\mu\pi/2}{F_{ct} T_{at} \left(\frac{SNR}{1+SNR}\right) (-\phi'_{ss}(T))} \quad (4)$$

and substituting in (1) gives

$$\sigma_{\hat{\tau}}^2 = \frac{\mu\pi^2}{16 F_{ct}^2 T_{at}^2 \left(\frac{SNR}{1+SNR}\right)^2 (\phi'_{ss}(T))^2} \quad (5)$$

where $SNR = \sigma_s^2 / \sigma_n^2$.

This is the variance of the time delay estimate of a clipped tracker whose time constant has been set equal to the adaptive tracker, and is not valid at high SNR.

In part VI of this report, the performance of an adaptive tracker for a broadband signal with an 800 Hz flat low pass spectrum was considered. Following the design procedure for the clipped tracker given in reference [1] gives the parameters

$$F_{ct} = \frac{1}{T} = 2400 \text{ Hz}$$

$$|\phi'_{ss}(T)| = 728.15 \text{ sec/sec}$$

For the adaptive tracker considered, $T_{at} = (1/2400)$. Substituting these parameters in (5) gives

$$\sigma_{\hat{\tau}}^2 = (1.1634 \times 10^{-6}) \mu \left(\frac{1+SNR}{SNR}\right)^2 \quad (6)$$

It should be stressed that the expressions (5) and (6) are not a generalized comparison of the particular clipped tracker with the adaptive tracker. The comparison is between an adaptive filter and a clipped tracker whose time constant has been adjusted at each signal-to-noise ratio to be equal to that of the adaptive tracker. This means, roughly, that the two trackers should be able to track dynamic targets with the same rate of change, or that the time to achieve the predicted bearing accuracy for an emerging target should be the same. Given the great difference in the structure of the two trackers, however, this equivalence is only approximate, and should be used only for order of magnitude comparisons, and not to predict fine differences in sensitivity.

Reference [1]: C. N. Pryor, "A Simplified Automatic Tracking Technique for Signal Correlation Systems," NOL Technical Report No. 67-152, 21 September 1967.

Unclassified

Security Classification

DOCUMENT CONTROL DATA - R & D

(Security classification of title, body of abstract and indexing annotation must be entered when the overall report is classified)

| | | | |
|---|--|---|------------------------------|
| 1. ORIGINATING ACTIVITY (Corporate author) Hughes Aircraft Company | | 2a. REPORT SECURITY CLASSIFICATION Unclassified | |
| | | 2b. GROUP | |
| 3. REPORT TITLE Final Report on Phase 1 of the Adaptive Tracking System Study | | | |
| 4. DESCRIPTIVE NOTES (Type of report and inclusive dates) Research Report | | | |
| 5. AUTHOR(S) (First name, middle initial, last name) Paul L. Feintuch, Francis A. Reed, Neil J. Bershad | | | |
| 6. REPORT DATE October 1978 | | 7a. TOTAL NO. OF PAGES 159 | 7b. NO. OF REFS 20 |
| 8a. CONTRACT OR GRANT NO. N00024-77-C-6251 | | 9a. ORIGINATOR'S REPORT NUMBER(S) TF78-11-1345 | |
| b. PROJECT NO. SF 11 121 160, Task 20929 | | 9b. OTHER REPORT NO(S) (Any other numbers that may be assigned this report) | |
| c. | | | |
| d. | | | |
| 10. DISTRIBUTION STATEMENT Distribution of this document is unlimited | | | |
| 11. SUPPLEMENTARY NOTES | | 12. SPONSORING MILITARY ACTIVITY Naval Sea Systems Command, Code 06H1 | |
| 13. ABSTRACT <p>The application of LMS adaptive filters to bearing tracking is investigated for sum and splitbeam bearing trackers and a specific splitbeam adaptive tracker algorithm selected. The adaptive tracker does not require a priori information regarding the input statistics, and can track using broadband and narrowband signal energy simultaneously. Time and frequency domain implementations of the tracker are presented. The performance of the tracker with a stationary broadband signal is analyzed and shown to be within .5 dB of the Cramer-Rao bound. The performance predictions are verified by computer simulations. The adaptive tracker is shown to give smaller bearing error than a conventional splitbeam tracker. In addition, the behavior of the adaptive tracker with broadband or narrowband signals that have changing bearing is analyzed, and simulations with moving targets presented. The response of the adaptive filter to a sine wave with linearly varying frequency is also analyzed.</p> | | | |

DD FORM 1 NOV 65 1473

Unclassified

Security Classification

Initial Distribution List

Commander
Naval Sea Systems Command
Department of the Navy
Washington, D.C. 20362
Attn: J. E. Neely, 06H1-1

Commander
Naval Sea Systems Command
Department of the Navy
Washington, D.C. 20362
Attn: 660F

Commander
Naval Sea Systems Command
Department of the Navy
Washington, D.C. 20362
Attn: 660C

Commander
Naval Sea Systems Command
Department of the Navy
Washington, D.C. 20362
Attn: 661C

Commander
Naval Sea Systems Command
Department of the Navy
Washington, D.C. 20362
Attn: 660E

Commander
Naval Sea Systems Command
Department of the Navy
Washington, D.C. 20362
Attn: 06H 2

Commander
Naval Sea Systems Command
Department of the Navy
Washington, D.C. 02362
Attn: Library 09G3

Defense Documentation Center
Defense Services Administration
Cameron Station, Building 5
5010 Duke Street
Alexandria, Virginia 22314

Director
Naval Research Laboratory
Department of the Navy
Washington, D.C. 20375

Chief of Naval Research
800 N. Quincy Street
Arlington, VA 22217
Attn: Code 466

Commander
Naval Ocean Systems Center
San Diego, CA 92152
Attn: Library

Officer in Charge
New London Laboratory
Naval Underwater Systems Center
New London, Connecticut 06320

David Taylor Naval Ship Research &
Development Center
Bethesda, MD 20034

Commander
Naval Surface Weapons Center
White Oak
Silver Spring, MD 20910

Commanding Officer
Naval Coastal Systems Center
Panama City, Florida 32407

Officer in Charge
New London Laboratory
Naval Underwater Systems Center
New London, CT 06320
Attn: Library

Commanding Officer
Naval Air Development Center
Johnsville
Warminster, Pennsylvania

Office of the Director of Defense
Research and Engineering
Room 3C128, The Pentagon
Washington, D.C. 20301